FTO supported Co_3O_4 thin film biosensor for detection of fructose

by

TATENDA INNOCENT GOTA

Thesis submitted in fulfilment of the requirements for the degree

MASTER OF ENGINEERING: CHEMICAL

in the

FACULTY OF ENGINEERING

at the

CAPE PENINSULA UNIVERSITY OF TECHNOLOGY

Bellville Campus

Supervisor: Dr. Mahabubur Chowdhury

Co-Supervisor: Prof. Tunde Ojumu

July 2018

CPUT copyright information

The thesis may not be published either in part (in scholarly, scientific or technical journals), or as a whole (as a monograph), unless permission has been obtained from the University.

*…In whom are hid all the treasures of wisdom and knowledge. [**Colossians 2:3]***

*True education means more than the pursual of a certain course of study. It means more than a preparation for the life that now is. It has to do with the whole being and with the whole period of existence possible to man. It is the harmonious development of the physical, the mental, and the spiritual powers. It prepares the student for the joy of service in this world and for the higher joy of wider service in the world to come. [E.G White, **Education 13.1**]*

*Engineering is not merely knowing and being knowledgeable, like a walking encyclopedia; engineering is not merely analysis; engineering is not merely the possession of the capacity to get elegant solutions to non-existent engineering problems; engineering is practicing the art of the organized forcing of technological change…Engineers operate at the interface between science and society...[**Dean Gordon Brown**]*

*It is a great profession. There is the fascination of watching a figment of the imagination emerge through the aid of science to a plan on paper... The great liability of the engineer compared to men of other professions is that his works are out in the open where all can see them. His acts, step by step, are in hard substance. He cannot bury his mistakes in the grave like the doctors. He cannot argue them into thin air or blame the judge like the lawyers. He cannot, like the architects, cover his failures with trees and vines. He cannot, like the politicians, screen his shortcomings by blaming his opponents and hope the people will forget. The engineer simply cannot deny he did it. If his works do not work, he is damned… [**H.C. Hoover**]*

DECLARATION

I, **TATENDA INNOCENT GOTA**, declare that the contents of this thesis represent my own unaided work, and that the thesis has not previously been submitted for academic examination towards any qualification. Furthermore, it represents my own opinions and not necessarily those of the Cape Peninsula University of Technology.

Signed **Date**

ABSTRACT

Electrochemical and non-enzymatic fructose detection has evoked keen interest in the scientific literature. Several authors have reported on different methods of electrode preparation for fructose sensors. However, little systematic study has been conducted to design a cheap, efficient method of depositing metal oxides to detect fructose. To address the challenge, a Co_3O_4 thin film was fabricated using a simple solution step deposition on Fluorine doped Tin oxide (FTO) glass electrode

In this study, a report on the selective oxidation of fructose on Co_3O_4 thin film electrode surface is presented. Electrode characterization was done using X-ray diffraction (XRD), High Resolution Transmission Electron Microscopy (HR-TEM), Scanning Electron Microscope (SEM), Atomic Fluorescence Microscopy (AFM), and Electrochemical Impedance Spectroscopy (EIS). All cyclic voltammetry (CVs) and chronoamperometry tests were carried out by the use of an AUTOLAB POTENTIOSTAT 302 N, controlled by Nova 2.0 software instrumentation using a customized 50 cm^3 electrochemical cell. The cell consisted of a graphite rod as the counter electrode (CE), 3 M Ag/AgCl reference electrode (RE) and the fabricated Co_3O_4/FTO as the working electrode (WE). All experiments were carried out at 25±2 ºC.

From the results, the constructed sensor exhibited two distinctive linear ranges in the ranges of 0.021 – 1.74 mM and from 1.74 - ~15 mM, covering a wide linear range of up to ~15 mM at an applied potential of +0.6V *vs*. Ag/AgCl in 0.1M NaOH solution. The sensor demonstrated a high, reproducible and repeatable sensitivity of 495 (lower concentration range) & 53 (higher concentration range) μA cm^{-2} mM^{-1} for a low R.S.D of 5 %. The Co_3O_4 thin film produced a low detection limit of ~1.7 μM for a signal to noise ratio of 3 (*S/N* = 3); a fast response time of 6s and long term stability. The repeatability and stability of the electrode resulted from the chemical stability of Co_3O_4 thin film. The study showed that the sensor was highly selective towards fructose compared to the presence of other key interferences i.e. AA, AC, and UA. Because of such a favourable electrocatalysis of the Co_3O_4 sensor towards fructose, the ease of the electrode fabrication and reproducibility makes it a future candidate for commercial applications in the food and beverages sector.

ACKNOWLEDGEMENTS

I wish to thank:

- I gratefully acknowledge support, guidance and advice afforded to me by my supervisor, **Dr. M. Chowdhury**, who guided my first steps into the field of electrochemistry and enabled me to develop my skills in the area of research. His input of ideas and enthusiasm has ensured that this thesis has reached completion.

- **Prof. T.Ojumu** who co-supervised the project and ran the administrative processes regarding the work. His efforts could not go by unmentioned.

- **Dr Oyekola** and **Dr De Jager** for their useful and constructive remarks and comments. Their review of my work in its proposal stages ensured that it reached its full potential.

- I am grateful to those people with whom I worked with and who assisted me in the work detailed in this thesis. **Gabriella Ossinga** and **Gloria Kibambo** were particularly generous with their efforts and time.

- The **Flow Process and Rheology Centre** at the Cape Peninsula University of Technology are thanked for the utilisation of their laboratories. A special word goes to **Prof. V. Fester** for her patience and generous assistance, even when I taxed her patience at most times!

- **Mr Richards** for making sure that I had all the equipment whenever I needed it.

- I also want to acknowledge all the people who helped me during the course of my Masters programme. To my friends and family who were supportive and kept me motivated when I was moving along a rough patch, your words of encouragement mean a lot. Please do not reserve your words of encouragement to those who need them most!

The opinions expressed therein and the conclusions arrived at are solely those of the author and are not in any way attributed to the Cape Peninsula University of Technology.

TABLE OF CONTENTS

ABSTRACT ..... **i**

ACKNOWLEDGEMENTS ..... **ii**

TABLE OF CONTENTS ..... **iii**

LIST OF FIGURES ..... **vii**

LIST OF TABLES ..... **x**

LIST OF ABBREVIATIONS ..... **xi**

LIST OF SYMBOLS ..... **xiii**

Chapter 1 ..... **1**

INTRODUCTION **1**

1.1 Background 1

1.2 Problem statement 2

1.3 Aim and objectives 2

1.4 Research approach 2

1.5 Scope of the work 4

1.6 Structure of the thesis 4

Chapter 2 ..... **6**

LITERATURE REVIEW **6**

2.1. Introduction 6

2.2 Nature and sources of fructose 6

2.3. Background – Methods used in the detection of fructose 7

2.4 Electrochemical methods 7

2.4.1 Enzymatic sensors 8

2.4.2 Non-enzymatic sensors 10

2.5 Electroanalytical techniques 15

2.5.1 Basic components of an electroanalytical system 15

2.5.2 Voltammetry Techniques 17

2.5.3 Cyclic Voltammetry 18

2.5.4 Chronoamperometric studies 23

2.5.5 Electrochemical Impedance Spectroscopy (EIS) Studies 24

2.6 Conclusions 29

Chapter 3 31

EXPERIMENTAL METHODOLOGY 31

3.1 Introduction 31

3.2 Materials and methods 31

3.2.1 Reagents and chemicals 31

3.3 Surface morphology of the thin film Co_3O_4 FTO glass electrode 32

3.3.1 X-diffractometry (XRD) 32

3.3.2 Transmission electron microscopy 33

3.3.3 Scanning electron microscopy (SEM) 34

3.4 Electrochemical experiments 34

3.5 Preparation of FTO glass electrodes 36

3.6 Calcination of thin film Co_3O_4 layers on FTO glass electrodes 36

3.7 Cyclic voltammetry 38

3.8 Chronoamperometric studies 38

3.8.1 Interference tests 41

3.9 Electrochemical Impedance Spectroscopy (EIS) Studies 41

3.10 Shelf life of the electrode 41

3.11 Reproducibility and chemical stability tests 42

3.12 Conclusions 42

Chapter 4 43

RESULTS AND DISCUSSION 43

4.1 Introduction 43

4.2 Surface Morphology of the Co_3O_4/FTO thin film 43

4.3 Electrochemical behaviour of the Co_3O_4-modified FTO electrode 45

4.3.1 Cyclic voltammetry of the Co_3O_4 modified thin film FTO 45

4.3.2 Effect of various concentrations of electrolyte 49

4.3.3 Electrochemical Impedance Spectroscopy (EIS) studies 51

4.3.4 Effect of scan rate study 54

4.3.5 Chronoamperometric studies of fructose detection 56

4.3.7 Reproducibility of the Co_3O_4 thin film 63

4.3.8 Chemical stability of the Co_3O_4 thin film electrode 63

4.3.9 Shelf-life of the sensor 64

4.3.10 Repeatability of the Co_3O_4/FTO thin film electrode 65

4.4 Conclusion 66

Chapter 5 68

CONCLUSION AND RECOMMENDATIONS 68

5.1. Introduction 68

5.2 Significance of the research 69

5.3 Further work and recommendations 69

References 70

LIST OF FIGURES

Figure 1.1: Experimental protocol used for conducting the thesis work.....3

Figure 2. 1: (a) A typical experimental set-up showing the reference electrode (RE),the working electrode (WE) and the counter electrode immersed into an electrolyte solution.(b) A simple electronic scheme equivalent to the electrochemical cell (Brownson & Banks,2014).....16

Figure 2. 2: Potential time (E-*t*) profiles used to perform linear sweep and cyclic voltammetry (Hess, 2010).....19

Figure 2. 3: Cyclic voltammogram for a reversible reduction of A to B (Compton & Banks, 2007).....20

Figure 2. 4: (a) Reversible and (b) irreversible cyclic voltammetry responses (Bard & Faulkner, 2000).21

Figure 2. 5: A typical chronoamprogram for an addition of analyte (shown are four step additions) (Neiva *et al*., 2016).....24

Figure 2. 6:A simplified Nyquist plot with a Randles equivalent circuit for a typical electrochemical cell (Randviir & Banks, 2013).....26

Figure 2. 7: A bode plot showing the logarithmic frequency and frequency for a number of layers a,b and c (Vora et al.,2013).....27

Figure 3. 1: Diffraction of X-rays by crystal lattice (Veqter Technologies,2018).....33

Figure 3. 2: A cell set-up utilised for both cyclic voltammetry and chronoamperometry (1) custom-made 3 electrode cell equipped with a magnetic stirrer,(2) Autolab potentiostat, (3) monitor to display electrical output.....35

Figure 3. 3: Schematic diagram of the solution step electrode fabrication of Co_3O_4 thin film on FTO glass electrode.....37

Figure 4.1: (a) Cross sectional SEM image of the Co_3O_4 film deposited on FTO (insert b & c: SEM and AFM image of the surface of the film respectively),(d) TEM image of the Co_3O_4 film (insert e:SAED of the Co_3O_4 partciles) and (f) XRD pattern of the Co_3O_4 thin film.....45

Figure 4. 2: Electrochemical behaviour of the Co_3O_4 thin film electrode in the absence and presence of 1 mM fructose in 0.1 M NaOH (scan rate: 25mV/s)..... 46

Figure 4. 3: CVs in the presence of 0 - 5 mM fructose in 0.1 M NaOH electrolyte (scan rate: 25 mV/s). 48

Figure 4. 4: CVs of Co_3O_4 in NaOH (0.05 – 1 M) electrolyte solution without fructose (scan rate = 25 mV/s) 50

Figure 4. 5: CVs of Co_3O_4 thin film in the presence of 1 mM fructose and NaOH (0.05 – 1 M NaOH) (scan rate: 25 mV/s)..... 51

Figure 4.6: Nyquist plots for bare FTO and Co_3O_4 FTO electrodes in 0.1 M NaOH solution containing 5 mM Fe $(CN)_6^{3-}$ 52

Figure 4.7: Equivalent circuit for the studied impedance system in 0.1 M NaOH containing 5 mM $Fe(CN)_6^{3-}$..... 52

Figure 4.8: Bode plots of the bare FTO and the Co_3O_4 thin film in 0.1 M NaOH solution containing 5 mM $Fe(CN)_6^{3-}$ 53

Figure 4. 9: (a) The influence of scan rate on the peak current density of Co_3O_4; (b)The plot of peak current density *vs*. scan rate (a) and (b) plot of current density against scan rate in the presence of 1.0 mM fructose and 0.1 M NaOH..... 55

Figure 4.10: Electrochemical response studies of Co_3O_4 film upon successive addition of fructose in 0.1 M NaOH in varying applied potentials..... 56

Figure 4. 11: Current density-time response for Co_3O_4 thin film upon successive addition of fructose in 0.1 M NaOH at + 0.60 V (response time, t = 6 s, of the sensor is also displayed) 57

Figure 4. 12: Linear range of the sensor for 0.021 - 15 mM fructose..... 58

Figure 4.13: Current density-time response of Co_3O_4 thin film upon successive addition of fructose and other interfering species in 0.1 M NaOH solution at an applied of + 0.60 V 60

Figure 4.14: Inter-electrode reproducibility of 6 Co_3O_4/FTO electrodes in 1 mM fructose in 0.1 M NaOH (scan rate:25 mV/s)..... 63

Figure 4.15: Chemical stability of the Co_3O_4/FTO electrode in 1 mM fructose in 1 M NaOH subjected to 100 cycles (scan rate:25 mV/s) 64

Figure 4.16: Shelf-life of the Co_3O_4/FTO electrode for 4 week period 65

Figure 4.17: Electrode repeatability tests for 1 electrode in 6 tests (error bars shown) 66

LIST OF TABLES

Table 2. 1: Enzymatic and non-enzymatic electrochemical sensors utilised in the detection of fructose..14

Table 3. 1: List of equipment used for thin film preparation and cyclic voltammetry 36

Table 3. 2: Parameters for CV analysis for scan rate tests and CV with the addition for different concentrations of fructose 38

Table 3. 3: Chronoamperometry tests at different applied potentials 39

Table 4. 1: Electrochemical parameters obtained by simulation of the EIS results on the FTO/Co_3O_4 in a 0.1 M NaOH containing 5 mM $Fe(CN)_6^{3}$.....54

Table 4. 2: Results of the scan rate in relation to the peak current density,1 mM fructose in 0.1 M NaOH 55

Table 4. 3: Comparison of the fabricated Co_3O_4/FTO thin film against previously reported fructose sensing characteristics of various nanomaterial modified electrodes prepared by different methods in literature 62

LIST OF ABBREVIATIONS

AA	Atomic Absorption
AAS	Atomic Absorption Spectroscopy
AFS	Atomic Fluorescence Spectroscopy
AuNP	Gold Nanoparticle
CCNFs	Cobalt oxide copper oxide composite nanofibers
CS-PDDA	Chitosan- poly (diallyldimethylammoniumchloride)
CE	Counter electrode
CNT	Carbon Nanotube
CNTP	Carbon Nanotube Paste
CPE	Carbon Paste Electrode
CV	Cyclic Voltammetry
DHB	Dihydroxybenzaldehyde
DNA	Deoxyribonucleic Acid
DP	Degree of Polymerisation
EIS	Electrochemical Impedance Spectroscopy
FDH	Fructose 5-Dehydrogenase
FRA	Frequency Response Analyser
GCE	Glassy Carbon Electrode
GE	Graphite Electrode
gL^{-1}	Gram per litre
HR-TEM	High Resolution Transmission Electron Microscopy
ICP-MS	Inductively Coupled Plasma-Mass Spectrometry
LOD	Limit of Detection ($g\ L^{-1}$)
NP	Nanoparticle
MPBA	Mercaptophenylboronic acid

MWNT	Multi-walled carbon nanotubes
OCV	Open circuit voltage
ppb	Parts per Billion
PBS	Phosphate Buffer Solution
PCS	Carbamoylsulphonate
PEI	Polyethylemine
PPY	Polypyrrole
RE	Reference electrode
RSD	Relative Standard Deviation
SDBS	Sodium dodecyl benzene sulfonate
SEM	Scanning Electron Microscope
SPE	Screen Printed Electrode
SWCNT-GCE	Single-Walled Carbon Nanotube Glassy Electrode
SWV	Sweeping Wave Voltammetry
TEM	Transmission Electron Microscopy
t_L	Shelf-life of an electrode at time ,t
t_{L50}	Shelf-life of the electrode after 50 % decrease in activity
WE	Working electrode

LIST OF SYMBOLS

Symbol	Description	Unit
A	Ampere	amps
A	Geometrical electrode area	cm^2
D	Diffusion coefficient	$cm^2\ s^{-1}$
Da	Molecular weight	$gmol^{-1}$
F	Faraday	-
f	Frequency	s^{-1}
S	Sensitivity	$u.A.cm^{-2}$
V	Applied potential	V

Greek symbols

μ	micro

Chapter 1

INTRODUCTION

The research encompasses the investigation of the electro catalytic properties of thin film metal oxide, cobalt oxide. This chapter provides a background to this work. ***Section 1.1*** *is an overview of the sensors.* ***Section 1.2*** *is a description of the problem statement in this context.* ***Section 1.3*** *expresses the rationale and motivation for carrying the project.* ***Section 1.4*** *presents the aims and objectives of the project, as well as the research approach and methods. The focus and scope of the work is described in* ***Section 1.5****. The chapter concludes with an outline of the thesis in* ***Section 1.6.***

1.1 Background

The accurate monitoring and detection of fructose has been extremely important to clinical and food and beverages industries. The demand for accurate sensing technologies for fructose has been increasing since the turn of the decade (Esswein *et al*., 2009). Frequent testing of physiological and food sample fructose are necessary to avoid and address adverse medical conditions influenced by diabetes in patients; and to enhance quality control and productivity. For decades, the development of fast, selective, wide linear range, low-cost, reliable fructose electrochemical sensors has been a subject of intense study and research. As for the last four decades, Fructose-5-dehydrogenase (FDAH)-based fructose biosensors have been extensively utilised as principal fructose sensors in research commercial applications. Similarly, there has been a high demand for sensitive and reliable blood fructose monitoring, and for the food processing industries.

1.2 Problem statement

A variety of electrochemical sensors for detection of fructose have been in use and some are being currently developed. On the other hand, the development most of these sensors is still in its infancy and hence they are not feasible for market applications. This therefore meets the need for the fabrication of cheap and portable sensors which are easy to operate for the detect fructose in body fluids and foods.

1.3 Aim and objectives

The overall aim of this research is to fabricate a cheap and efficient sensor by solution casting cobalt oxide on a FTO glass electrode using a simple solution method.

The objectives of this study are:

1. To prepare a sensor by a solution deposition of cobalt oxide onto a conductive Fluorine-doped Tin Oxide (FTO) glass support;
2. To evaluate the electrochemical properties of the sensor by characterisation methods such as CV and EIS and;
3. To conduct interference studies on sensor performance by selected compounds (fructose, acetaminophen, uric acid, glucose, sodium chloride, potassium chloride).

1.4 Research approach

In line with the research objectives and the research methodology, the research plan is illustrated in **Figure 1.1**:

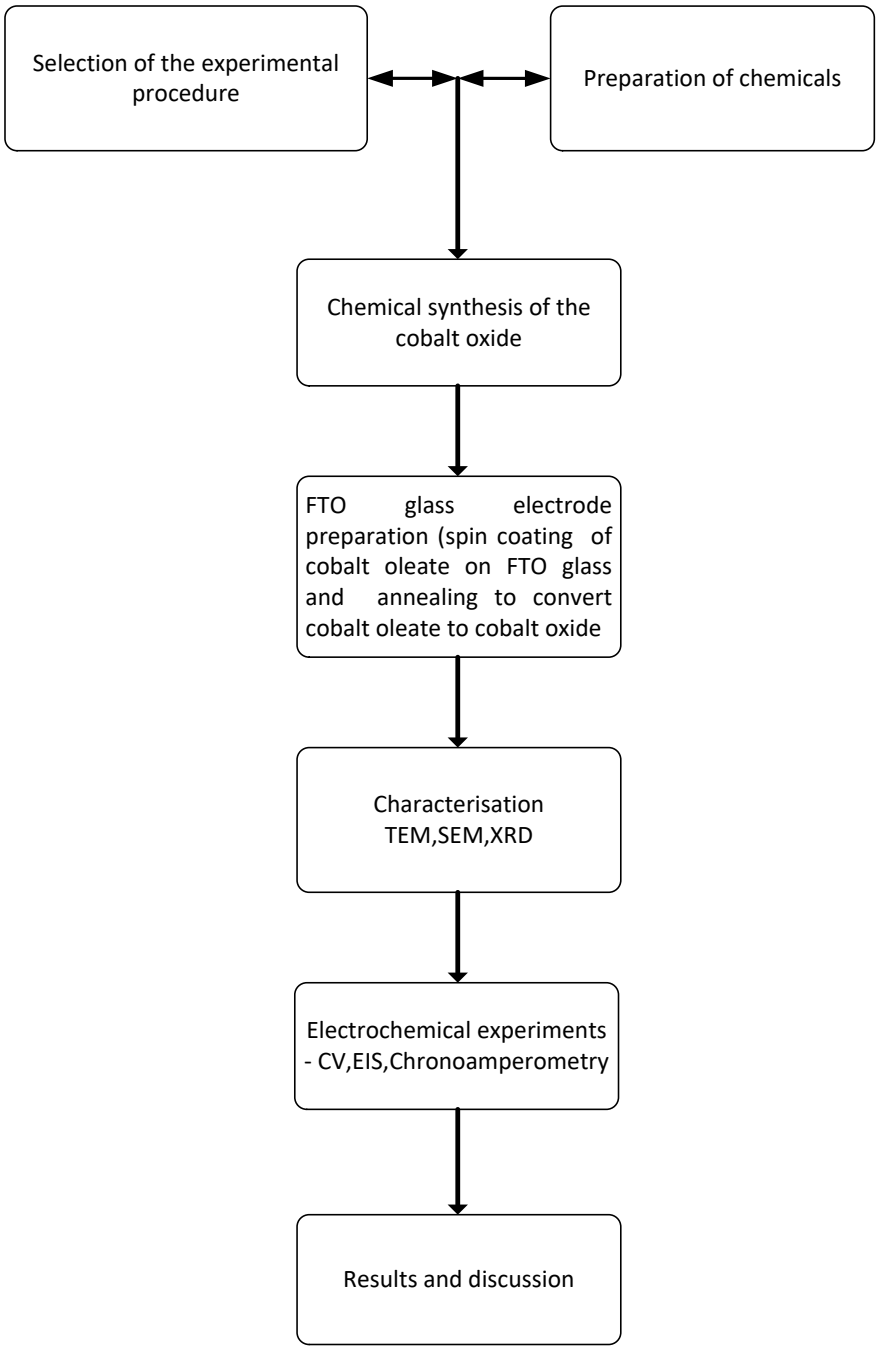

Figure 1.1: Experimental protocol used for conducting the thesis work

1.5 Scope of the work

The work focused on the fabrication of the electrode surface using Co_3O_4 FTO supported thin film as the sensing material.

1.6 Structure of the thesis

Chapter 1: Background

Chapter 1 places the problem statement (research motive) into context. It introduces, contextualizes, provides a motivation for the research that is reported in this thesis, and establishes the need for quantitative analysis of the sensor performance. The chapter also defines the scope of the research.

Chapter 2: Literature review

Chapter 2 describes of the various studies and methods on the fabrication of the sensors. The chapter provided a literature review that acted as a guide to the methodology and data analysis. The relevant literature dealing with electrochemical sensors are discussed. In it, principles sensing mechanisms are explained, as well as different views that have been proposed by different researchers as they try to sensor mechanisms.

Chapter 3: Research methodology

The methodology employed in achieving the objectives of this thesis is given in Chapter 3. A description of the experimental methodology used to conduct cyclic voltammetry test work is provided. Included in the methodology is the deposition technique, preparation of samples, testing techniques applied, and parameters that were varied to achieve the goals of the thesis.

Chapter 4: Results and Discussion

This chapter develops an analysis of the data generated from the experiments. Efforts to meaningfully interpret the data are made, in relation to available information. By analyzing the performance from the data it will be included whether or not the expectations can be met.

Chapter 5: Conclusions and recommendations.

Chapter 5 concludes with an overall description of the work performed, presents the significant findings and identifies areas not covered which can be explored in further research work. Based on the outcomes of this study, the inferences of the research are stated and recommendations for further studies are presented.

Chapter 2

LITERATURE REVIEW

2.1. Introduction

A review of the literature on the different non-enzymatic sensors that have been reported to date is presented in this chapter. The problem of the need to use a portable sensing mechanism is also given in context. The structure and the mode of operation of such are considered also. The fundamentals of electrochemistry are introduced in brief. **Section 2.1** gives a brief introduction to the chapter. **Section 2.2** introduces the occurrence of fructose and how they are significant. **Section 2.3** gives a background in the methods used to detect fructose and introduces electrochemical methods. **Section 2.4** evaluates the literature behind the development of the use of enzymatic fructose sensors. The section also focusses on non-enzymatic fructose sensors. Basic electro analytical techniques of electrochemistry are represented in **Section 2.5**. The chapter concludes with **Section 2.6** and demonstrates how the fabricated sensor would compare significantly to what has been found in previous studies.

2.2 Nature and sources of fructose

Fructose is a monosaccharide widely found in fruit pulp, cereal, soft drinks, as well as honey (Paredes *et al*., 1997). The sugar is chiefly utilised as a sweetener and ingredient of high fructose corn syrups (Xu *et al.*, 2014). Because of its superior sweetening ability compared to glucose or sucrose, fructose has been preferred over the preceding two sugars (Paredes *et al*., 1997). It is also present in the blood serum in comparable amounts although it is significantly higher in diabetic patients (Kawasaki *et al*., 2012).Higher fructose levels in fruits are an indication of the fruit ripening process. As diet trends are ever changing,

more and more fructose is being ingested through various foods (Xu *et al*., 2014).Currently, the traditional determination of fructose levels in fruits and fructose-containing syrups or soft drinks is employed as an expression of the sugar content in terms of the percentage of soluble solids content. For more accurate results, another method will be the evaluation of total inverted sugars content in the sample. In the medical industry, the blood serum is drawn from the patient and the samples tested for fructose content. This poses discomfort in terms of needle prick, and the method is invasive in nature. Therefore the determination of fructose has considerable application in food industry, biotechnology, and diagnostic medicine (Elahi *et al*., 2008).

2.3. Background – Methods used in the detection of fructose

Currently the determination and quantification of the fructose in food samples and serum is conducted via laboratory methods including high-performance liquid chromatography (HPLGC), gas chromatography–mass spectrometry (GCMS) (Katona *et al*., 1999), and the fluorescence method (Wang *et al*., 1999). Although these methods are accurate, however, they are restricted to the expensive apparatus used and tedious sample preparation. These drawbacks restrict the applicability and the development of these methods.

The use of electrochemical sensors and their advantages over laboratory methods has been well appraised in various bodies of literature (Stradiotto *et al*., 2003). The electrochemical detection of fructose offers a wide array of advantages over the use of conventional laboratory methods. These sensors have a great potential of use in the sensing field because they have high sensitivities, easier instrumentation, rapid detection, low cost and the potential of being mass reproduced. In addition to that, the use of these sensors has been promising in terms of portable personal use, which allows fast and continuous monitoring.

2.4 Electrochemical methods

Electrochemical methods have attracted an immense amount of attention from the scientific literature. Currently electrochemical detection of fructose can be considered as a cheap and viable mode of fructose detection. This can be attributed to their favourable characteristics such as low cost, ease of fabrication,

easy operation and a fast linear response. Electrochemical fructose sensors are classified into two categories: fructose dehydrogenase (FDH)-based sensor (enzymatic sensors) and non-enzymatic sensors.

2.4.1 Enzymatic sensors

Enzymatic sensors have been utilised due to their high selectivity and short response times. The use of the membrane-bound fructose dehydrogenase (FDH) has been well appraised in literature. Yamada *et al*. (1966) was the first to describe a systematic attempt to utilise FDH in fructose detection. The authors confirmed the catalysed the oxidation of d-fructose to 5-keto-d-fructose by FDH.

FDH contains a complex of three subunits with a total molecular weight of 140,000 Da (Tkáč *et al*., 2001). The enzyme contains one Flavin and one heame c group as the prosthetic groups (Ameyama *et al*., 1981). The heame group in FDH renders its catalytic properties in that the enzyme is a PQQ (pyrroloquinoline quinone) enzyme. The catalytic activity takes place when the PQQ to reduced pyrroloquinoline quinone ($PQQH_2$). Prabhulkar and co-authors (Prabhulkar *et al*., 2012) reported that FDH is able to participate in the electrocatalytic oxidation of fructose into 5-keto-fructose in the absence of an electron transfer mediatory compound. The action of FDH upon fructose is described by Equation 2.1:

$$D-fructose \;+\; FDH_{(ox)} \;\rightarrow\; 5-keto-D-fructose \;+\; FDH_{(red)} + \;2H^{+} + \;2e^{-} \quad \textbf{2.1}$$

In the first step, FDH is reduced as it attaches to the substrate; the enzyme regeneration is achieved by the device transducer (Swann *et al*., 1997;Yabuki & Mizutani, 1997). In this instance, as the the enzyme catalyses the oxidation of fructose to 5-keto-D-fructose, there is a reduction of the covalently bound cofactor PQQ to $PQQH_2$. Both the direct and the indirect re-oxidation of $PQQH_2$ are possible, and this yields a current which is proportional to fructose concentration. Because FDH has a high specificity for D-fructose as a substrate, the prospects are high that the enzyme might be applicable the field of food analysis and for clinical use (Marbán *et al*., 2008; Nam, 2006).

In order to enhance the kinetics of the surface-bound electrocatalytic activity of FDH, several electrodes and catalysing materials have been utilised to work in conjunction with the FHD enzyme. In addition to that, previous studies have also reported extensively on the direct electron transfer kinetics and reaction mechanisms of FDH on various electrode surfaces (Marbán *et al*., 2008; Kamitaka *et al*., 2007; Tominaga *et al*., 1999). Since then FDH biosensors based on platinum supports (Antiochia & Palleschi, 1997),

glassy carbon electrodes (Begum *et al*., 1993), carbon paste electrodes (Stredansky *et al*., 1999), have been developed and commonly utilised.

For instance Garcia and co-workers (Garcia *et al*., 1998) immobilized FDH on a polypyrrole film (PPY) over a platinum electrode containing sodium ferricyanide as an electron mediator. . A linear range of 0.1 – 0.8 mM was reported for the sensor. In another set of experiments conducted by Trivedi *et al*. (2009), a portable fructose sensor was developed for the detection of fructose. For their test work, FDH was immobilised on a platinum (Pt) tip of a screen printed graphite (SPE) electrode using polyethylenemine (PEI) and poly (carbamoylsulphonate) (PCS) and ferricyanide as the electron acceptor. The sensor was evaluated in a 1 mM d-fructose at pH 5.4. They reported the sensitivity of 0.62 ± 0.10 nAM^{-1} that is much lower than most of the fructose sensors that have been reported. The response of the sensor was best found in the ranges of 3 - 4 mM. The sensor had a shelf life of 3 – 5 days, with the electrode response decreasing with continued use. This lifetime was within the range for disposable types of biosensors. While the biosensor has numerous favourable features, the enzymes require more time for preparation and the samples need to have more rigorous preparatory and preservation procedures.

Antiochia *et al*. (2004) reported results describing the use of a mediated carbon nanotube paste (CNTP) electrode for the detection of fructose. The CNTP electrode was modified with an electropolymerized film of 3, 4-dihydroxybenzaldehyde (3, 4-DHB). In this work, the fructose dehydrogenase was immobilized on the surface of the CNTP. The biosensor was utilized to detect fructose in the range of 0.005 to 2 mM. Results of the study showed that the sensor displayed a fairly low limit of detection of 1 µM. The sensor also had a good reproducibility and a low relative standard deviation (RSD) of 1.8 for a set of 5 tests.

A novel approach of applying a sensor using modified commercial screen-printed ferrocyanide/carbon electrodes (SPFCE) was reported by Biscay *et al*. (2012a). For the sensor, a commercial screen-printed electrode was utilized as a support for the electrode. For this sensor 10 µL FDH was cast on the electrode surface and dried (approximately 1 h) at room temperature. The sensor had a good sensitivity of fructose up to 1.25 μAmM^{-1}. A satisfactory linear range of the sensor was developed in the range of 0.1 - 1 mM of fructose and a low limit of detection (LOD) of 0.05 mM. The sensor also displayed satisfactory results when placed in real fruit and beverage samples. Whilst the sensor performance appears to be ideally suitable for real-time monitoring of fructose, information on the time response of the sensor was not available.

However, FDH-based biosensors are prone to problems such as the requirement for different cofactors and the complexity of the immobilisation procedures (Ding *et al*., 2010; Thevenot *et al*., 2001; Paredes *et al*., 1997). Further, there have been some drawbacks of enzyme-based fructose determination which include complex enzyme immobilization, critical operating temperature and pH, chemical instability, and high cost.

To counteract these challenges and setbacks, research has turned to explore the applicability of enzyme-less sensors for fructose detection. This has been achieved by incorporating different sensing materials such as precious inert metals, metal oxides, nanocomposites of metals and carbon nanotubes (CNTs) (Bang & Suslick, 2010). However, the performance of these materials is limited because of high costs, quick loss of activity by adsorption as well as by accumulation of intermediates and poisoning by potassium or chloride ions (Chen & Ostrom, 2015). Therefore in light of this, the development of fast, selective, sensitive non-enzymatic fructose sensors is imperatively needed.

2.4.2 Non-enzymatic sensors

More attention has been furnished for the non-enzymatic sensors due to their favourable inherent features such as stability, simplicity and reproducibility (Biscay *et al*., 2012a). Some sensors have been explored by (Biscay *et al*. (2012a) and Sung & Bae, (2000). Unlike enzymes, they are not susceptible to fouling or denaturation, and do not require stable storage conditions.

Over the past years, there have been a number of non-enzymatic techniques of fructose detection focussing on the application of nano-scale metal oxides, noble metal-doped metal oxides, metal oxide-CNTs nanocomposites, and metal oxide-polymer composites. Studies have also proved that simple designs of nanostructured metal oxide films were cost-effective, highly sensitive (due to the contribution of large surface-to-volume ratio of the nanostructure), and in addition exhibited excellent selectivity when combined with bio-molecules (Huang & Wan, 2009; Zhai *et al*., 2009; Liu, 2008; Sung & Bae, 2000). Metal oxides such as ZnO and CeO_2 have been reported to possess high isoelectric points (IEP), excellent bio-compatibility, and ease of synthesis (Ansari *et al*., 2010a; Ansari *et al*., 2010b). Thus, the catalytic ability of transition metal oxides to detect fructose has been a promising feature for the fabrication of cost-effective and stable fructose sensors.

A non-enzymatic fructose sensor was fabricated based on the electrooxidation of fructose based on the activity of Ni (II)-curcumin catalyst (Elahi *et al*., 2008). In this work, Elahi and co-workers employed a nano-structured Ni (II)–curcumin modified glassy carbon electrode (GCE) in a 0.1 M NaOH electrolyte solution comprising Ni (II)–ammonia complex. Their results indicated that this sensor displayed a wider linear range of 10 µM to 10 mM, as well as a lower limit of detection (LOD) of 0.98 µM. Such a lower detection limit is commendable. Good EIS results were also demonstrated. However, in spite of the excellent catalytic properties of the sensor, issues such as detailed sensor fabrication remain a drawback in the full realisation of the use of the sensor.

Another area of sensor can be seen in the work of Wang *et al*. (2011). Cobalt oxide-doped copper (Cu/Co_3O_4) composite nanofibers (CCNFs) were effectively prepared via electro-spinning followed by thermal treatment processes. The fabricated electrode was then utilised as active catalyst for non-enzymic fructose detection. The electrocatalytic activity of the Cu/Co_3O_4 binary sensor was excellent as revealed by the good sensitivity of 18.988 µA mM^{-1} with an applied potential of + 0.30 V, with a fast response time of 1 second. A current response ranging from 0.01 to 6 mM was observed, coupled with a satisfactory electrode reproducibility and stability. It can be argued that the results might have been influenced by the absorbent nature of Cu/Co_3O_4.

An electrochemical fructose sensor based on the of $LaMnO_3$ was reported by Xu and co-workers (Xu *et al*., 2014).They utilised an electrospinning technique in which the $LaMnO_3$ was electrodeposited on a solid glassy carbon electrode. The sensor had a relatively high sensitity of 1238.5 µ $A.cm^{-2}.Mm^{-1}$.

Zhou *et al*. (2013) studied the use of graphene as a support with the sodium dodecyl benzene sulfonate complexed with cobalt and copper (SDBS/Co-Cu). Their results showed fairly high sensitivity of 932 $\mu AmM^{-1} cm^{-2}$) when applied at a potential of +0.40 V and a linear range of 0.003 – 1 mM of fructose.

The use of nickel has been investigated in depth. Literature from tests carried by Elahi et *al*. (2008) provided for the use in the electrocatalytic sensing of fructose. They used Nickel (II)-curcumin for their test. The use of nanoparticles of nickel has also been investigated by the same author (Elahi *et al*., 2008). Electrodeposition was used in the deposition of the cobalt oxide. However, the detailed sensor fabrication and analyte performances were not studied into detail.

More complex combinations have been dealt with recently in the literature concerning the electrochemical sensing of fructose. An example is the combination of the chitosan-poly (diallyldimethylammoniumchloride)-nano-Prussian blue/nano-Au/4-mercaptophenylboronic acid (CS-

PDDA-nano-PB/nanoAu/MPBA) (Bian *et al*., 2010). The combination, though complex was favoured on the premise that boric acid and its derivatives has the ability to form reversible bonds with the diol group of sugars to form complexes. Thus combined with other metals, boric acid can be useful to form electrochemical transducers in the detection of fructose. The response time of approximately 10 s was relatively satisfactory. A detection limit of 0.022 mM was reported for the fructose concentration in the range of 0.1 – 100 mM. In spite of the superiority of the technique, its use is still under development and in its maiden stages and more has to be done before the sensor can find any commercial value.

Recently, nanomaterials possessing favourable physical and chemical properties have been widely employed as efficient electrochemical sensors (Le & Liu, 2009). Of the nanomaterials, carbon nanotubes have been a strong candidate for their use in electrochemical sensors as they have high electrochemical conductivity, excellent chemical stability, high surface/volume ratio, enhanced mechanical strength and a highly chemically modifiable surface (Ensafi et al., 2012; Yang *et al*., 2010; Le & Liu, 2009). For instance, Shekarchizadeh *et al*. (2013) reported observations of non-enzymatic fructose sensor fabricated using a GCE modified with a copper oxide (CuO)/multiwalled carbon nanotube (MWCNT) nanocomposite. (CuO/MWCNT/GCE). Wide linear fructose detection was possible as suggested by the range of 0.1 – 20 mM. They reported a LOD of fructose of 0.04 mM. The reproducibility was fairly good, with an RSD of 1.9 %. An argument given for that was the fact that the catalyst was not easily deactivated by oxidation. The sensor was used in samples as blood serum, and this demonstrated its future potential to be used as a non-enzymatic carbohydrate sensor. The sensor was novel in that it was able to detect both fructose and glucose, since fructose and glucose are structurally related to one another, and they are isomers of each other. Fructose and glucose co-exist, and therefore the work was innovative in itself (Shekarchizadeh *et al*., 2013).

Electrodes coated with metal oxides have undergone intensive study with regard to modification of their surface properties in which the materials can be utilised as efficient electrocatalyst for the oxidation of reducing sugars on the electrode surfaces (Elahi *et al*., 2008). These metal oxide based non-enzymatic sensors are interesting due to their ability of electrocatalytic oxidation of both organic and inorganic materials. Of these metal oxides, cobalt oxides namely cobaltic oxide (Co_2O_3), cobaltous oxide (CoO), and cobaltosic oxide (Co_3O_4), are increasingly gaining momentum in sensor applications (Monk & Ayub, 1997). Studies have also demonstrated that these oxides of cobalt can be deposited on the electrode surfaces by methods such as hydrothermal deposition (Wang *et al*., 2011), electrochemical radiation (Koza *et al*., 2012), electroprecipitation (Polo da Fonseca *et al*., 1994), electrodeposition (Casella, 2002), spray deposition (Patil *et al*., 1998), sol-gel process (Buratti *et al*., 2008) and powder immobilization

(Jiang & Tseung, 1990) to form stable modified electrodes applicable for the amperometric detection of carbohydrates. However, most of these techniques are not commercially scalable and electrodes prepared via these routes exhibit an undesirably low electronic conductance due to low electron transport as well as high contact resistances (Gowda *et al*., 2012;Ding *et al*., 2011), hindering their electrocatalytic efficiency. In addition to this, high vacuum processes such as, plasma sputtering (Arriola & Cordón, 2010), electron beam evaporation (Seike *et al*., 1991), atomic layer deposition (Donders *et al*., 2011) have also been used to deposit $Co_3 O_4$ directly on substrates. Equally, the preparation methods are tedious and require lengthy processing time. Moreover, the involvement of high vacuum equipment in some of the processes requires maintenance and is capital intensive, which hinders the roll out of cheap and efficient non-enzymatic sensors.

Compared to other cobalt oxides, much preference has been placed on Co_3O_4 due to its high specific area and good electrochemical activity (Wang *et al*., 2010; Reitz *et al*., 2008). The use of Co_3O_4 and other binary Co_3O_4/metal in the electrochemical detection of sugars is well appraised in scientific literature, particularly in the detection of glucose (Chowdhury *et al*., 2017). A limited number of studies have been reported on non-enzymatic detection of fructose using Co_3O_4 thin film (Xu *et al*., 2014a; Zhou *et al*., 2013; Arvinte *et al*., 2011; Wang *et al*., 2011;Wang *et al*., 2010). Despite this, the literature surveyed from the previous studies indicated low sensitivity, high detection limit and short linear range for fructose detection.

From this review, **Table 2.1** can thus be constructed for the sensing methods that have been reported so far with the focus on detection methods, electrode material, mode (enzymatic or non-enzymatic) of operation, sensitivity, LOD, response time, and applied bias potential.

Table 2. 1: Enzymatic and non-enzymatic electrochemical sensors utilised in the detection of fructose.

Electrode materials	Electrode preparation route	Supporting electrode	Applied potential V *vs.* Ag/AgCl	Linear range (mM)	Sensitivity ($\mu A.cm^{-2}.mM^{-1}$)	LOD (µM)	Response time (s)	Reference
PVD/CP	-	-	-	-	-	-	-	(Kamitaka *et al*., 2007)
Pt+PCS + PEI	Enzyme immobilisation	Platinum	+ 0.40	3 - 14	0.62±0.10	0.65	18 - 25	(Trivedi *et al*., 2009)
CNTP/FDH/3,4 DHB	Enzyme immobilisation	CNTP	-	0.005 – 2.0	-	1	-	(Antiochia *et al*., 2004)
SPFCE	Enzyme immobilisation	Screen Printed Carbon	+ 0.25	0.1 - 1	1.25 ± 0.02	0.05	-	(Biscay *et al*., 2012b)
FHD/Carbon Paste	Enzyme immobilisation	Carbon Paste	-	0.2 – 20 0.5 - 15	15 ± 2	35 115		(Paredes *et al*., 1997)
SDBS/GR/CuO–Cu	Electrodeposition	Graphene	+ 0.4	0.003 - 1	932		1	(Zhou *et al*., 2013)
$LaMnO_3$	Electrospinning	Glassy Carbon	+0.60	0.4 – 4	1238.5	63	15	(Xu *et al*., 2014)
CS–PDDA–nano-PB	Simple solution casting	Glassy Carbon		0.1 – 0.5 0.5 - 100	-	0.022	10	(Bian *et al*., 2010)
SDBS/Co-Cu	Electrodeposition	Graphene	+0.40	0.003 - 1	932	-	<1	(Zhou *et a*l., 2013)
CuO/MWCNTs	Solution step calcination	Glassy Carbon Electrode	-	0 - 30	-	4	-	(Shekarchizadeh *et al*., 2013)
CNT- NiCo-oxide	Simple deposition	Screen-printed	+0.35	0.02 – 0.675 0.675-12.12	2.5±0.8 1.08±0.009	9.5	-	(Arvinte *et al*., 2011)
CuO/Co_3O_4	Electrospinning	Glassy carbon	+0.30	0.01-3	18.988	3	1	(Y. Wang *et al*., 2011)
Au/Co	Electrochemical & hydrothermal	Au	+0.26	0.001– 0.01	12.5	0.005	<1	(Lang *et al*., 2013)
Nano-Ni(II)-curcumin	Electrodeposition	Glassy Carbon	+0.70	0.01-0.10	8.8285	≈0.98	~10	(Elahi *et al*., 2008)
CS–PDDA–nano-PB/nano-Au/MPBA	Solution casting	Glassy Carbon	+0.5	-	70	10	~10	(Bian *et al*., 2010)

2.5 Electroanalytical techniques

Electrochemistry has become one of the most sensitive and helpful analytical techniques which can be used by chemists (Labib *et al*., 2016; Urdea *et al*., 2006; Baird, 1993). Electroanalytical methods such as cyclic voltammetry, stripping voltammetry, differential pulse polarography, square wave and chronoamperometry complement other analytical techniques such as chromatography and spectroscopy. They are not only capable of assaying trace concentrations of an electroactive analyte, but also supply useful information concerning its physical and chemical properties (Bonfilio *et al*., 2010). Electrochemical methods of analysis include all methods of analysis that measure current, potential and resistance and relate them to analyte concentration (Riu *et al*., 2006). Quantities such as oxidation potentials, diffusion coefficients, electron transfer rates, and electron transfer numbers can be readily obtained using electroanalytical methods which would have been difficult to obtain using other electrochemical techniques (Rassaei, 2008; Bergren, 2006). Perhaps, the most popular electroanalytical techniques are cyclic voltammetry and square wave voltammetry (Pavinatto *et al*., 2015). This section describes the basic components of the modern electroanalytical system, the principles of cyclic voltammetry and square wave voltammetry.

2.5.1 Basic components of an electroanalytical system

Commercial instrumentation for controlled-potential experiments has been recently developed and is currently in use (Bard & Zoski, 2000).The basic necessities include a cell (with a three electrode system), a voltammetric analyzer (consisting of potentiostatic circuitry and a voltage ramp generator), and an X-Y-t recorder (or plotter).Three electrode cells (**Figure 2.1**) are commonly used in controlled-potential experiments.

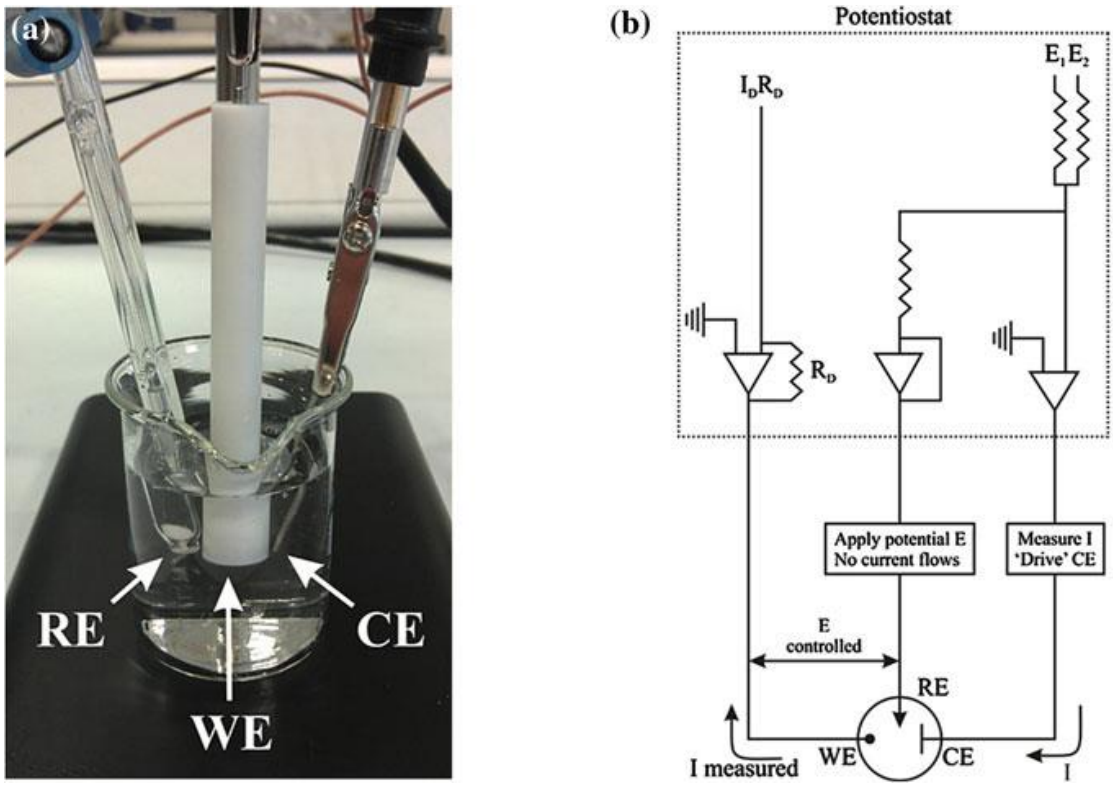

Figure 2.1: (a) A typical experimental set-up showing the reference electrode (RE),the working electrode (WE) and the counter electrode immersed into an electrolyte solution.

(b) A simple electronic scheme equivalent to the electrochemical cell (Brownson & Banks,2014)

The cell is usually a covered beaker of 5 – 50 ml volume, and contains the three electrodes (working, reference, and auxiliary), which are immersed in the sample solution. The working electrode is the electrode at which the reaction of interest occurs. Commonly used materials for working electrodes include platinum, gold or glassy carbon and in this case fabricated conductive cellulose paper is used as a working electrode; the reference electrode provides a stable and a reproducible potential (independent of the sample composition), against which the potential of the working electrode is compared. Such buffering against potential changes is achieved by a constant composition of both forms of its redox couple, for example Ag/AgCl reference electrode. To minimize contamination of the sample solution, the reference electrode may be insulated from the sample through an intermediate bridge. An inert conducting material, such as a platinum wire or graphite rod, is usually used as a current carrying auxiliary electrode

(Gasana *et al*., 2000). At the onset, an electrochemical cell usually consists of a working electrode and reference electrode. The working electrode (WE) facilitates the transfer of electron to and from the electrolyte while the reference electrode (RE) is used as a standard to indicate the potential of the working electrode. Using this two-electrode structure, it is extremely difficult for an electrode to maintain a constant potential while passing current to counter redox events at the working electrode. To solve this problem, a third electrode called auxiliary or counter electrode (CE) has to be introduced to pass or sink all the current needed to balance the current observed at the WE. Thus in a three electrode system, the RE only acts as a reference in measuring and controlling the working electrodes potential and at no point does any current pass through it. The auxiliary electrode acts as a sink for electrons so that current can be passed from the external circuit through the cell. Reactions occurring at the counter electrode surface are unimportant as long as it conducts current well. The basic components of a modern electroanalytical system for voltammetric measurements are a potentiostat, an electrochemical cell and a computer. The role of the potentiostat is to apply accurate and controlled potential and monitor the current produced. In this three-electrode system, voltage is carefully regulated between the working and the reference electrodes, while the current passes between the working and the counter electrode. It is noteworthy that at no time does current pass through the reference electrode; this is ensured by the use of a potentiostat.

2.5.2 Voltammetry Techniques

Voltammetric techniques are characterized by the application of the potential *E* to an electrode and the monitoring of the resulting current *i* flowing through the electrochemical cell (Wu *et al*., 2008). The applied potential is varied or the current is monitored over a period of time *t.* Thus, voltammetry can be broadly defined as the exploration of the three-dimensional space that relates potential (*E*), current (*i*), and time (*t*). The term "voltammetry" was first introduced to describe experiments in which the current as a function of potential at a solid working electrode is measured and this field of study has undergone tremendous changes to date (Batchelor-Mcauley *et al*., 2015). The basic components of a modern electroanalytical system for voltammetry are a potentiostat, computer and an electrochemical cell. The general theory of voltammetry is stabilised on the effect of the applied potential and the behaviour of the redox current, which are described by several well-known laws. As summarized by Bard and Zoski (2000) the applied potential controls the concentrations of the redox species at the electrode surface C_O^0 and C_R^0 and the rate of the reaction k_0 as described by the Nernst or Butler–Volmer equations, respectively. In cases where diffusion plays a controlling part, the current resulting from the redox process (known as the Faradaic current) is related to the material flux at the electrode–solution interface

and is described by Fick's law. The interplay between these processes is responsible for the characteristic features observed in the voltammograms of the various techniques. A reversible electrochemical reaction (that is, a reaction so fast that equilibrium is always re-established as changes are made), can be described by the redox equation:

$$O + ne^- \rightarrow R \qquad \text{Equation 2.2}$$

where O is the oxidized species and n is the number of electrons transferred in the redox reaction, and R is the reduced species.

The application of a potential *E* forces the respective concentrations of O and R at the surface of the electrode i.e. C_O, C_R a ratio in compliance with the Nernst equation:

$$E = \frac{(E^0 - RT \ln C^0{}_O)}{nFC^0{}_R} \qquad \text{Equation 2.3}$$

where R is the molar gas constant (8.314 J mol^{-1} K^{-1}), T is the absolute temperature (K), n is the number of electrons transferred, F the Faraday constant (96,485 C mol^{-1}), and E^0 is the standard reduction potential for the redox couple. A change in the applied potential affects the ratio of C_O, C_R at the electrode surface since it is at equilibrium, and the ratio will adjust to satisfy the Nernst equation. A shift in the potential applied toward the negative will cause reduction while a positive shift will cause oxidation.

Apart from the actual electron transfer that occurs at the electrode interface, mass transport can also determine the faradaic current or general electrochemical rate. This is why we say an electrode process can be kinetically controlled or diffusion controlled. Diffusion, which is one of the means of mass transport (the others are migration and convection) is usually governed by Fick's law, which states that the flux of matter Φ is directly proportional to the concentration gradient and is given by:

$$\phi = -D_O\left(\frac{dC_O}{dx}\right) \qquad \text{Equation 2.4}$$

where D_0 is the diffusion coefficient of O and *x* is the distance from the electrode surface.

2.5.3 Cyclic Voltammetry

Cyclic voltammetry is the first and currently the *de facto* technique used for acquiring qualitative information about electrochemical reactions (Wang *et al*., 2008). This is a type of potentiodynamic

electrochemical measurement, which offers rapid identification of redox potentials that are characteristic of the electroactive species under study, and provide significant information about the thermodynamics of a redox process, kinetics of heterogeneous electron-transfer reactions and the analysis of coupled electrochemical reactions or adsorption processes (Astruc, 2012). In particular, it offers a rapid location of redox potentials of the electroactive species, and convenient evaluation of the effect of media upon the redox process.

Figure 2.2 illustrates cyclic voltammetry, which comprises a linear scanning of the potential of the working electrode using a triangular potential waveform.

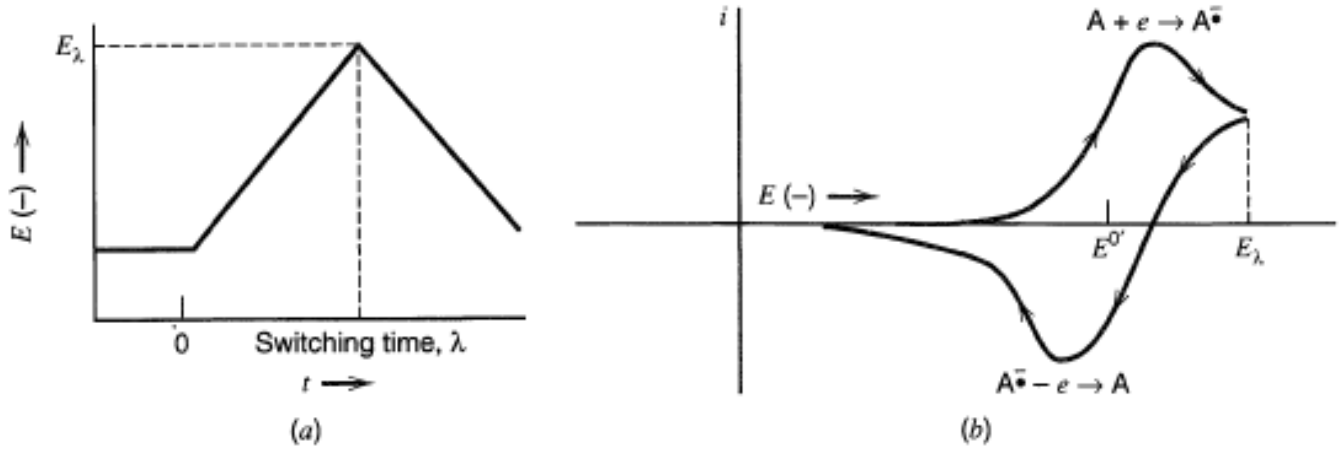

Figure 2. 2: Potential time (E-*t*) profiles used to perform linear sweep and cyclic voltammetry (Hess, 2010)

The potential is swept from E_1 to some potential E_λ and the rate at which this is achieved is the voltammetric scan rate (or the gradient of the line, V/s), as presented in the illustration. In this case, if the potential is stopped, this is known as a linear sweep experiment. As the scan is returned to E_1, a full potential cycle is obtained, which is referred to as cyclic voltammetry. Depending on the information sought, either single or multiple cycles can be performed (Bard & Faulkner, 2001). For the duration of the potential sweep, the potentiostat measures the resulting current that arises via the applied voltage (potential). The plot of current versus potential (voltage) is termed a 'cyclic voltammogram', CV. A

cyclic voltammogram is complex and dependent on time along with many other physical and chemical properties.

Figure 2.3 depicts how the concentration profiles and surface concentrations change during the voltammogram. Point A on the graph corresponds to the formal potential ($E = E_f^{\,0}$).The peak size and peak potential seen on the forward and backward scan reflects the reversibility of reaction.

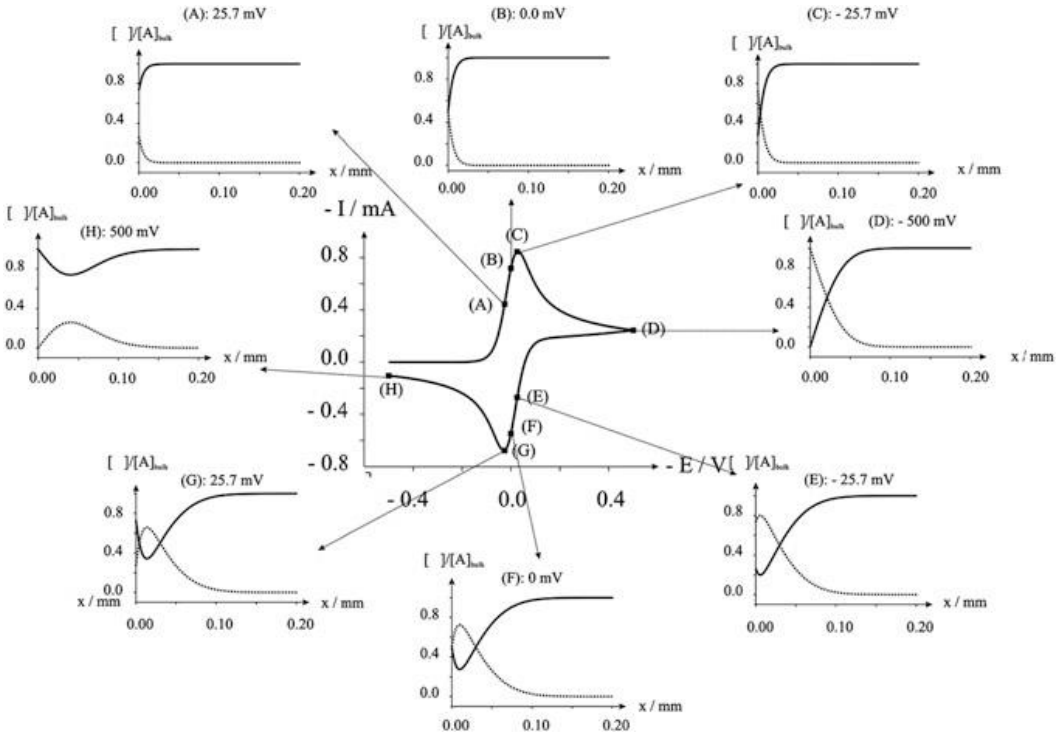

Figure 2. 3: Cyclic voltammogram for a reversible reduction of A to B (Compton & Banks, 2007)

At point A, prior to the start of the peak corresponding to the reduction of A, only a small amount of A has been consumed at the electrode surface and only a small layer of B has consequently built up. This diffusion layer is relatively small, typically in the order of around 10 μm. At point C the maximum reduction current in the voltammetry wave is evident and the diffusion layer has increased in thickness.

At point D the current is decreasing with increasing potential; the concentration profile plot shows the concentration of A at the electrode surface to be close to zero so that this part of the voltammogram is under diffusion control, whereas at (A) it is the electrode kinetics which controlled the response. The diffusion layer at this point has reached a thickness of approximately 40 μm. At point D, the direction of the voltammetry scan is reversed. At point F the working electrode potential has the value of 0 V corresponding to the formal potential of the A/B couple. At this point the electrode potential is insufficient to noticeably reduce A or oxidize B. Point G corresponds to the peak in the reverse scan due to the re-conversion of B to A. The concentration profiles show the build-up of A and depletion of B. Point H corresponds to a point on the reverse peak beyond the maximum G and shows that the concentration of B is very close to zero at the electrode surface whilst that of A has returned to almost its original value nearly that in the bulk solution.

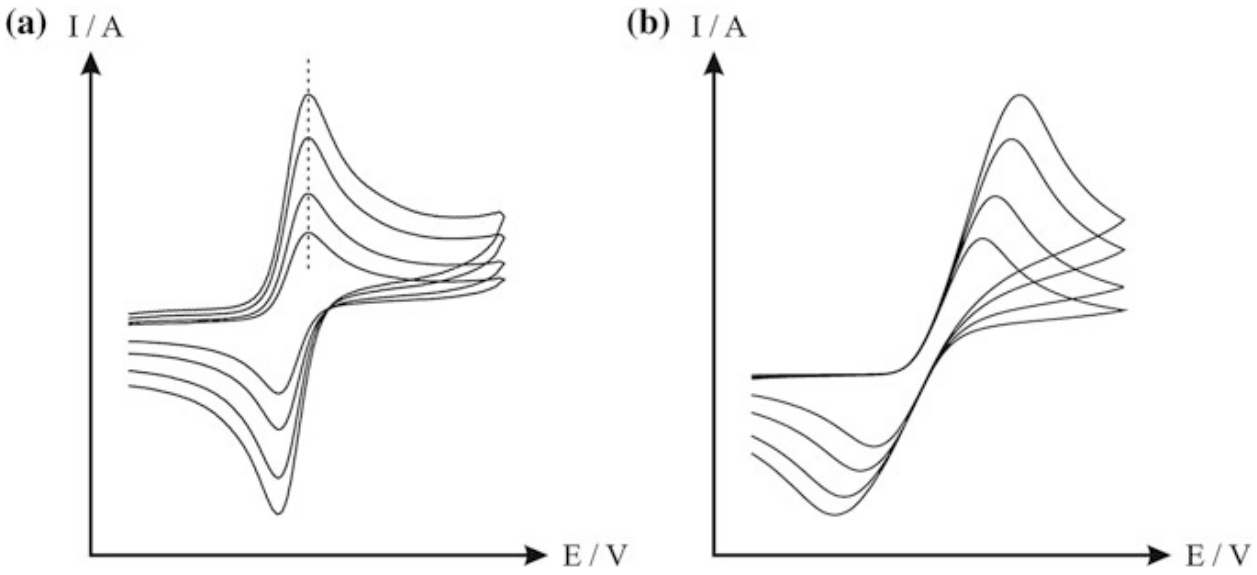

Figure 2. 4: (a) Reversible and (b) irreversible cyclic voltammetry responses (Bard & Faulkner, 2000)

It is evident that each voltammetric signature is the same but that the current increases with increasing scan rate. A point worth noting is when the position of the maximum current occurs at the same potential; this peak maximum, which does not shift in potential with scan rate, is characteristic of electrode

reactions which exhibit rapid electron transfer kinetics, usually termed reversible electron transfer reactions.

For reversible reaction, the concentration is related to peak current by the Randles-Sevčik equation (at 25 °C) (Neghmouche & Lanez, 2013):

$$I_p = 2.69\times10^5 n^{\frac{3}{2}} A D^{\frac{1}{2}} v^{\frac{1}{2}} C \qquad \text{Equation 2.5}$$

where I_p is the peak current (A), v is the potential scan rate (V/s), A is the electrode area (cm^2), n is the number of electrons transferred, D is the diffusion coefficient ($cm^2\ s^{-1}$), and C the concentration (mol cm^{-3}). Accordingly, the current is directly proportional to concentration and increases with the square root of the scan rate. Such dependence on the scan rate is indicative of electrode reaction controlled by mass transport (semi-infinite linear diffusion). For, instance, when the peak current is plotted against the square root of the scan rate, the slope of the linear plot can be used to estimate the diffusion coefficient according to the Randles-Sevčik, equation.

For an irreversible reaction, which displays a sluggish electron exchange, the individual peaks are reduced in size and are widely separated. A totally irreversible electron reaction is characterised by a shift of the peak potential with the scan rate:

$$E_p = E_o - \frac{RT}{\alpha n_a F}\left(0.78 - \ln\frac{k^o}{D^{\frac{1}{2}}} + \ln\left(\frac{\alpha n_a F v}{RT}\right)^{\frac{1}{2}}\right) \qquad \text{Equation 2.6}$$

where α is the transfer coefficient and n_a, is the number of electrons involved in the charge transfer step. Thus, E_p occurs at potentials higher than $E°$, with the over-potential related to $k°$ and α. Independent of the value $k°$, such peak displacement can be compensated by an appropriate change of the scan rate. The peak potential and the half-peak potential (at 25°C) will differ by $48/\alpha n$ mV. Hence, the voltammogram becomes more drawn-out as αn decreases.

The peak current is given by:

$$I_{pc} = (2.99\times10^5) n(\alpha n_a) A C D^{\frac{1}{2}} v^{\frac{1}{2}} \qquad \text{Equation 2.7}$$

When plotted, the log of peak current versus the log of scan rate gives a linear plot whose slope distinguishes between diffusion controlled peaks, adsorption peaks or even a mixture of the two. At plot of the log I_p versus log *v* there is linearity, in which a slope of 0.5 for a diffusion peak and a slope of 1 for an adsorption peak is obtained. Intermediate values of the slope are sometimes observed, suggesting a mixed diffusion-adsorption peak. In some cases, the sample to be characterized may be deposited on the surface of the electrode (chemically modified electrodes). In such cases, the surface concentration of the adsorbed material can be estimated by the use of the Brown-Anson equation (Brown & Anson, 1977):

$$I_p = \frac{n^2 F^2 \Gamma A v}{4RT} \qquad \text{Equation 2.8}$$

where Γ represents the surface coverage concentration (mol/cm^2), *v* is the scan rate (V/s), A is the electrode surface area A (cm^2) , I_p is the peak current (A), n is the number of electrons per reactant molecule, and F is the Faraday constant.

2.5.4 Chronoamperometric studies

Chronoamperometry methods have been utilized in assessing the sensor performance using stepping-potential techniques where the transient response from the cell current is recorded (Kamat *et al*., 2010). A step potential is applied and the current, *i*, is measured as a function of time, *t*. The current-time (*i*-*t*) comprises two elements: the current due to charging the double-layer, and current due to the electron transfer reaction with the electroactive species. The occurrence of the double-layer charge and the electron transfer reaction depends on the initial and final applied potentials. The technique is employed under stirred conditions at a constant applied potential over a determined period of time. Although the method is excellent at handling qualitative analysis, it is generally not very efficient at the handling of capacitive current.

To accomplish the measurement of capacitative current, the cell voltage is stepped down from open circuit voltage (OCV) to lower than 0.2 V. The corresponding transient cell current can be described by Equation 2.8:

$$i_{cell} = i_d + i_{cap} \qquad \text{Equation 2.8}$$

where i_{cell} is the total current, i_d is the diffusion limiting current, and i_{cap} is the capacitative current. In such cases the Cortell equation for diffusion limiting current is applied to the system:

$$i_d(t) = \frac{nFAD_{O_2}^{\frac{1}{2}} C_{O_2}}{\pi^{\frac{1}{2}} t^{\frac{1}{2}}} \qquad \text{Equation 2.9}$$

where π is the number of electrons transferred in one electrochemical reaction step,F is the Faraday constant, A is the active electrode area, D is the diffusion coefficient of oxygen in electrolyte, C is the initial bulk concentration of oxygen in electrolyte, and *t* is time.

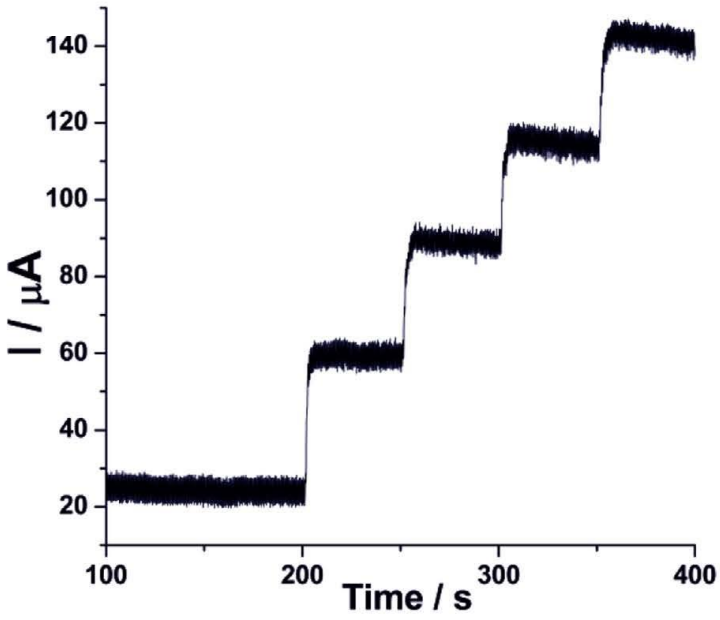

Figure 2. 5: A typical chronoamprogram for an addition of analyte (shown are four step additions) (Neiva *et al*., 2016)

2.5.5 Electrochemical Impedance Spectroscopy (EIS) Studies

Electrochemical Impedance Spectroscopy (EIS) has been applied in many fields such as corrosion analysis, electrode interfacial behaviour (adsorption of molecules), and also in batteries and fuel cells (He

& Mansfeld, 2009; Gomadam & Weidner, 2005). The EIS measurement is a simple procedure usually conducted with the help of a Frequency Response Analyser (FRA) coupled to a potentiostat (Fasmin & Srinivasan, 2017). Consequently, the term impedance is defined as the complex ratio of the voltage and current in an AC circuit (MacDonald, 2006) which is expressed mathematically as:

$$Z(j\omega) = \frac{V(j\omega)}{I(j\omega)} \qquad \text{Equation 2.10}$$

where Z is the impedance, V is the applied voltage, *I* is the current, *j* is the imaginary component and ω is the frequency. In its correct term, impedance applies to the opposition force against an electrical current in a circuit and has the same units as electrical resistance, Ω. However resistance differs from impedance because resistance obeys Ohm's law, and is observed in DC circuits where the resistance is technically the impedance with zero phase angle, since the current is not alternating. The concept of resistance can only be applied in an AC circuit if certain criteria are met: i) the AC voltage and current must be in phase with each other; ii) the resistance is frequency-independent; and iii) the resistance can be applied to all currents and voltages. Unfortunately, in the vast majority of cases the phase angle is not equal to zero, as capacitative and/or inductive effects are observed at almost all frequencies, hence a more general principle must be used to account for frequency-dependence; the concept of impedance essentially allows a quantitative representation of the opposition force to electrical current in these cases (as in AC circuits).

In an EIS experiment, a fixed sinusoidal voltage is applied by a potentiostat across a three- electrode cell containing a solution of electrolyte that contains the molecule under investigation. It is also agreed that the amplitude and load (*i.e.* magnitude of the voltage) of the fixed sinusoidal voltage is dependent upon the type of molecular system under investigation (Kandalkar *et al*., 2008). In essence, biological molecules are subjected to smaller applied voltages than non-biological ones as the biological molecules are easily denatured at slightly high potentials. An EIS experiment is commonly carried out by constructing a composite upon the electrode surface which will attract target analytes and thus affect the conductivity of the system through either a blocking or a molecularly wired admittance mechanism. In cases such as these it is common for impedance measurements to be performed in a blank buffer solution or a known redox probe (such as potassium ferricyanide (II) ($K_4Fe(CN_6)$ (Brownson *et al*., 2012) or hexamine-ruthenium (III) chloride ($Ru(NH_3)_6Cl_3$) (Randviir *et al*., 2012) after the composite and target analyte has been assembled upon the electrode surface. When the load is applied at a set frequency, a current will flow through the electrochemical cell which is recorded by the potentiostat and converted by the software into an impedance value with a real and an imaginary component. This process is repeated

across a frequency range where different values are deduced for the real and imaginary components of the overall impedance value. The frequency ranges usually from 100 KHz to 1 mHz, and a small AC signal of amplitude 5 or 10 mV is usually applied to analyse the current response of the circuit without disturbing its operation (a large potential well).

The impedance data can be presented in a variety of ways. For instance real and imaginary impedance components are plotted against one another in Nyquist plots (**Figure 2.6**) which have to be interpreted properly to deduce solution resistances, charge transfer resistances, and Warburg impedance, as well as time constants. In Bode plots, however the impedance and phase angle is plotted against frequency which can be helpful to find capacitative or inductive effects of electrochemical systems (**Figure 2.7**).

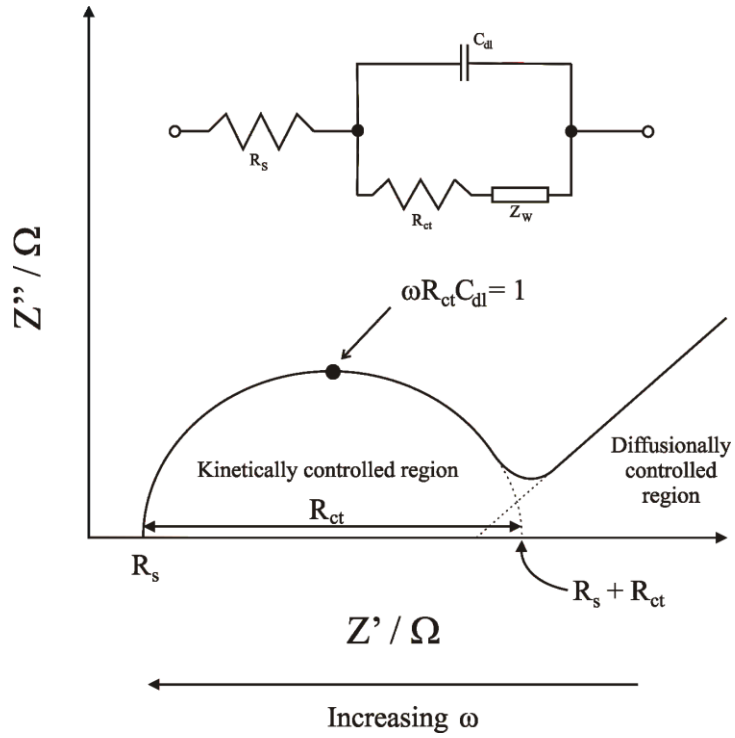

Figure 2.6:A simplified Nyquist plot with a Randles equivalent circuit for a typical electrochemical cell (Randviir & Banks, 2013)

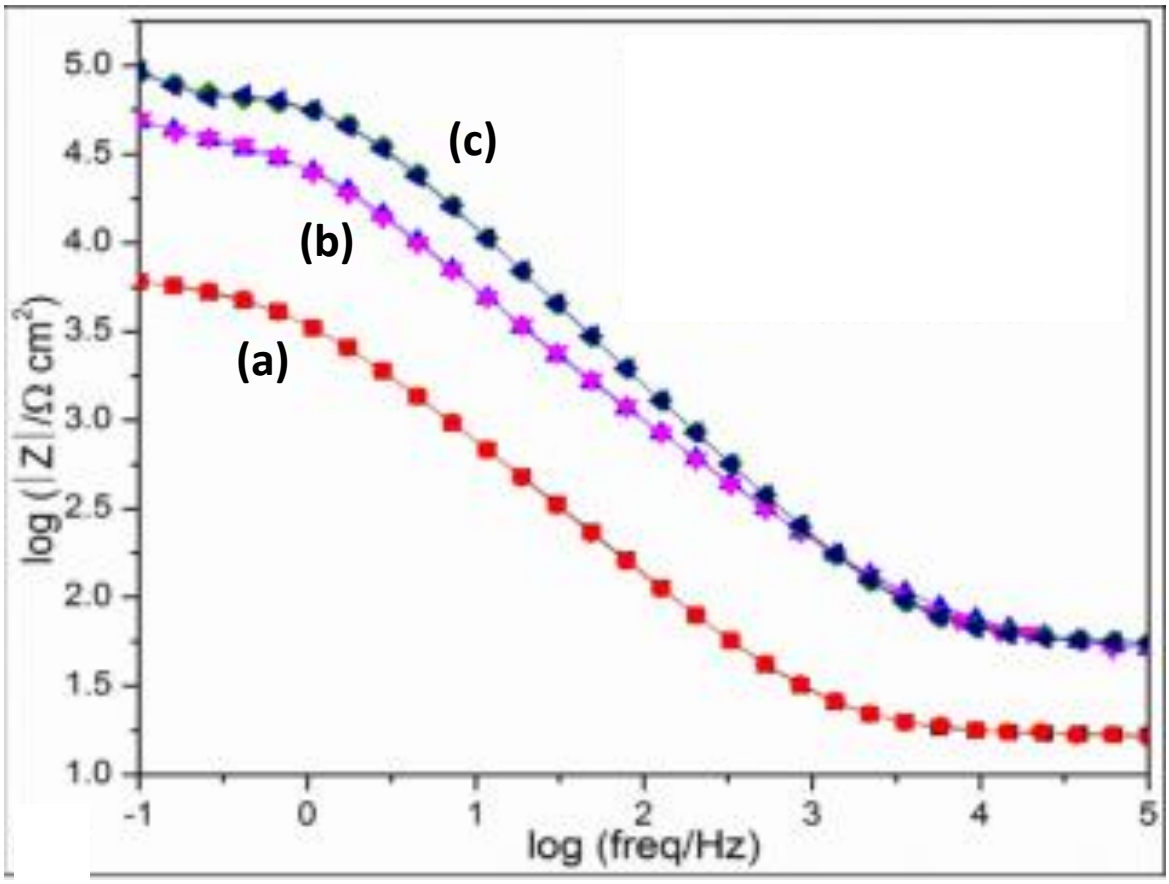

Figure 2.7: A Bode plot showing the logarithmic frequency and frequency for a number of layers a, b and c (Vora *et al*., 2013)

The application of layers of chemicals, polymers, or coatings to electrodes (to form composite electrodes) has been known to provide useful enhancements in terms of electron transfer and sensitivity (Li *et al*., 2009). For instance, (Yang *et al*., (2012) and Gao *et al*. (2012) established that the effects of these different layers and coatings can be identified using EIS, including electrochemical contributions from polar, ionic and dielectric relaxation processes in the electrolyte system as well as within the electrode, at the electrode surface and within the double-layer region. Using the same method, it was found possible to investigate key parameters of an electrochemical system such as exchange-current densities, charge-transfer resistances and double-layer capacitances.

Equations 2.11 and 2.12 describe the real and imaginary impedances the Nyquist plot from an EIS experiment,

$$Z' = R_S + \frac{R_{ct}}{1+\omega^2 R_{ct}^{\ 2} C_{dl}^{\ 2}} \qquad \text{Equation 2.11}$$

and

$$Z'' = \frac{R_{ct}^{\ 2} C_{dl} \omega}{1+\omega^2 R_{ct}^{\ 2} C_{dl}^{\ 2}} \qquad \text{Equation 2.12}$$

where Z' and Z' are the observed impedances due to the real and imaginary parts respectively, R_s is the solution resistance, R_{ct} is the charge transfer resistance, ω is the angular frequency and C_{dl} is the double layer capacitance. Furthermore, the capacitance and inductance are related to current and voltage *as* reflected in Equations 2.13 and 2.14:

$$I = CV \qquad \text{Equation 2.13}$$

$$I = VjL \qquad \text{Equation 2.14}$$

where I is the current, j is the imaginary quantity, C is the capacitance, V is the voltage, and L is the inductance. Hence, from Equation 2.15 the relationship of impedance function, $Z(j\omega)$, in terms of capacitance or inductance can be expressed as:

$$Z(j\omega) = \frac{1}{C} = L \qquad \text{Equation 2.15}$$

The total impedance of an EIS circuit connected with a number of components can be represented with a relationship similar to Ohm's Law by the summation of the impedances of each component (impedance components in series):

$$Z_{TOTAL} = Z_1 + Z_2 + Z_3 ... Z_x \qquad \text{Equation 2.16}$$

The Warburg Element describes the diffusion of the ions in solution in an electrochemical reaction (Skale *et al*., 2007). For instance, at high frequencies, Warburg impedance is not observed as migration occurs over much longer time periods than the operational frequency and thus a slow diffusion of molecules in solution suppresses the effect of the impedance (Zaban *et al*., 1996). Hence, Warburg effects are generally observed in the low frequency region. The right hand side of **Figure 2.6** illustrates the diffusional

controlled region of a Nyquist plot obtained using EIS. The solution resistance is independent of the frequency and is observed at the highest frequency where the real axis is intersected (R_s). The charge transfer resistance (R_{ct}) is the opposition experienced to electron movement and is a real quantity. The R_{ct} as observed at the second extrapolated intersection with the real axis in the mid- to low-frequency region is marked as the kinetically controlled region of the Nyquist plot and is related to the heterogeneous electron transfer rate constant, k_0, by following Equation 2.17 for a simple one electron process:

$$R_{ct} = \frac{RT}{F^2 k^0 C} \qquad \text{Equation 2.17}$$

where R is the molar gas constant, T is the temperature, F is the Faraday constant and C is the concentration of the electroactive species.

In order to enhance understanding of the different components contributing to the overall impedance of the circuit, EIS circuits simplified into circuit diagrams are employed for computer simulations of impedimetric systems (Grieshaber *et al*., 2008). For instance, in an electrochemical experiment, the impedance will arise from the solution resistance (R_e), double layer charging at the electrode surface (C_d), charge transfer resistance (R_{ct}), and the Warburg Element (Z_w). A combination of these elements is known as a Randles circuit (Macdonald, 1987) and such circuits are conveniently utilised to simulate EIS experiments. The double layer capacitance (C_{dl}) can be roughly estimated by the Z''_{max} of the semi-circle. The capacitative element of an electrochemical cell is often represented by a constant phase element (C_{PE}) which, simply put, accounts for factors which affect the capacitance of a system like surface heterogeneities resulting in differing reaction rates upon the surface which introduces multiple time constants (Wang & Pilon, 2012).

2.6 Conclusions

In view of the importance of the sugars like fructose in body fluids (like blood serum, urine) and the food and beverage industries, a great deal of continuing research is needed to develop a rapid detection and quantification of fructose in these samples. It would be imperative to have a detection method that is simple, fast and sensitive which could be effectively used in these areas. A comprehensive overview on the different electrochemical sensors has been presented, highlighting the necessity of conducting such a study. To date, some authors have recently tried to use enzymes in the fabrication of electrochemical

sensors using well-documented procedures. As pointed out, while enzymes are highly specific, their preparation and preservation is still a prominent challenge. The features and previous works regarding non-enzymatic fructose sensors and their limitations have been discussed. The application of metal oxides as catalysts for fructose oxidation on electrode surfaces has been presented.

It has also been demonstrated that both electrode surface and substrate both affect the transfer of electrons from the solution to the electrode surface. This therefore highlights these remarkable differences.

The properties of the electrochemical sensors seem to be strongly dependent upon the chemical structure of the thin film and the groups that are embedded on the support. Metals and CNTs provide more stable potential and influence the transport of electrons on electron-solution interface.

The interest in such highly efficient sensors is that they have numerous potential technological applications in the food and beverages industries and in medicinal practices. It is thus, justified and useful to research the development of low cost and disposable sensors for the detection of fructose for analysis purposes. It is proposed that a simple fructose sensor based upon a Co_3O_4 thin film on FTO glass electrode should offer a cost-effective, portable and disposable alternate method for fructose detection.

Chapter 3

EXPERIMENTAL METHODOLOGY

3.1 Introduction

Having studied the various methods of detecting fructose, it appears that electrochemical methods utilising cobalt oxide are an attractive approach in the detection of fructose. **Section 3.2** is a description of the experimental procedures that were used to carry out the characterisation of the Co_3O_4 thin film on FTO glass electrode. Transparent FTO substrates have been commonly used as conductive electrodes (Jasiecki *et al*., 2013). A summary of the experimental work is given in **Section 3.3**.

3.2 Materials and methods

3.2.1 Reagents and chemicals

All the reagents and chemicals used in this work were of the analytical reagent grade and were used as received without any further purification. D (-) fructose ($C_6H_{12}O_6$), Sodium Hydroxide pellets (NaOH) (99.9%), Phosphate Buffer Solution (PBS, pH 7.4), Toluene ($C_6H_5CH_3$), Ethanol (C_2H_5OH), Ascorbic acid (AA), D(-) Glucose ($C_6H_{12}O_6$), Uric Acid (UA), Acetaminophen (AC), Sodium Chloride (NaCl), Potassium Chloride (KCl), Potassium Ferricyanide Trihydrate ($K_4Fe(CN)_6.3H_2O$) were all obtained from Sigma-Aldrich, South Africa. Deionised water (18.2 MΩ) purified by the Purite™ system was used for all aqueous solution preparations.

3.3 Surface morphology of the thin film Co_3O_4 FTO glass electrode

Direct determination of the crystal structure of the electrodes was achieved by XRD. The X-ray patterns of the electrodes were recorded using a PANalytical X'pert PRO PW 3040/60 diffractometer. An FEI Tecnai F20 TEM operated at 200kV, equipped with a Gatan GIF-2001 energy filter was utilised to extract High-Resolution Transmission Electron Microscopy (HR-TEM) images, Selected Area Electron Diffraction (SAED) data. Atomic Force Microscopy (AFM) was used to analyse the surface roughness of the thin film electrode. The AFM measurements were carried out in air under ambient conditions with a commercial Agilent 5500 AFM (Agilent Technologies, USA) in the contact mode at a scanning rate of 1 line per second.

3.3.1 X-diffractometry (XRD)

An X-ray powder diffraction provides information regarding the crystal size and the disorder, structural parameters (i.e. unit cell edge lengths), degree of isomorphous substitution and surface area (Han,2001).The ordered arrangement of a crystal atom is described by a number of symmetry elements. The position of any plane of atoms within the crystal can be characterised by the intercepts the plane makes with the stem axes. These intercepts are usually expressed as their reciprocal value, *hkl* (Miller indices), and thus converted into smaller integer numbers. The interaction of the electromagnetic waves with the atoms of the crystal is observed in the X-ray diffraction (Han,2001).When a monochromatic beam of X-rays is directed towards a crystalline material, the incident X-ray photons interact with the electrons that surround the atoms. The electron clouds scatter the X-rays in all directions. However, at certain angles (θ), the distance travelled by the incident and scattered X-rays differs by a complete number (n) of wavelengths. These directions are related to the distances between atomic planes, the d-vales, and the angle (θ) at which X-rays enter and leave a crystal. The constructive interface of scattered waves is illustrated in **Figure 3.1**:

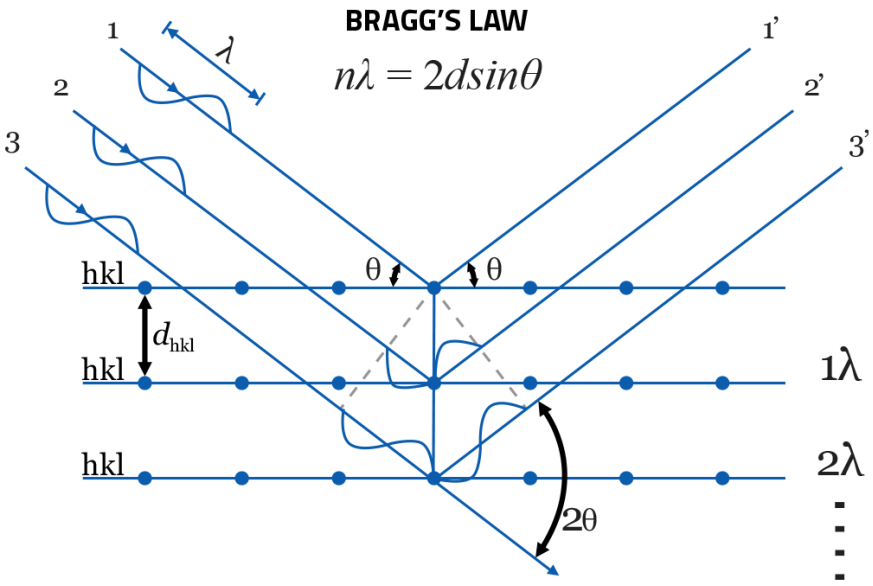

Figure 3. 1:Diffraction of X-rays by crystal lattice (Veqter Technologies,2018)

The relationship is best described by the Bragg equation (Graef & Henry, 2007):

$$n\lambda = 2d_{hkl} \sin\theta \qquad \text{Equation 3.1}$$

where,λ, is the wavelength of the X-rays used,θ,the angle at which the X-rays strike the crystal and for which the maximum interface intensity is observed, and d_{hkl}, the distance between the set of *hkl* planes in the crystal (or lattice spacings).

3.3.2 Transmission electron microscopy

In Transmission electron microscopy (TEM), a beam of electrons is transmitted through an ultrathin specimen (< 100 nm).As the beam passes through the specimen interacts with the specimen. An image is magnified and focused onto an imaging device, such as a fluorescent screen, on a layer of photographic film or detected by a sensor. Only the transmitted beams of some of the forward scattered beams are used in conventional TEM to form a diffraction contrast image. In High-resolution TEM (HRTEM) transmitted

and scattered beams are used to create an interface image. Material preparation is specific to the desired information that needs to be obtained from such a study.

3.3.3 Scanning electron microscopy (SEM)

The Co_3O_4 layers were analysed using Scanning Electron Microscope (SEM).SEM uses a fine electron probe to (7 – 10 nm diameter) to illuminate samples by scanning them with a high-energy beam of electrons in a raster scan pattern (Williams,1984). As illustrated by Han (2001), the electrons interact with the atoms that make up the sample producing signals that contain information about the sample's surface topography, composition, and other properties such as electrical conductivity. Appropriately sized samples are mounted rigidly on a specimen stub. For the SEM, an electron beam is thermionically emitted from an electron gun fitted with a tungsten filament cathode. Tungsten is normally used in thermionic electron guns because it has the highest melting point and lowest vapour pressure of all metals, thereby allowing it to be heated for electron emission. When the primary electron beam interacts with the sample, the electrons lose energy by repeated random scattering and absorption within a teardrop-shaped volume of the specimen known as the interaction volume, which extends from less than 100 nm to ≈5μm into the surface. The size of the interaction volume depends on the electron's landing energy, the atomic number of the specimen and the specimen's density. The energy exchange between the electron beam and the sample, results in the reflection of high-energy electrons by elastic scattering. Several models of SEM can examine any part of a 6-inch (15cm) semiconductor wafer, and some can tilt an object of that size to 45°.For conventional imaging in the SEM, the specimens must be electrically conductive, at least at the surface, and electrically grounded to prevent the accumulation of electrostatic charge at the surface. Non conducting materials are therefore usually coated with an ultrathin coating of electrically conducting material, such as gold, deposited on the sample either by low vaccum splutter coating or by high vacuum evaporation (Suzuki, 2002)..

3.4 Electrochemical experiments

All electrochemical measurements were performed using an Autolab PGSTAT302N potentiostat (Metrohm Autolab, Netherlands) controlled by Nova 2.0 software (**Figure 3.2**). A conventional three electrode setup was used, i.e. a graphite rod as the counter electrode, Co_3O_4 thin film modified FTO as the

working electrode (geometrical area, A = 1 cm^2), and Ag/AgCl (3M KCl) as the reference electrode. All experiments were carried out at temperature of 25±2 ºC. Cyclic voltammetry and chronoamperometry studies were conducted in a 0.1 M NaOH electrolyte solution. Chronoamperometric studies were carried out at applied bias potential of + 0.60 V *vs*. Ag/AgCl.

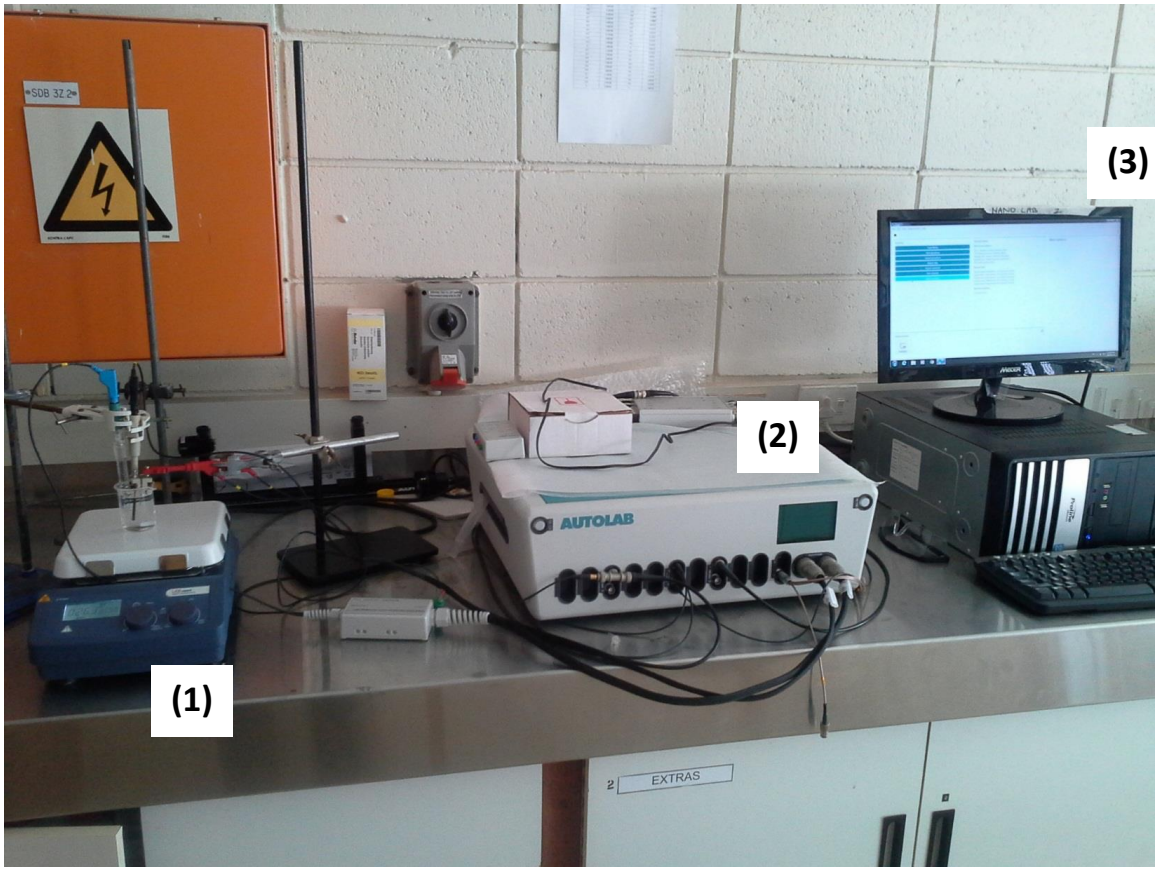

Figure 3. 2: A cell set-up utilised for both cyclic voltammetry and chronoamperometry (1) custom-made 3 electrode cell equipped with a magnetic stirrer,(2) Autolab potentiostat, (3) monitor to display electrical output

Table 3. 1: List of equipment used for thin film preparation and cyclic voltammetry

Instrument Description	Purpose
Autolab Potentiostat 302N	To conduct the cyclic voltammetry tests and chronoamperometry tests
Furnace/Oven	To calcinate the Co_3O_4 on the surface of the FTO electrode
Spin coater	To drop cast the Co_3O_4 on the surface of the FTO by gravity.
Other utilities (water, blown air, balances, stirrers)	To provide stirring, cleaning and heating

3.5 Preparation of FTO glass electrodes

FTO glass strips (surface resistivity~7 $\Omega.m^2/m$) purchased from Sigma-Aldrich, South Africa were prepared. For the removal of the adsorbed particles, such prepared FTO glass strips were pre-cleaned by immersion in a 100 cm^3 Pyrex glass beaker containing a soap solution in distilled water. The beaker with the contents was then placed in a sonicator for 30 minutes at a set temperature of 37 ºC for the removal of the adsorbed particles. For further cleaning of the surfaces, the glass slides were immersed in 100 cm^3 of ethanol and sonicated for 30 min at 37 ºC. The procedure was repeated again using 100 cm^3 distilled water. For drying, the glass slides were air blown and placed in the oven maintained at 60ºC to dry for 8 hrs. Conductive sides of the FTO glass were determined using a multimeter. For the preparation for spin coating, 1 cm^2 area on the conductive sides of the glass slides was marked using transparent tape to demarcate the area of the deposition of the Co_3O_4 catalyst.

3.6 Calcination of thin film Co_3O_4 layers on FTO glass electrodes

For this stage, a two-step spin-coating procedure of a chemical solution as previously described by Chowdhury and co-authors (Chowdhury *et al.*, 2017a and 2017b) was used to deposit the Co_3O_4 film on an FTO glass electrode. For this procedure, solutions of Co_3O_4 were prepared by dissolving 0.09 g of cobalt-oleate ($C_{36}H_{66}CoO_4$), which in turn oxidised to Co_3O_4, in 0.5 cm^3 toluene ($C_6H_5CH_3$) in a 20 cm^3

glass vial. Ultrasonication was carried on for 30 minutes at 30ºC for the complete dissolution of the Co_3O_4 in toluene.

For the calcination procedure, 50 µL of Co_3O_4 solution was spin-coated at 4 000 rpm for 60 s using a spin coater. The FTO glass slide was placed on the rotating table on the air hole. Afterwards, the vacuum pump was turned on, to hold the FTO glass slide securely on the rotating table by the vacuum. The lid was placed on the spin coater, and the spin coater was started. After the coating time had elapsed, the glass slide was then taken out and the tape removed and placed in a preheated oven at 350 ºC for the setting of the Co_3O_4 for 10 mins after which the glass slide was taken out and placed on a tile for cooling for 2 minutes. Repeating the procedure, different numbers of layers were added to the FTO glass (i.e. N = 1, 2…). The final layer was calcinated for 5 hrs. The modified electrodes were stored at ambient temperature (25 ºC) before being used in experiments. **Figure 3.3** is schematic illustration of the deposition of Co_3O_4 thin film on a FTO glass electrode.

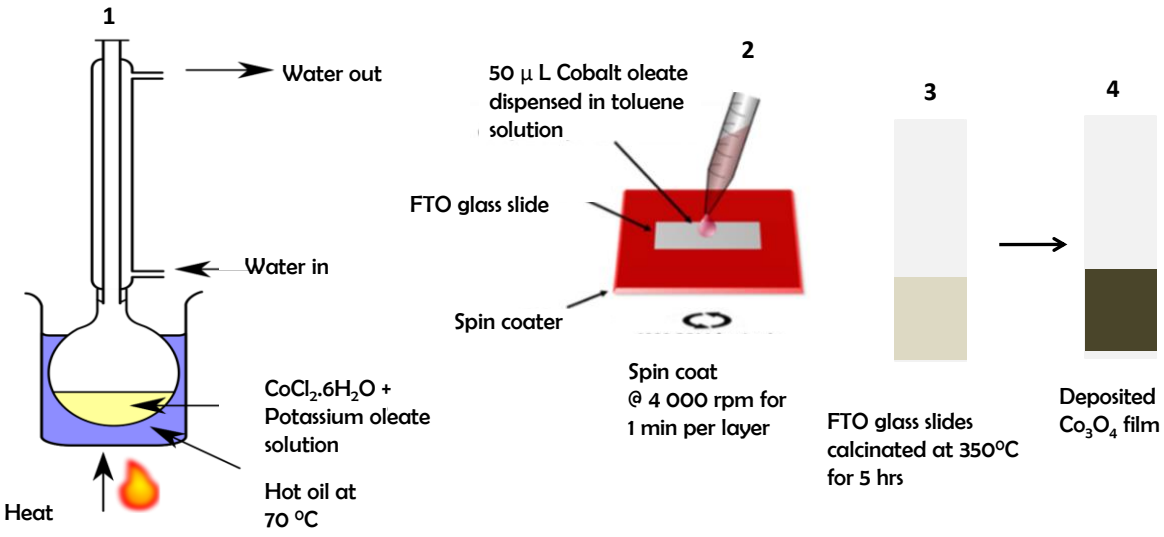

Figure 3. 3: Schematic diagram of the solution step electrode fabrication of Co_3O_4 thin film on FTO glass electrode

3.7 Cyclic voltammetry

Non-stirred cyclic voltammetry tests were conducted by immersing the three-electrode set-up in a 50 cm^3 glass beaker with 0.1 NaOH. The tests were conducted in blank and in fructose concentrations of various concentrations (i.e. 1 – 5 mM). **Table 3.2** illustrates the parameters that were varied in this study. Each test run included a setting up of a CV in the both the blank solution or fructose solution and then running the tests at fixed or varying scan rates as reflected. For comparison purposes with other literature, for the addition of analytes, 25 m V/s was chosen as the scan rate.

Table 3. 2: Parameters for CV analysis for scan rate tests and CV with the addition for different concentrations of fructose

Cyclic voltammetry parameters (no analytes)		**Cyclic voltammetry parameters (addition various analyte concentration)**	
Sensitivity	**100 nA**	Sensitivity	**100 nA**
Scan rates (mV/s)	**5, 10, 15, 20, 25, 30**	Scan rate (m V/s)	**25**
Amplitude (dB)	**50**	Amplitude (dB)	**50**
Start potential (V)	**- 0.2**	Start potential (V)	**- 0.2**
Stop potential (V)	**+ 0.8**	Stop potential (V)	**+ 0.8**

3.8 Chronoamperometric studies

Chronoamperometry under stirred conditions was performed to demonstrate the practical sensing utility of the fabricated Co_3O_4/FTO thin film. The tests were carried out at varying potentials of + 0.50V, +0.55 V, +0.60 V, +0.65 V and +0.70 V (to determine the optimum potential to use) for a time period of 780 s. The matrix for the chronoamperometric tests is shown in **Table 3.4**:

Table 3. 3: Chronoamperometry tests at different applied potentials

Parameter	Value (s)
Applied bias potential (V)	+ 0.50; +0.55; +0.60; +0.65; +0.70
Operating time (s)	780
Stirrer speed (rpm)	2 350
Addition time interval (s)	30

For this procedure, the three-electrode set-up was prepared, 45 cm^3 of 0.1 M NaOH was placed in a 50 cm^3 beaker, and the stirrer operated at 2 350 rpm. For all the chronoamperometric experiments, an initial fructose concentration of 100 mM stock solution was used and serial dilutions were done using the dilution formula:

$$C_1V_1 = C_2V_2 \qquad \text{Equation 3.2}$$

where C_1 and C_2 are the initial and final concentration in solution, and V_1 and V_2 are initial and final volumes in cm^3. For chronoamperometric measurements under stirred conditions, starting with a volume of NaOH of 45 cm^3, fructose was pipetted in aliquots of 0.5 up to 2 300 µ L as illustrated in **Table 3.4**.

Firstly, 300 s was allowed to elapse so that the current would stabilise. After stabilisation of the current, at the 300 s mark fructose solution was added stepwise at 30 s interval until the experiment was terminated after a 780 s run. From these results, the chronoamperograms were then plotted for use in sensitivity analyses and tests. The detection limits were estimated based on the signal-to-noise characteristics (S/N = 3) of these data.

Table3. 4: Amperometric fructose addition table for response studies

Stock solution concentration (M)	V_1 added (µ L)	Total volume in beaker V_2 (ml)	Actual fructose concentration in solution (m M)	Time (s)
100	0	45	0	0
100	0.5	45.0005	0.001	200
100	1	45.0015	0.003	230
100	3	45.0045	0.010	260
100	5	45.0095	0.021	290
100	10	45.0195	0.043	320
100	15	45.0345	0.077	350
100	56	45.0905	0.201	380
100	100	45.1905	0.422	410
100	100	45.2905	0.643	440
100	100	45.3905	0.863	470
100	100	45.4905	1.083	500
100	100	45.5905	1.302	530
100	100	45.6905	1.521	560
100	100	45.7905	1.740	590
100	1 000	46.7905	3.877	620
100	1 100	47.8905	6.174	650
100	2 200	50.0905	10.566	680
100	2 300	52.3905	14.956	780

3.8.1 Interference tests

The interference of other species on the function of the fructose sensor was evaluated in the presence of the key species that are found in typical biological and other fluids chiefly glucose, AA, , AC, KCl and NaCl. Different concentrations of the species were used as follows: Glucose (0.46mM); UA (0.46 mM); KCL (57 mM); NaCl (63 mM) and fructose (0.46 mM).

3.9 Electrochemical Impedance Spectroscopy (EIS) Studies

Electrochemical impedance spectroscopy (EIS) studies were performed in a PBS solution containing 5.0 mM Potassium ferricyanide ($K_4Fe\ (CN)_6.3H_2O$) at an applied bias potential of + 0.25 V with 5 mV amplitude, in the frequency range from 0.1 Hz to 100 kHz. This was used to investigate the solution impedance on the mode of action of the catalyst surface. The results were plotted as Nyquist and Bode plots. This was used to evaluate the effect of the interference of ions with respect to the number of layers of the thin film Co_3O_4 that were used to evaluate the optimum number of layers of performance. The results of such interference and layer study are reported in Chapter 4.

3.10 Shelf life of the electrode

The shelf life of an electrode (t_L), is defined as the storage or operational time necessary for the sensitivity, within the linear concentration range, to decrease by a factor of 10 (tL10) or50% (t_{L50}) (Thévenot *et al*., 2007).The shelf life of the Co_3O_4/FTO thin film was evaluated by the use of the prepared FTO electrode over a four week period at a one week intervals. For the tests, a CV in 1 mM fructose was conducted, and the readings were noted. After the test, the potentiostat was disconnected and the electrode removed. After each test, the electrode was thoroughly rinsed with distilled water and dried by air blowing. When not in use, the electrode was stored at an ambient temperature of 25±2 ^{0}C until the next test.

3.11 Reproducibility and chemical stability tests

Electrode reproducibility is one of the fundamental operational parameters of an electrochemical sensor. Reproducibility is a measure of the scatter or the drift in a series of observations or results performed over a period of time. It is generally determined for the analyte concentration with in a usable range (Thévenot *et al*., 2007). In order to evaluate the reproducibility of the Co_3O_4 sensor, a series of 6 electrodes, 4 layers of Co_3O_4 were prepared and CV's were carried out with 1 mM fructose in 0.1 M NaOH. Each of the electrodes was stored under ambient temperature. The tests were done in triplicates and the RSD was used to determine the repeatability of the results. From a batch of 6 thin film Co_3O_4/FTO electrodes, the electrochemical response was studied and reported.

Chemical stability tests were performed in a similar type of cell arrangement as that used for cyclic voltammetry. For this procedure, CV tests (50 cycles, scan rate: 25 mV/s) were conducted in 1 mM fructose in 0.1 M NaOH.

3.12 Conclusions

This chapter has described the solution step for the deposition of Co_3O_4 on FTO glass electrodes. It has also been noted that the calcination of the Co_3O_4 was conducted at optimum conditions. Additionally, the solution step fabrication procedure offers immense simplicity and a more economical of electrode fabrication as compared to other methods of fructose detection.

In sum, the experimental section described procedures that address the challenge of developing a Co_3O_4 thin film electrode for use in further development of sensors.

Chapter 4

RESULTS AND DISCUSSION

4.1 Introduction

The results of results of the experimental investigations conducted as detailed in Chapter 3 are presented and interpreted. **Section 4.1** presents the introduction and focuses on key areas that will be addressed in the thesis. An extensive presentation of the results is made in **Section 4.2**, whereas the electrocatalytic behaviour of the Co_3O_4 electrode is discussed in **Section 4.3**. The chapter ends with a summary in **Section 4.4.**

4.2 Surface Morphology of the Co_3O_4/FTO thin film

High-resolution Scanning Electron Microscopy (HR-SEM) and TEM were used to evaluate the morphology and structure of the solution deposited film. The SEM and TEM images of the prepared film are shown in **Figure 4.1**. The resultant film thickness was found to be 665 nm and was measured from the cross sectional view of the film (**Figure 4.1 a)**. **Figure 4.1 (a)** shows that the Co_3O_4 thin film is homogenously spread and coated on the surface of the FTO glass. The film has interconnected aggregated porosity and a rough surface, as can be observed from the SEM (**Figure 4.1b**) and AFM topography image (**Figure 4.1c**). The roughness of the film can provide an increased surface area for enhanced electrocatalytic oxidation of fructose. The aggregated particles are nanoclusters of a single crystalline state as was observed from the HR-TEM image (**Figure 4.1 d**). The first three diffraction patterns (SAED, **Figure 4.1 e**) from the film yields d (111) = 0.481 nm, d (220) = 0.294 nm and d (311) = 0.249 nm, with a lattice constant a = 0.831 nm which corresponds largely to the diffraction from the Co_3O_4 lattice. XRD patterns (**Figure 4.2.1f**) matches very well with the diffraction pattern of crystalline cubic

Co_3O_4 structure (JCPDS card no: 76-1802) with the exposed {111} facet (TEM data not shown) corresponding to the exposure of high density, low surface energy planes. The XRD results correspond very well with the recorded SAED patterns of the Co_3O_4 film.

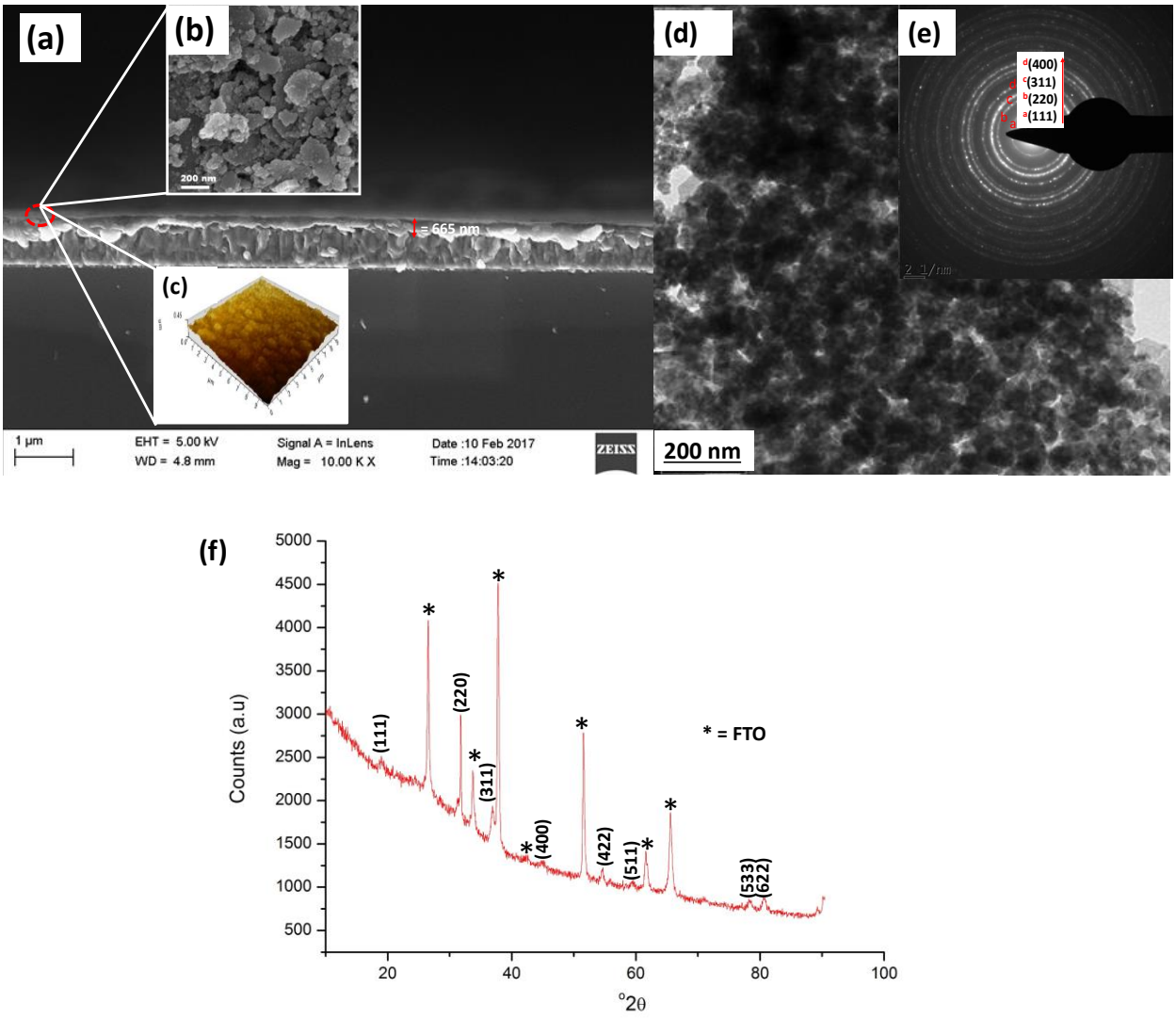

Figure 4. 1: (a) Cross sectional SEM image of the Co_3O_4 film deposited on FTO (insert b & c: SEM and AFM image of the surface of the film respectively), (d) TEM image of the Co_3O_4 film (insert e: SAED of the Co_3O_4 particles) and (f) XRD pattern of the Co_3O_4 thin film

4.3 Electrochemical behaviour of the Co_3O_4-modified FTO electrode

4.3.1 Cyclic voltammetry of the Co_3O_4 modified thin film FTO

The electrocatalytic activity of the bare FTO and the Co_3O_4 towards the oxidation of fructose in alkaline solution was investigated by Cyclic Voltammetry. An alkaline media such as 0.1 M NaOH solution was used to evaluate the performance of Co_3O_4 modified electrode by CV for the electrocatalytic detection of fructose. The CV's were recorded in the potential range of -0.2 to +0.8 V *vs*. Ag/AgCl as shown in **Figure 4.2**.

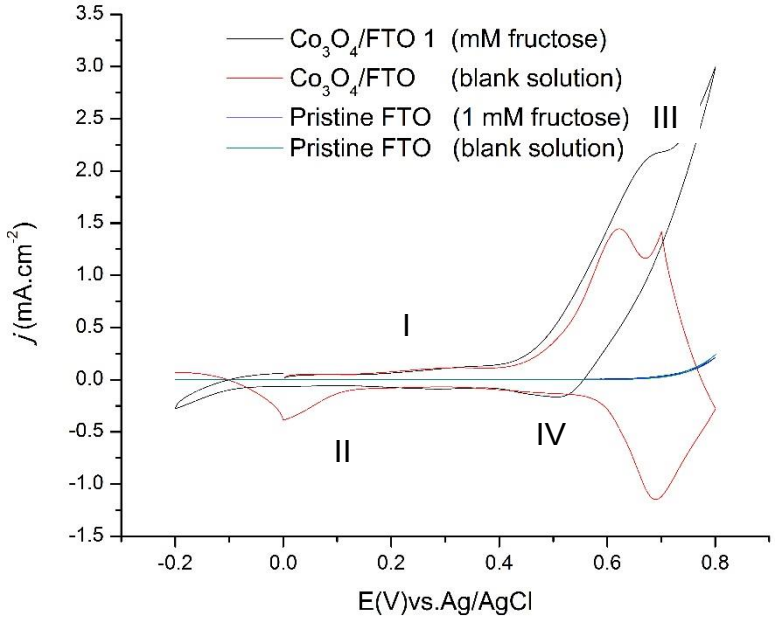

Figure 4. 2: Electrochemical behaviour of the Co_3O_4 thin film electrode in the absence and presence of 1 mM fructose in 0.1 M NaOH (scan rate: 25mV/s).

Displayed are the CV's of Co_3O_4 electrode in both the absence and presence of 1 mM fructose at 25 mVs^{-1} in 0.1 M NaOH electrolyte solution. It was observed that FTO displayed no oxidation behaviour both in the absence and presence of fructose in the potential range of -0.2 to +0.8 V. The Co_3O_4 thin film electrode resulted in an increase in the anodic current in the presence and absence of fructose. Two sets of redox peaks were observed. The first set of peaks (I / II) are attributed to the reversible transition between Co and CoOOH. The second redox pair (III / IV) is attributed to the conversion between CoOOH and CoO_2 (Yuan *et al*., 2014). It is also envisioned that the interconversion between the Co_3O_4 and COOH

formation in alkaline media can be influenced by the hydroxide concentration in the electrolyte solution. Spataru *et al*. (2003) reported that the oxidation of cobalt oxide in alkaline media is likely to follow the sets of reactions as: peak I being attributed to the formation of Co_3O_4 via the following reaction:

$3Co(OH)_2 + 2\ OH^- \rightarrow Co_3O_4 + 4\ H_2O + 2\ e^-$ Equation 4.1

The subsequent reaction that gives peak II will be attributed to the formation of CoOOH, which is a result of the oxidation of $Co(OH)_2$ and/ or the Co_3O_4 formed:

$Co(OH)_2 + OH^- \rightarrow CoOOH + H_2O + e^-$ Equation 4.2

$Co_3O_4 + H_2O + OH^- \rightarrow 3CoOOH + e^-$ Equation 4.3

And the oxidation of the CoOOH to CoO_2 can be according to the flowing reaction:

$CoOOH + OH^- \rightarrow CoO_2 + H_2O + e^-$ Equation 4.4

The effect of fructose concentration was evaluated in the range of 0 – 5 mM and the electrocatalytic activity of the Co_3O_4 prepared electrode is illustrated in Figure **4.3.**

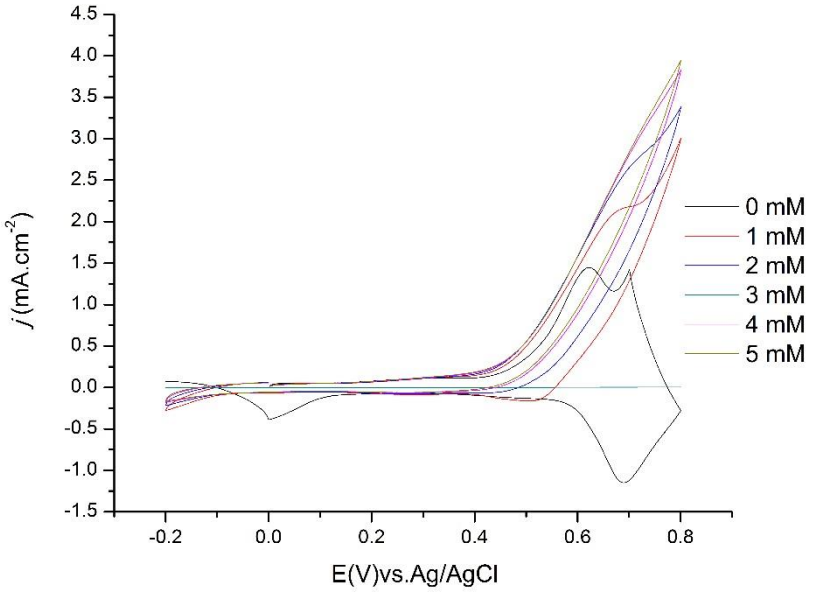

Figure 4.3: CVs in the presence of 0 - 5 mM fructose in 0.1 M NaOH electrolyte (scan rate: 25 mV/s)

The anodic current increased significantly with increasing concentration of fructose due to the catalytic oxidation of fructose, while the reduction peak largely diminished. Comparing the conditions before the addition of fructose and after the addition of fructose, the peak current intensity increased with the increase of the electroactive surface of the Co_3O_4 catalyst. As the concentration of fructose is continuously added up to 5 mM the definition of the voltammogram continues to be less and less defined. This could be a property attributed to the saturation of the surface of the electrode due to oxidation of fructose, or the adsorption of the fructose itself on the electrode surface. This suggests that the Co_3O_4 nanoparticles are suitable mediators for the shuttling of electrons between the fructose molecules and the working electrode, resulting in high catalytic activity for fructose oxidation.

The mechanism of electrocatalytic oxidation of fructose by Co_3O_4 is not well understood, although the most widely accepted one was suggested in previous studies (Karim-Nezard *et al*., 2009). With the subsequent addition of fructose, the cobalt acts as an electron delivery to shuttle electrons from the fructose to the electrode, thereby increasing the peak current. The electrocatalytic mechanism of fructose sensing on the Co_3O_4 surface is a multistep which can be presented in the following manner (Karim-Nezhad *et al*., 2009):

$$Co(III) \longleftrightarrow Co(IV) + e$$ Equation 4.5

The fructose is oxidised on the Co_3O_4 surface according to the reaction:

$$Co(IV) + fructose \rightarrow Intermediate + Co(III)$$ Equation 4.6

Subsequently, the intermediate formed oxidises to the product by a similar reaction mediated by Co (IV):

$$Co(IV) + Intermediate \rightarrow \text{Product} + Co(III)$$ Equation 4.7

It was thought that initially the Co(III) is oxidised to Co(IV) in a reversible aqueous reaction as in Equation 4.5. The addition of fructose enhances a surface-based reaction that further leads to the oxidation of the hydroxyl (OH) group of the fructose to give a reactive intermediate and Co(III) through an irreversible reaction as indicated by Equation 4.6. The intermediate is thought to be a fructaran intermediate; however the uncoated FTO does not display an increased current as displayed by the fructose oxidation peaks (**Figure 4.2**). The intermediate reacts with the Co(IV) to generate the product and regenerate the Co(III) as in Equation 4.7. Thus, it is likely that the Co(IV) generated in reaction (Equation 4.6) is the active species that is effective in the speeding up the oxidation of fructose. It is worthy of emphasis that an increment in the concentration of fructose results in a shift in the peak current toward the positive potential window, while a high concentration of fructose could have been significant to the decrease in the catalytic oxidation of fructose by Co_3O_4. It is proposed that as the reaction goes on there is a slight decrease in the pH of the electrolyte which subsequently results in the slight shift in potential towards the more positive values (Lee & Coates, 2000). Hayashi *et al*. (2012) indicated a direct electrolysis of water with the simultaneous generation of a hydroxyl radical on the surface may cause the potential to display such a shift. However, it is yet to be ascertained the exact mechanism that takes place (see **Figure 4.2.**).

4.3.2 Effect of various concentrations of electrolyte

It is well known that an alkaline medium is required to enhance the synergistic effect of the Co_3O_4 for the oxidation of carbohydrates (Prasad & Bhat, 2015). In this study, the effect of the varying concentrations of the NaOH electrolyte solution on fructose (1 mM) oxidation at Co_3O_4 was used to evaluate the effect of OH^- ions on the oxidation of fructose as shown in **Figure 4.4**. The concentrations of NaOH investigated

were 0.05, 0.1, 0.5 and 1 M. As presented in Figure **4.4** with the increasing NaOH concentration, the oxidative applied potential decreased slightly to values of around + 0.50 V, until the NaOH concentration would be close to 1 M. This indicated that higher concentrations of NaOH tend to bring instability to the Co_3O_4 electrode material. It is, therefore, most likely that the CV of the solution was influenced significantly by the presence of the OH^-. However, in this study, 0.1 M NaOH solution was used as a base electrolyte for comparison purpose with previous literature (Wang *et al*., 2010; Lang *et al*., 2013; Elahi, 2008). From the results in **Figure 4.4**, 0.1 M was selected as the optimum concentration of NaOH to obtain the highest fructose oxidation at lower applied potential and low current.

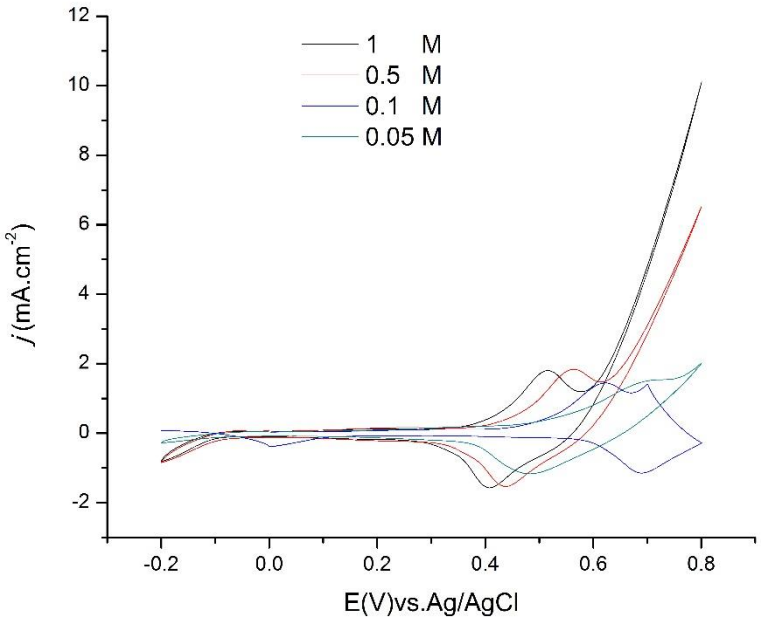

Figure 4. 4: CVs of Co_3O_4 in NaOH (0.05 – 1 M) electrolyte solution without fructose (scan rate = 25 mV/s)

Without fructose in the electrolyte solution it was observed that there was not much increase in the peak current. As shown in **Figure 4.5**, with the increasing NaOH concentration, the oxidative applied potential decreased slightly towards the negative potential to values of around + 0.50 V, until the NaOH concentration would be close to 1 M. Then as the NaOH concentration increases further, the current decreased. The tests showed that a high concentration of NaOH tended to bring instability to the Co_3O_4

electrode material. This could be easily understood as being the oxidation of the electrolyte itself, a phenomenon that was dealt with in section **4.2**.

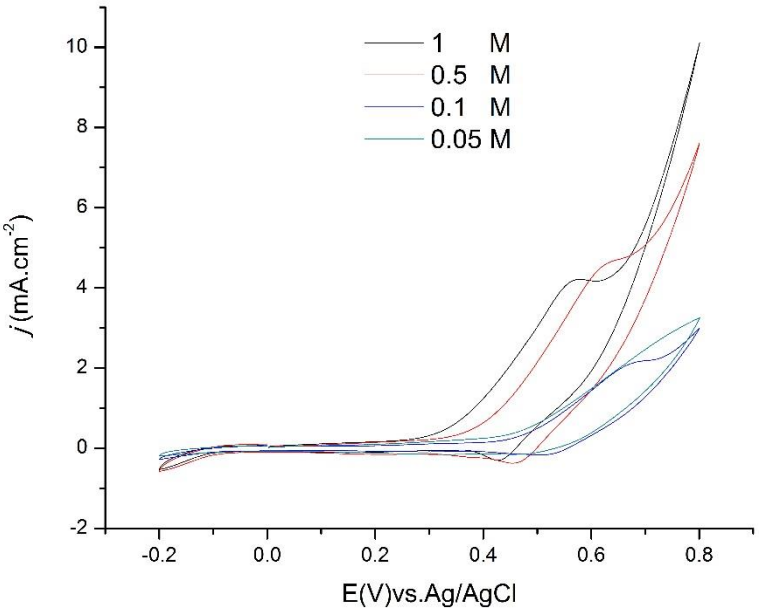

Figure 4.51: CVs of Co_3O_4 thin film in the presence of 1 mM fructose and NaOH (0.05 – 1 M NaOH) (scan rate: 25 mV/s)

4.3.3 Electrochemical Impedance Spectroscopy (EIS) studies

Figure 4.6 shows the corresponding Nyquist plot (**Figure 4.6**) obtained for the FTO and Co_3O_4/FTO various layer coated electrodes (N =1,2,3, 4…. where N is the number of layers) at 0.25 V (applied bias potential). In EIS, the diameter of the semicircle in the Nyquist plots corresponds to the electron transfer limited process and is equivalent to the electron transfer resistance (R_{ct}). The Nyquist diagrams in **Figure 4.6** showed depressed semicircles due to the combination of the effect of the charge transfer resistance of the Co (III) to Co(IV) (Gao *et al.*, 2010). This could be attributed to the effect of the instant chemical reaction of Co_3O_4 by ferricyanide (Koza *et al.*, 2012). The closer the diagram is to the vertical axis, the greater the decrease in solution resistance (R_s) (Walter, 1986). It can be seen from **Figure 4.6** that by addition of each layer, charge transferability increases, resulting in enhanced electrochemical activity.

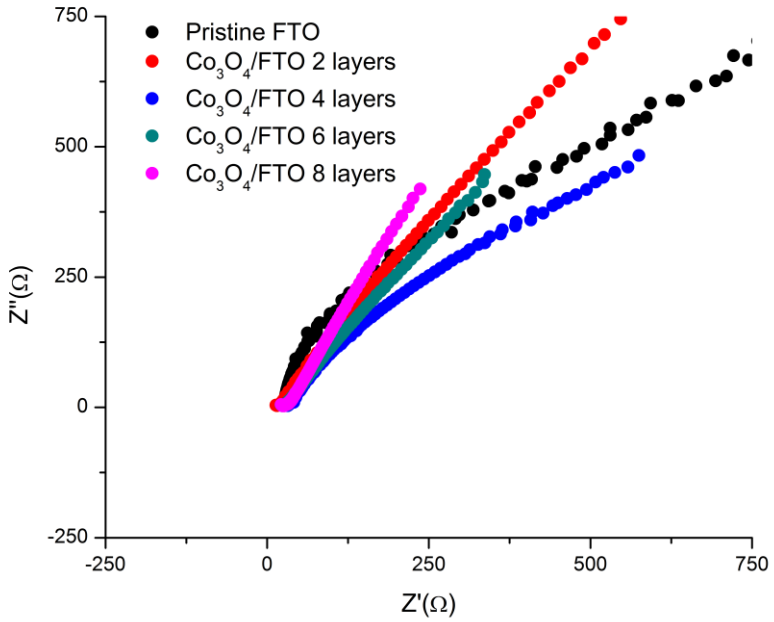

Figure 4.6: Nyquist plots for bare FTO and Co_3O_4 FTO electrodes in 0.1 M NaOH solution containing 5 mM Fe $(CN)_6^{3-}$

For a good approximation of the studied electrochemical system, the equivalent Randles circuit (**Figure 4.7**) that was chosen to fit the experimental data was based on the Boukamp model (Boukamp, 1986). The circuit was modelled by incorporating the electrolyte solution resistance (R_s), in series with an electrical double-layer capacitor (C_{DL}), which is in parallel with R_{ct}.

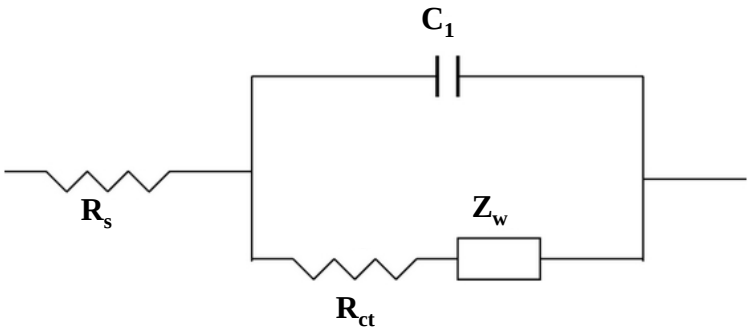

Figure 4.7: Equivalent circuit for the studied impedance system in 0.1 M NaOH containing 5 mM $Fe(CN)_6^{3-}$

In the equivalent circuit, R_s, C_1, R_{ct}, and Z_w represent the resistance of the electrolyte solution, capacitance, charge transfer resistance, and Warburg impedance, respectively. A Warburg element (Z_w) was used in series with the R_{ct} to accommodate the linear part of the EIS. The obtained impedance parameters are presented in **Table 4.1**.After the addition of the subsequent layers of Co_3O_4 thin film onto the FTO, the R_{ct} decreased from 500 to 0.514 $\Omega.cm^2$.The results demonstrated that the Co_3O_4 thin film FTO electrode acts as a powerful electrode mediator to shuttle electrodes from the solution to the electrode-solution surface. The effect of Co_3O_4 FTO support is also confirmed by the Bode plot in **Figure 4.8**.

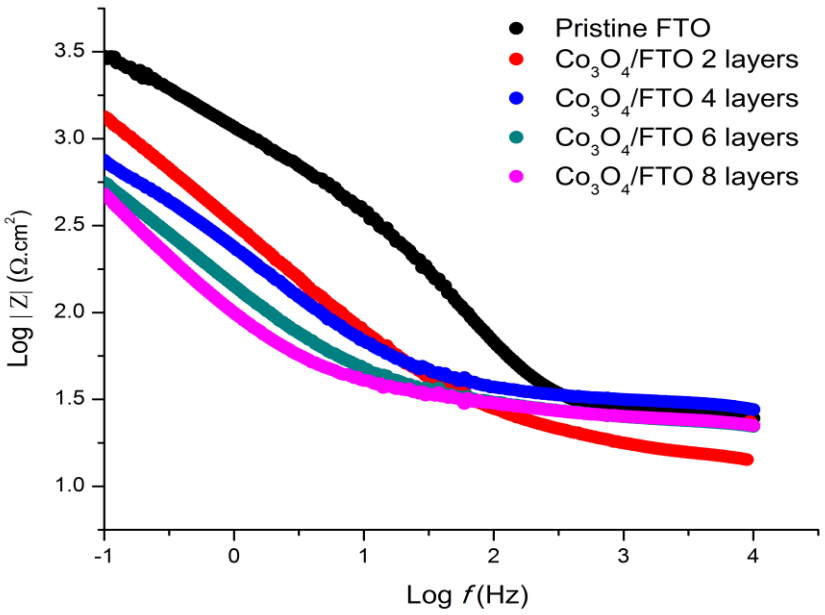

Figure 4.82: Bode plots of the bare FTO and the Co_3O_4 thin film in 0.1 M NaOH solution containing 5 mM $Fe(CN)_6^{3-}$

The Bode plot represents the logarithm of the impedance modulus (log $|Z|$ *vs*. the logarithm of the frequency (log *f* (Hz)) for the Co_3O_4 modified thin film FTO. The comparison of log |Z| *vs*. log *f* for the FTO and the Co_3O_4 distinctively shows that the charge transfer resistance decreased significantly with the presence of Co_3O_4 highlighting the good electrochemical activity of Co_3O_4.

However, it was observed from the CV data that the oxidation potential shifted slightly towards positive value when 6 layers of Co_3O_4 were deposited. This was due to the rate of the catalysis of fructose being

faster than its diffusion as the film thickness increased. Hence for the purposes of this study, only 4 layers of Co_3O_4 were considered to be optimum.

Table 4.1: Electrochemical parameters obtained by simulation of the EIS results on the FTO/Co_3O_4 in a 0.1 M NaOH containing 5 mM $Fe(CN)_6^{3-}$

Electrode	**R_s ($\Omega.cm^2$)**	**R_{ct}($\Omega.cm^2$)**	**W($mMhos.cm^2$)**
Pristine FTO	500	500	100×10^{-6}
Co_3O_4/ FTO (2 layers)	16.9	428	1.12×10^{-6}
Co_3O_4/ FTO (4 layers)	31.3	514	1.68×10^{-3}
Co_3O_4/ FTO (6 layers)	25.7	490	2.55×10^{-6}
Co_3O_4/ FTO (8 layers)	26.8	274	2.97×10^{-6}

4.3.4 Effect of scan rate study

The CVs of the oxidation of fructose solution were measured at different scan rates as illustrated in **Table 4.2**. Comparisons of the CV's at various scan rates were conducted and a direct correlation between the peak current and the square root of the scan rate was found. The anodic peak current of glucose oxidation is proportional to the square root of scan rate. A linear equation of I/μA = (186.00±0.092)/μA + (65.480±0.001)υ/μA mV^{-1} s with a correlation coefficient (R) of 0.995 was determined. The results are indicative that the kinetics of the electrocatalytic oxidation of fructose is controlled by the diffusion of fructose to the surface of the electrode. It can also be seen that the peak potential of the oxidation of fructose exhibits a positive shift with the increase in the scan rates.

Table 4.2: Results of the scan rate in relation to the peak current density,1 mM fructose in 0.1 M NaOH

Scan rate (mV/s)	Root scan rate ($^{1/2}$)	Anodic Current density (j)(A/m^{-2})	Cathodic Current density (j)(A/m^{-2})
5	2.236	4.32	-2.42
10	3.162	7.87	-5.06
15	3.872	9.99	-7.26
20	4.472	12.7	-9.95
25	5	14.9	-12.1
30	5.477	16.5	-13.1

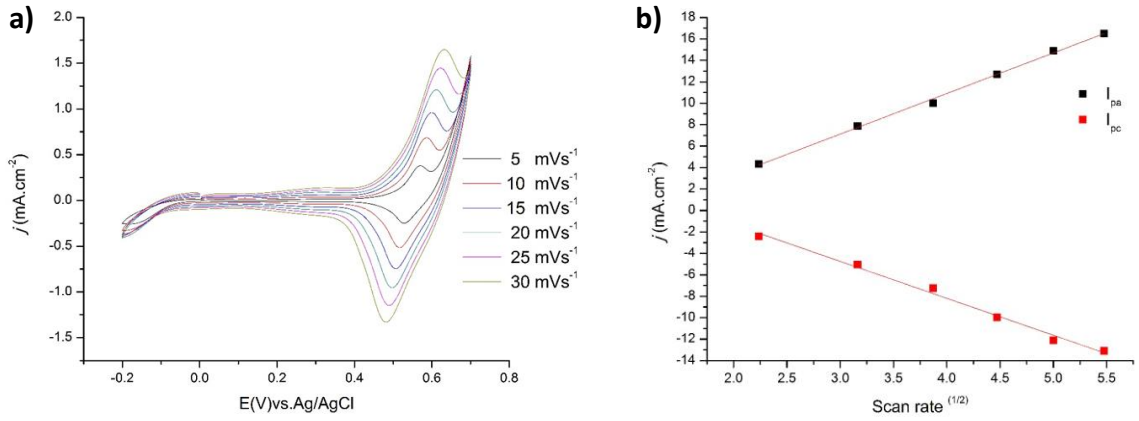

Figure 4.9: (a) The influence of scan rate on the peak current density of Co_3O_4; (b)The plot of peak current density *vs*. scan rate (a) and (b) plot of current density against scan rate in the presence of 1.0 mM fructose and 0.1 M NaOH

4.3.5 Chronoamperometric studies of fructose detection

To optimize the potential for fructose detection, the Co_3O_4 thin films were subjected to chronoamperometry using applied potentials of + 0.50 V, + 0.55 V,+ 0.60 V and + 0.65 V, and for each potential seven additions of 1mM fructose were carried out. The stirred chronoamperometric response studies were conducted for a total time of 780 s. **Figure 4.10** exhibits the analytical staircase chronoamperograms obtained at applied bias potentials of + 0.50 V, + 0.55 V, + 0.60 V, and + 0.65 V on the Co_3O_4/FTO film, showing the increase of the current according to fructose additions, as expected. However, at + 0.65 V the background current increased significantly, but the oxidation current decreased, compared to +0.6 V. The decrease in the oxidative current was due to the initiation of parasitic reaction from the electrolysis of water. So, the potential of + 0.60 V was employed for the detection of fructose in the concentration range from 0.4 to 15 mM. These potentials were used to find the optimum potential for fructose oxidation.

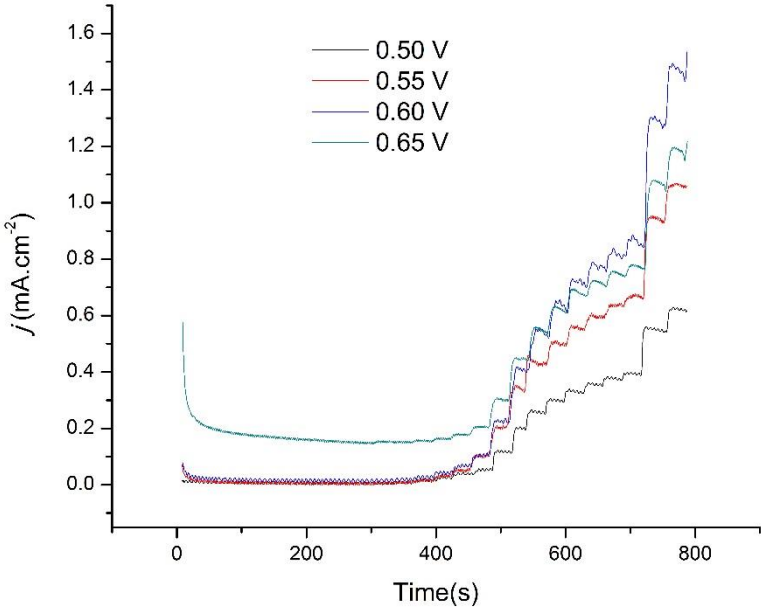

Figure 4.10: Electrochemical response studies of Co_3O_4 film upon successive addition of fructose in 0.1 M NaOH in varying applied potentials

A fast response time of 6 s (to reach 95% steady state after injection) was recorded during the successive addition of fructose (**Figure 4.11**). A fast response time translates to an easy electron transfer process on the Co_3O_4 surface. The shorter response time was attributed to the enhanced kinetics of the fructose catalysis that took place at the sensor surface.

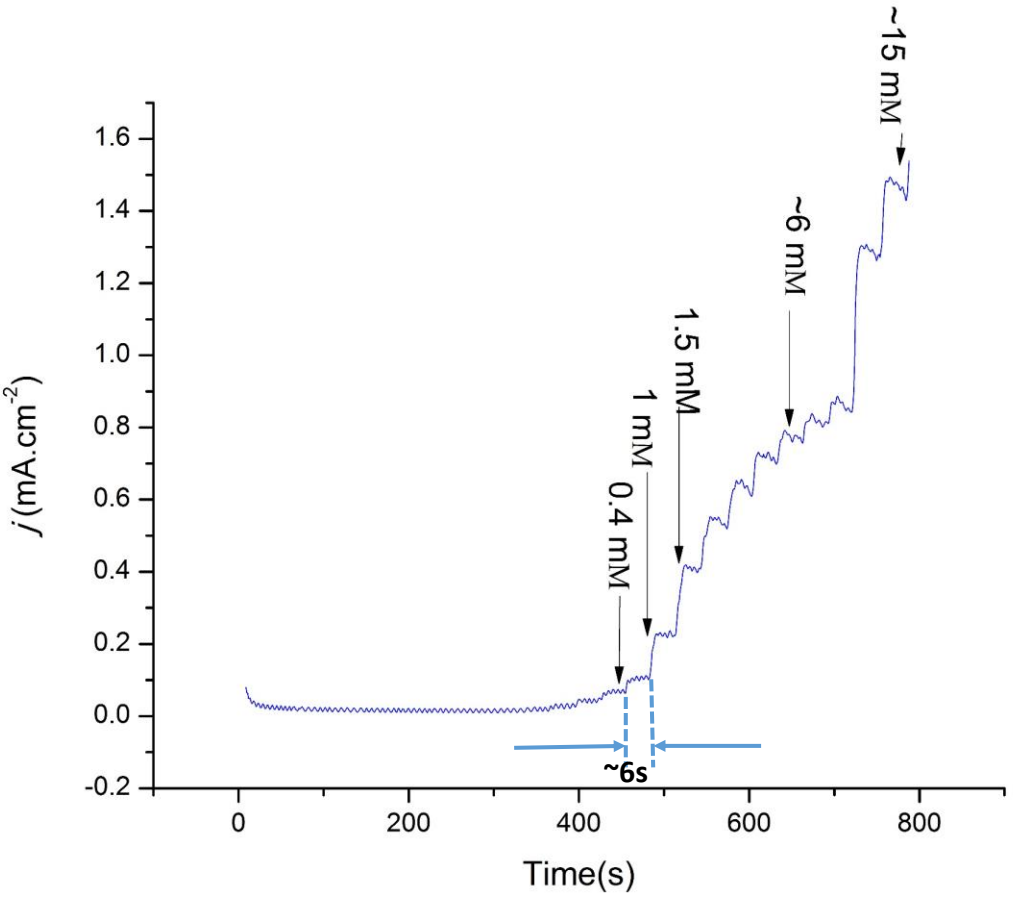

Figure 4.11: Current density-time response for Co_3O_4 thin film upon successive addition of fructose in 0.1 M NaOH at + 0.60 V (response time, t = 6 s, of the sensor is also displayed)

It could be observed that there was a slight baseline drift at high fructose concentration. This is due to the variation of the localised pH, the rate of the catalysis of fructose being faster than its diffusion and also adsorption of intermediates on catalyst surface (Chowdhury *et al*., 2017).

Figure 4.12 demonstrates two distinctive linear ranges (0.021 – 1.74 mM; 1.74 - ~15 mM) covering a wide linear range of up to ~15 mM obtained from the dose response curve of fructose.

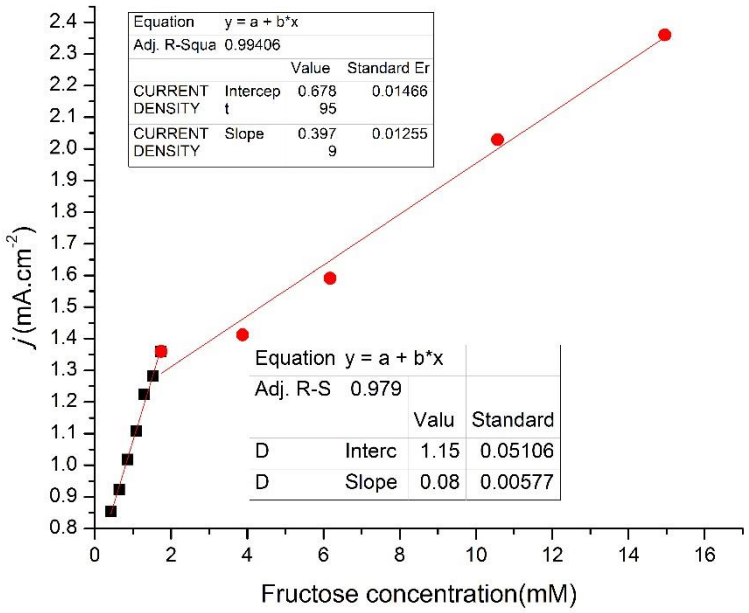

Figure 4. 123: Linear range of the sensor for 0.021 - 15 mM fructose

The sensor exhibited a high sensitivity of 495 µA cm^{-2} mM^{-1} for the lower concentration range. For higher concentration range the sensitivity was calculated to be 53 µA cm^{-2} mM^{-1}. The limit of detection (LOD) was determined using Equations 4.8 and 4.9:

$$\text{Sensitivity} = \text{slope of the calibration curve} \qquad \text{Equation 4.8}$$

$$LOD = \frac{3.3 \times \sigma}{slope} \qquad \text{Equation 4.9}$$

From the calculations in Equations 4.8 and 4.9, the LOD of the sensor was found to be 1.7 µM at a signal-to-noise ratio (S/N) = 3(see Appendix).

The fabricated Co_3O_4/FTO thin film was also compared with previously reported fructose sensors based on nano-metal and is as listed in **Table 4.3.** As displayed in **Table 4.3** the fabricated sensor shows a

highly enhanced sensitivity and LOD due to the excellent catalytic activity of Co_3O_4. Like enzyme bound electrodes or Co_3O_4 based electrodes, however the fabricated electrode displays some advantages that may not be found in other electrodes. For instance, from a practical point of view, the electrode based on FTO glass can be easily integrated into a custom-made circuit. This can effectively reduce the volume of the circuit used as compared to electrodes that are modified using other materials, such as glassy carbon electrodes. Secondly, the preparation method involves solution deposit of fructose and therefore this will be a far more economically viable process for electrode fabrication. The detection limit (LOD) of fructose at a signal-to-noise ratio ($S/N = 3$) was calculated to be 1.7 μM. The shorter response time was attributed to the enhanced kinetics of the fructose catalysis that took place at the sensor surface.

4.3.6 Selectivity studies of the sensor

For further verification of the performance of the sensor, the selectivity of the fructose sensor in the presence of the common key constituents that are contained in typical biological fluids, such as, glucose (0.46 mM), AA (0.46 mM),UA (0.46 mM), AC (0.46 mM), KCl (67 mM) and NaCl (53 mM) was examined as shown in **Figure 4.13**. Although the concentration of the interfering species in the typical human serum is 12 times less than that of fructose (Kawasaki *et al*., 2012), the much higher concentration of the interfering species i.e. fructose: interfering species 1: 15 (for example, fructose : uric acid), was used in the present analysis to ensure the sensitivity of the sensor. As is clearly observed in **Figure 4.13**, the current responses of the key interfering species had little effect compared to that of fructose.

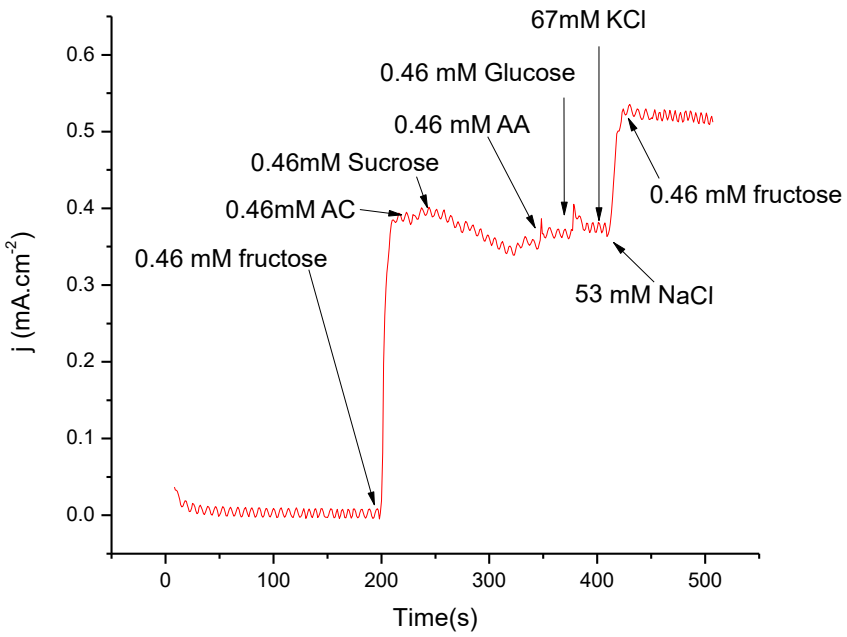

Figure 4.13: Current density-time response of Co_3O_4 thin film upon successive addition of fructose and other interfering species in 0.1 M NaOH solution at an applied of + 0.60 V

The results indicated that glucose and other key interference species did not cause any significant response. It would have been expected for glucose to interfere significantly with the detection of fructose. However, the non-interference of glucose in the detection of fructose might be attributed to the inhibitory action of other key interfering species in the simulated sample. It is also understood that fructose is isomeric with glucose in many biological and food items (Qi *et al*., 2008), that there is a coexistence between the two, and that it is difficult to detect glucose when fructose is present (Fang *et al*., 2009). Prevention of interference species (AA, AC and UA) oxidation at +0.6 V can be due to the repelling effect on the Co_3O_4 surface (Ding *et al*., 2010). The current responses of the interference species are relatively low in the presence of 0.46 mM of fructose. This could be as a result of the Co_3O_4 and the anionic species being negative in 0.1 M NaOH solution. However, low oxidation of glucose might result from the application of low potential in this study. It has been reported previously that chloride poisoning is a challenge for most of the precious metal and non-enzymatic glucose sensor (Reitz *et al*., 2008; Park *et al*., 2003). It was noticeable that the injection of chloride ions did not result in any obvious amperometric response. This means that the developed sensor can be used to determine precise fructose

concentrations in high chloride environments, e.g. blood. The sensing characteristics of the fabricated Co_3O_4/FTO thin film are listed **Table 4.3** along with those reported in literature. It is evident that the sensitivity of the Co_3O_4 thin film compares well with that of the other reported electrodes. The results demonstrate that the Co_3O_4/FTO thin film is a better and more promising candidate over conventional electrodes.

Table 4. 3: Comparison of the fabricated Co_3O_4/FTO thin film against previously reported fructose sensing characteristics of various nanomaterial modified electrodes prepared by different methods in literature

Electrode materials	**Electrode preparation route**	**Supporting electrode**	**Applied potential V *vs.* Ag/AgCl**	**Linear range (mM)**	**Sensitivity ($\mu A.cm^{-2}.mM^{-1}$)**	**LOD (µM)**	**Response time (s)**	**Reference**
$LaMnO_3$	Electrospinning	Glassy Carbon	+0.60	0.4 – 4	1238.5	63	15	(Xu *et al*., 2014a)
SDBS/Co-Cu	Electrodeposition	Graphene	+0.40	0.003 - 1	932	-	<1	(Zhou *et al*., 2013)
CNT- NiCo-oxide	Simple deposition	Screen-printed	+0.35	0.02 – 0.675 0.675-12.12	2.5±0.8 1.08±0.009	9.5	-	(Arvinte *et al*., 2011)
CuO/Co_3O_4	Electrospinning	Glassy carbon	+0.30	0.01-3	18.988	3	1	(Y. Wang *et al*., 2011)
Au/Co	Electrochemical & hydrothermal	Au	+0.26	0.001– 0.01	12.5	0.005	<1	(Lang *et al*., 2013)
Nano-Ni(II)-curcumin	Electrodeposition	Glassy Carbon	+0.70	0.01-0.10	8.8285	≈0.98	~10	(Elahi *et al*., 2008)
CS–PDDA–nano-PB/nano-Au/MPBA	Solution casting	Glassy Carbon	+0.5	-	70	10	~10	(Bian *et al*., 2010)
Co_3O_4	Spin-coating	FTO	+0.6	0.021 – 1.74 1.74 - ~15	398 & 53	1.7	~6	This abstract

4.3.7 Reproducibility of the Co_3O_4 thin film

Figure 4.14 illustrates the electrochemical response of 6 different Co_3O_4/FTO thin film electrodes fabricated under the same set of conditions in the presence of 1 mM fructose in 0.1 M NaOH. It is found that the Co_3O_4/FTO thin film electrode shows good inter-electrode reproducibility for six different electrodes with a constant geometric area. This was evidenced by the RSD which was determined to be 3.97 %.

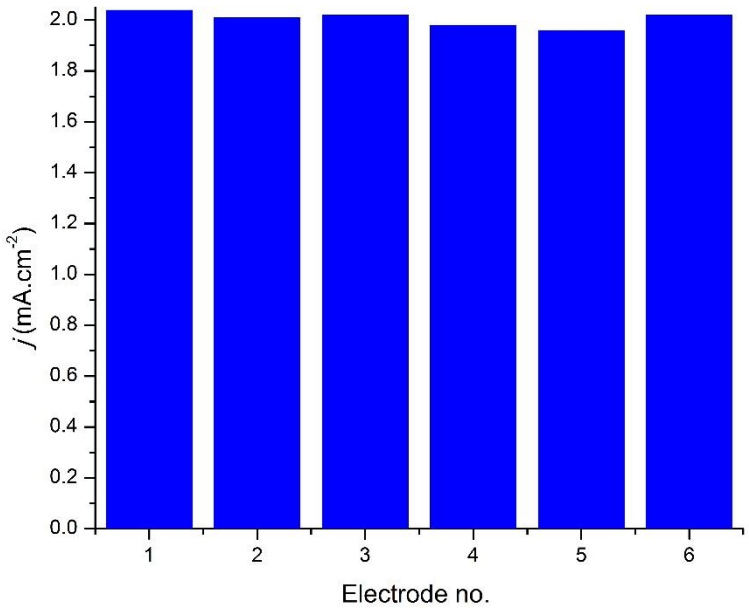

Figure 4.14: Inter-electrode reproducibility of 6 Co_3O_4/FTO electrodes in 1 mM fructose in 0.1 M NaOH (scan rate:25 mV/s)

4.3.8 Chemical stability of the Co_3O_4 thin film electrode

Chemical stability of the sensor was determined by conducting CV experiments for 50 cycles in 1 mM fructose solution at a scan rate of 25 mV/s (**Figure 4.15**). No new redox pairs were observed and no significant changes occurred in the existing redox peaks. This highlights good chemical stability and repeatability of the sensor.

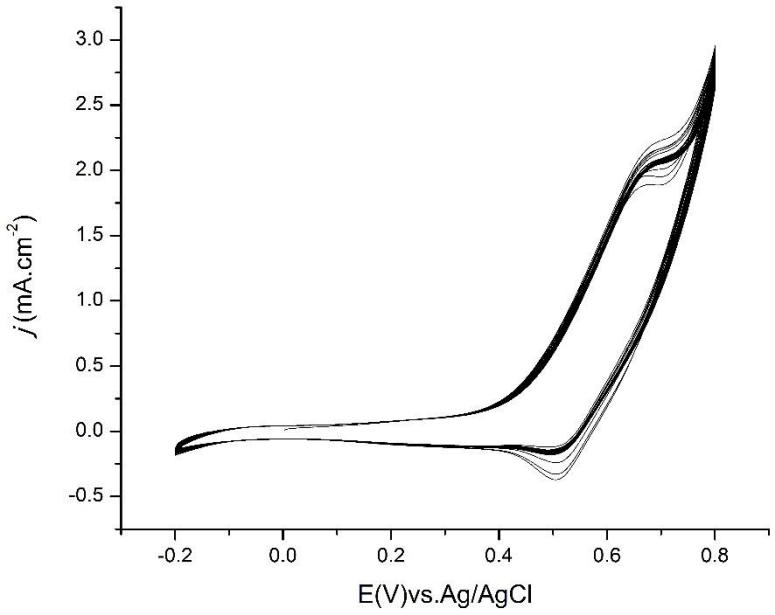

Figure 4.15: Chemical stability of the Co_3O_4/FTO electrode in 1 mM fructose in 1 M NaOH subjected to 100 cycles (scan rate:25 mV/s)

4.3.9 Shelf-life of the sensor

The storage stability this Co_3O_4/FTO 4-layer thin film electrode was monitored at an interval of 4-weeks as shown in **Figure 4.16**. The investigations were conducted by the consecutive measurements of the current response for 1 mM fructose solution over that 4-week period. It was found that the fabricated electrode maintained 83 % of its initial peak current even after 4 weeks when stored at ~ 25 ^{0}C after which the current response dropped to less than 80 % in about 30 days. This indicates that the fabricated FTO electrode exhibits a reasonably good shelf-life for at least 4 weeks of use before a significant drop in current response is observable. The shelf life of the sensor could have been influenced by factors such as the oxidation of the fructose on the surface of the Co_3O_4 thin film, or the deposition the fructose itself on the surface of the sensor.

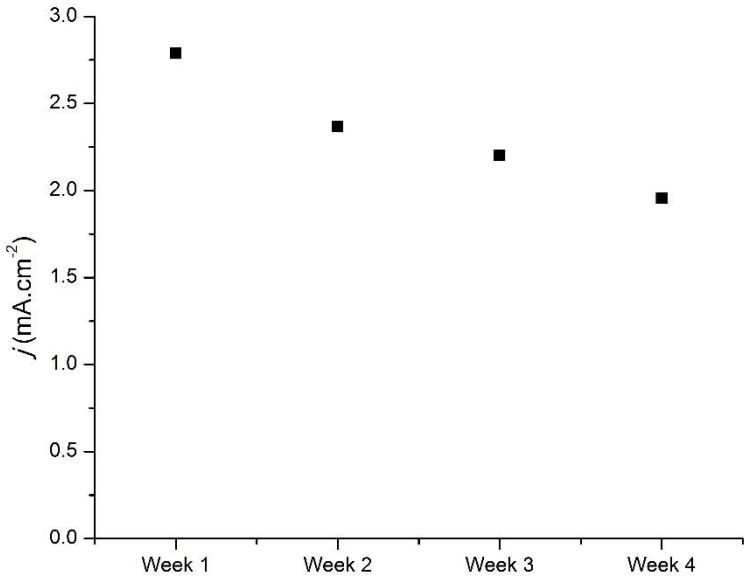

Figure 4.16: Shelf-life of the Co_3O_4/FTO electrode for 4 week period

4.3.10 Repeatability of the Co_3O_4/FTO thin film electrode

The repeatability of the Co_3O_4 regarding the electrocatalytic oxidation of fructose was tested. For the tests, an electrode was used repeatedly in cyclic voltammetry in the presence of 1 mM fructose in 0.1 M NaOH electrolyte six times. The electrode was used, then rinsed thoroughly in distilled water and allowed to dry at room temperature. Once dry, the same electrode was used again for the tests. The results are illustrated in **Figure 4.17**. The low RSD (5 %) displayed by the electrode indicated good electrode repeatability.

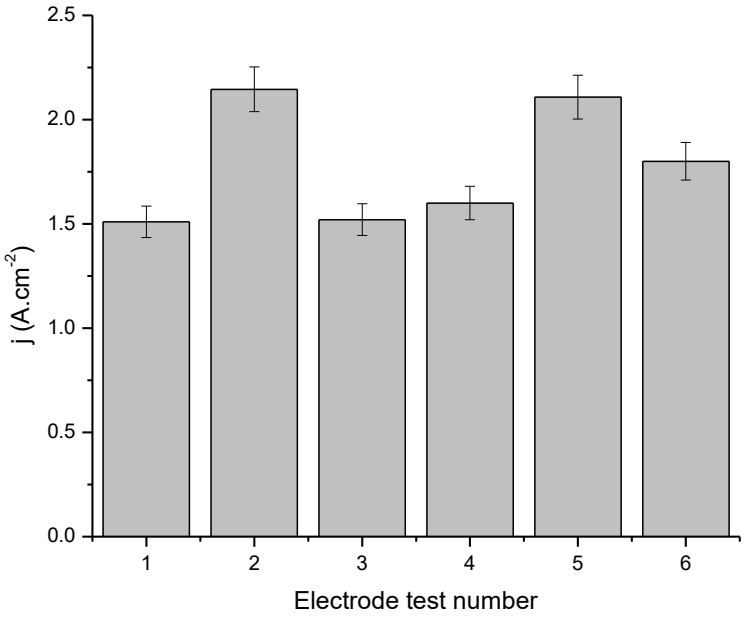

Figure 4.17: Electrode repeatability tests for 1 electrode in 6 tests (error bars shown)

4.4 Conclusion

This chapter deals with the results obtained during tests conducted on the Co_3O_4 thin film electrode. The Co_3O_4/FTO thin film electrode has shown excellent electrocatalytic activity toward the oxidation of fructose in alkaline media and a wider range of fructose concentrations. The fabricated electrode can be utilised for micromolar or millimolar concentration ranges of fructose using cyclic voltammetry and chronoamperometric techniques, respectively. The fabricated electrochemical system was applicable to the analysis of simulated fructose samples containing different reducing sugars with minimal interference from interfering species in analytical samples. The electrode had a remarkable sensing ability, a significantly lower LOD, a greater analytical sensitivity, stability and shelf-life, and it compared favourably with other modified electrodes employed as fructose sensors. Additionally, the fabrication procedure offers greater simplicity and economy of electrode fabrication as compared to other methods of fructose detection. The work in this thesis has demonstrated that a Co_3O_4 thin film electrode, which was prepared via a simple solution-based spin coating method, can be used in the development of the next

generation of non-enzymatic fructose sensors. From the calculations, the fabricated sensor exhibited a wide linear range of up to 15 mM and a low LOD of 1.7 mM. The sensor displayed a fast response time of 6 s. Thus the sensor can be used in the detection of key monosaccharides in medicinal and food and beverages applications.

The work in this thesis was aimed at demonstrating the sensing potential of Co_3O_4 thin film for electrocatalytic fructose oxidation. Hence no real sample testing was done for the purpose of this study.

Chapter 5

CONCLUSION AND RECOMMENDATIONS

5.1. Introduction

The highly catalytic, stable and non-sensitive thin film Co_3O_4 supported FTO electrodes have been successfully prepared by simple two-step spin-coating procedure. The thin film Co_3O_4 surface morphology was evaluated and confirmed by the use of the TEM, XRD and the SEM microscopy. Consequently, the fabricated Co_3O_4/FTO was characterised by electrochemical methods using cyclic voltammetry and EIS. The sensor exhibited strong electrocatalytic activity towards the selective oxidation of fructose in the presence of other key interfering species as uric acid, ascorbic acid, glucose, acetaminophen, potassium chloride and sodium chloride. Moreover, the electrode was able to sustain close to 90 % of its original activity when used for a period of 4 weeks. This makes the method better and more viable as compared to other fabrication techniques.

Applying the cyclic voltammetry techniques, the lower limits of detection (LODs) were estimated to be in the order of ~1.7 μM (*S/N* = 3). The fabricated sensor also displayed two distinct linear ranges from 0.021 – 1.74 mM (lower linear range) and 1.74 - ~15 mM (upper linear range) covering an overall wide linear range of up to ~15 mM at an applied potential of +0.6V vs Ag/AgCl in 0.1M NaOH solution. For the same sensor, with the two linear ranges, the sensor also presented two distinct sensitivities of 495 $\mu A cm^{-2} mM^{-1}$ (lower concentration range) & 53 $\mu A cm^{-2} mM^{-1}$ (higher concentration range) respectively. The sensor also displayed a chemical stability as evidenced by its behaviour when it was subjected to a series of 100 cycles without altering the cyclic oxidation potential. The constructed sensor exhibited a fast response rate of 6s. This work has presented a new approach of fabricating a non-enzymatic fructose sensor using simple electrode coating techniques.

This work demonstrated that Co_3O_4 thin film electrode, prepared via simple spin coating of chemical solution can be utilised in rapid, sensitive, selective and wide linear range detection of fructose. The LOD

falls within the range of typical fructose concentration in biological fluids for both diabetic and healthy patients.

5.2 Significance of the research

The Co_3O_4/FTO thin film electrode exhibited strong potential for its use as a non-invasive, selective, and non-enzymatic fructose sensor which can be applicable in the food industry, and the pharmaceutical and medical industries.

5.3 Further work and recommendations

Based on the results obtained from these experiments, there are two areas that key to improve understanding of the operation of the oxidation of fructose on electrodes.

- Though the work has presented the use of pristine Co_3O_4 film on a FTO glass electrode, future work will endeavour to utilise different combinations of Co_3O_4 with other electrodes.
- Further work needs to be focussed on the use of the Co_3O_4 to detect the presence of fructose under physiological conditions and in physiological samples.

References

Ameyama, M., Shinagawa, E., Matsushita, K. & Adachi, O. 1981. D-fructose dehydrogenase of Gluconobacter industrius: purification, characterization, and application to enzymatic microdetermination of D-fructose. *Journal of Bacteriology*, 145(2): 814–823.

Ansari, A.A., Alhoshan, M., Alsalhi, M.S. & Aldwayyan, A.S. 2010a. Nanostructured Metal Oxides Based Enzymatic Electrochemical Biosensors.In Serra,P.A.(ed.) *Biosensors*.Available: (February). http://www.intechopen.com/books/biosensors/nanostructured-metal-oxides-based-enzymatic-electrochemical-biosensors.Accessed:September 21,2017.

Ansari, A.A., Alhoshan, M., Alsalhi, M.S. & Aldwayyan, A.S. 2010. Prospects of nanotechnology in clinical immunodiagnostics. *Sensors*, 10(7): 6535–6581.

Antiochia, R., Lavagnini, I. & Magno, F. 2004. Amperometric Mediated Carbon Nanotube Paste Biosensor for Fructose Determination. *Analytical Letters*, 37(8): 1657–1669.

Antiochia, R. & Palleschi, G. 1997. A tri-enzyme electrode probe for the sequential determination of fructose and glucose in the same sample. *Analytical Letters*, 30(4): 683–697.

Arriola, E.R. & Cordón, A.C. 2010. Effective interactions and long distance symmetries in the nucleon-nucleon system. *AIP Conference Proceedings*, 1322(1): 483–487.

Arvinte, A., Sesay, A.M. & Virtanen, V. 2011. Carbohydrates electrocatalytic oxidation using CNT-NiCo-oxide modified electrodes. *Talanta*, 84(1): 180–186.

Astruc, D. 2012. Electron-transfer processes in dendrimers and their implication in biology, catalysis, sensing and nanotechnology. *Nature Chemistry*, 4(4): 255–267.

Baird, D. 1993. Analytical chemistry and the ‘big’ scientific instrumentation revolution. *Annals of Science*, 50(3): 267–290.

Bang, J.H. & Suslick, K.S. 2010. Applications of ultrasound to the synthesis of nanostructured materials. *Advanced Materials*, 22(10): 1039–1059.

Bard, A.J. & Zoski, C.G. 2000. Voltammetry Retrospective. *Analytical Chemistry*, 72(9): 346 A-352 A.

Batchelor-Mcauley, C., Kätelhön, E., Barnes, E.O., Compton, R.G., Laborda, E. & Molina, A. 2015. Recent Advances in Voltammetry. *ChemistryOpen*, 4(3): 224–260.

Begum, A., Kobatake, E., Suzawa, T., Ikariyama, Y. & Aizawa, M. 1993. New electrocatalytic biomolecular interface for fabricating a fructose dehydrogenase-based sensing system. *Analytica Chimica Acta*, 280(1): 31–36.

Bergren, A.J. 2006. Electron transfer reactivity patterns at chemically modified electrodes: Fundamentals and application to the optimization of redox recycling amplification systems.PhD.dissertation,Iowa Sate University. *ProQuest Dissertations and Theses*.Available: https://search-proquest-com.libproxy.cput.ac.za/docview/305317447/F44016DE69AB498APQ/1?accountid=26862. Accessed: October 27, 2017.

Bian, X.Z., Luo, H.Q. & Li, N.B. 2010. Electrochemical recognition for sugars on the chitosan-poly(diallyldimethylammonium chloride)-nano-Prussian blue/nano-Au/4- mercaptophenylboronic acid modified glassy carbon electrode. *Bioprocess and Biosystems Engineering*, 33(8): 971–978.

Biscay, J., Rama, E.C, García, M.B.G., Reviejo, A.J., Carrazón, J.M.P & García, A.C. 2012a. Amperometric fructose sensor based on ferrocyanide modified screen-printed carbon electrode. *Talanta*, 88: 432–438.

Biscay, J., Rama, E.C, García, M.B.G, Reviejo, A.J., Carrazón, J.M.P & García, A.C. 2012b. Amperometric fructose sensor based on ferrocyanide modified screen-printed carbon electrode. *Talanta*, 88(April): 432–438.

Bonfilio, R., De Araujo, M.B., Salgado, H.R.N. 2010. Recent applications of analytical techniques for quantitative pharmaceutical analysis : a review. *WSEAS Transactions on Biology and Biomedicine*, 7(4): 316–338.

Boukamp, B.A. 1986. A nonlinear least squares fit procedure for analysis of immittance data of electrochemical systems. *Solid State Ionics*, 20(1): 31–44.

Brown, A.P. & Anson, F.C. 1977. Cyclic and differential pulse voltammetric behavior of reactants

Confined to the Electrode Surface. *Analytical Chemistry*, 49(11): 1589–1595.

Brownson, D.A.C. & Banks, C.E. 2014. Interpreting Electrochemistry (in The Handbook of Graphene Electrochemistry).Springer London. pp.23 – 77.

Brownson, D.A.C., Lacombe, A.C., Gómez-Mingot, M. & Banks, C.E. 2012. Graphene oxide gives rise to unique and intriguing voltammetry. *RSC Advances*, 2(2): 665–668.

Buratti, S., Brunetti, B. & Mannino, S. 2008. Amperometric detection of carbohydrates and thiols by using a glassy carbon electrode coated with Co oxide/multi-wall carbon nanotubes catalytic system. *Talanta*, 76(2): 454–457.

Casella, I.G. 2002. Electrodeposition of cobalt oxide films from carbonate solutions containing Co(II)-tartrate complexes. *Journal of Electroanalytical Chemistry*, 520(1–2): 119–125.

Chen, A. & Ostrom, C. 2015. Palladium-Based Nanomaterials: Synthesis and Electrochemical Applications. *Chemical Reviews*, 115(21): 11999–12044.

Chowdhury, M., Cummings, F., Kebede, M. & Fester, V. 2017. Binderless Solution Processed Zn Doped Co 3 O 4 Film on FTO for Rapid and Selective Non-enzymatic Glucose Detection.*Electroanalysis*, 578–586.

Chowdhury, M., Ossinga, C., Cummings, F., Chamier, J. & Kebede, M. 2017. Novel Sn Doped Co_3O_4 Thin Film for Nonenzymatic Glucose Bio-Sensor and Fuel Cell. *Electroanalysis*,29(8) 1176 - 1886.

Compton, R.G. & Banks, C.E. 2007. Understanding Voltammetry (World Scientific, Singapore)

Ding, Y., Liu, Y., Parisi, J., Zhang, L. & Lei, Y. 2011. A novel NiO-Au hybrid nanobelts based sensor for sensitive and selective glucose detection. *Biosensors and Bioelectronics*, 28(1): 393–398.

Ding, Y., Wang, Y., Su, L., Bellagamba, M., Zhang, H. & Lei, Y. 2010. Electrospun Co3O4 nanofibers for sensitive and selective glucose detection. *Biosensors and Bioelectronics*, 26(2): 542–548.

Donders, M.E., Knoops, H.C.M., M.C.M., Kessels, W.M.M. & Notten, P.H.L. 2011. Remote Plasma Atomic Layer Deposition of Co3O4 Thin Films. *Journal of The Electrochemical Society*, 158(4): G92 - G96.

Elahi, M.Y., Mousavi, M.F. & Ghasemi, S. 2008. Nano-structured Ni(II)-curcumin modified glassy carbon electrode for electrocatalytic oxidation of fructose. *Electrochimica Acta*, 54(2): 490–498.

Ensafi, A.A., Lotfi, M. & Karimi-Maleh, H. 2012. New modified-multiwall carbon nanotubes paste electrode for electrocatalytic oxidation and determination of hydrazine using square wave voltammetry. *Chinese Journal of Catalysis*, 33(3): 487–493.

Esswein, A.J., McMurdo, M.J., Ross, P.N., Bell, A.T. & Tilley, T.D. 2009. Size-Dependent Activity of Co3O4 Nanoparticle Anodes for Alkaline Water Electrolysis. *The Journal of Physical Chemistry C*, 113(33): 15068–15072.

Fang, B., Gu, A., Wang, G., Wang, W., Feng, Y., Zhang, C. & Zhang, X. 2009. Silver oxide nanowalls grown on cu substrate as an enzymeless glucose sensor. *ACS Applied Materials and Interfaces*, 1(12): 2829–2834.

Fasmin, F. & Srinivasan, R. 2017. Nonlinear Electrochemical Impedance Spectroscopy. *Journal of The Electrochemical Society*, 164(7): H443–H455.

Gao, Y., Chen, S., Cao, D., Wang, G. & Yin, J. 2010. Electrochemical capacitance of Co3O4 nanowire arrays supported on nickel foam. *Journal of Power Sources*, 195(6): 1757–1760.

Garcia, C.A.B., De Oliveira Neto, G. & T. Kubota, L. 1998. New fructose biosensors utilizing a polypyrrole film and D-fructose 5-dehydrogenase immobilized by different processes. *Analytica Chimica Acta*, 374(2–3): 201–208.

Gasana, E., Westbroek, P., Temmerman, E., Thun, H.P. & Twagiramungu, F. 2000. Influence of changes of platinum electrode surface condition on the kinetics of the oxidation of sodium dithionite and sulfite in alkaline solution. *Electrochemistry Communications*, 2(10): 727–732.

Gomadam, P.M. & Weidner, J.W. 2005. Analysis of electrochemical impedance spectroscopy in proton exchange membrane fuel cells. *International Journal of Energy Research*, 29(12): 1133–1151.

Gowda, S.R., Leela Mohana Reddy, A., Zhan, X., Jafry, H.R. & Ajayan, P.M. 2012. 3D nanoporous nanowire current collectors for thin film microbatteries. *Nano Letters*, 12(3): 1198–1202.

Graef,M. & Henry,E.H.2007.*Structure of materials*.Cambridge press.New York.

Grieshaber, D., MacKenzie, R., Vörös, J. & Reimhult, E. 2008. Electrochemical Biosensors - Sensor Principles and Architectures. *Sensors*, 8(3): 1400–1458.

Han,J.2001.*A study of α-iron oxide as a gas sensing material*.PhD Thesis.University of South Australia.

Hayashi, T., Sakurada, I., Honda, K., Motohashi, S. & Uchikura, K. 2012. Electrochemical Detection of Sugar-related Compounds Using Boron-doped Diamond Electrodes. *Analytical Sciences*, 28(2): 127.

He, Z. & Mansfeld, F. 2009. Exploring the use of electrochemical impedance spectroscopy (EIS) in microbial fuel cell studies. *Energy Environ. Sci.*, 2(2): 215–219.

Hess, E. 2010. Boron-doped Diamond Sensors for the Determination of Organic Compounds in Aqueous Media. MSc Thesis. University of Western Cape.

Huang, J. & Wan, Q. 2009. Gas sensors based on semiconducting metal oxide one-dimensional nanostructures. *Sensors*, 9(12): 9903–9924.

Jasiecki, S., Czupryniak, J., Ossowski, T. & Schroeder, G. 2013. FTO coated glass electrode functionalization with transition metal cations receptors via electrostatic self-assembly. *International Journal of Electrochemical Science*, 8(12): 12543–12556.

Jiang, S.P. & Tseung, A.C.C. 1990. Homogeneous and Heterogeneous Catalytic Reactions in Cobalt Oxide/Graphite Air Electrodes III . Deposition of Cobalt Oxide Catalysts onto Graphite Electrodes for Oxygen Reduction. *Journal of The Electrochemical Society*, 137(11): 3442–3446.

Kamat, A., Huth, A., Klein, O. & Scholl, S. 2010. Chronoamperometric investigations of the electrode-electrolyte interface of a commercial high temperature PEM fuel cell. Fuel Cells, 10 (6):983 - 992.

Kamitaka, Y., Tsujimura, S., Setoyama, N., Kajino, T. & Kano, K. 2007. Fructose/dioxygen biofuel cell based on direct electron transfer-type bioelectrocatalysis. *Physical Chemistry Chemical Physics*, 9: 1793–1801.

Kandalkar, S.G., Gunjakar, J.L. & Lokhande, C.D. 2008. Preparation of cobalt oxide thin films and its use in supercapacitor application. *Applied Surface Science*, 254(17): 5540–5544.

Karim-Nezhad, G., Hasanzadeh, M., Saghatforoush, L., Shadjou, N., Earshad, S. & Khalilzadeh, B. 2009. Kinetic Study of Electrocatalytic Oxidation of Carbohydrates on Cobalt Hydroxide Modified Glassy Carbon Electrode. *Journal of the Brazilian Chemical Society*, 20(1): 141–151.

Katona, Z.., Sass, P. & Molnár-Perl, I. 1999. Simultaneous determination of sugars, sugar alcohols, acids and amino acids in apricots by gas chromatography–mass spectrometry. *Journal of Chromatography A*, 847(1–2): 91–102.

Kawasaki, T., Igarashi, K., Ogata, N., Oka, Y., Ichiyanagi, K. & Yamanouchi, T. 2012. Markedly increased serum and urinary fructose concentrations in diabetic patients with ketoacidosis or ketosis. *Acta Diabetologica*, 49(2): 119–123.

Koza, J.A., He, Z., Miller, A.S. & Switzer, J.A. 2012. Electrodeposition of Crystalline Co 3 O 4 —A Catalyst for the Oxygen Evolution Reaction. *Chemistry of Materials*, 24(18): 3567–3573.

Labib, M., Sargent, E.H. & Kelley, S.O. 2016. Electrochemical Methods for the Analysis of Clinically Relevant Biomolecules. *Chemical Reviews*, 116(16): 9001–9090.

Lang, X.-Y., Fu, H.-Y., Hou, C., Han, G.-F., Yang, P., Liu, Y.-B. & Jiang, Q. 2013. Nanoporous gold supported cobalt oxide microelectrodes as high-performance electrochemical biosensors. *Nature Communications*, 4: 1–8.

Le, W.Z. & Liu, Y.Q. 2009. Preparation of nano-copper oxide modified glassy carbon electrode by a novel film plating/potential cycling method and its characterization. *Sensors and Actuators, B: Chemical*, 141(1): 147–153.

Lee, H.S. & Coates, G.A. 2000. Quantitative Study of Free Sugars and Myo-Inositol in Citrus Juices By Hplc and a Literature Compilation. *Journal of Liquid Chromatography & Related Technologies*, 23(14): 2123–2141.

Li, X., Zhu, Y., Cai, W., Borysiak, M., Han, B., Chen, D., Piner, R.D., Colombo, L. & Ruoff, R.S. 2009. Transfer of Large-Area Graphene Films for High-Performance Transparent Conductive Electrodes.Nano Letters,9(12):4359 - 4363.

Liu, A. 2008. Towards development of chemosensors and biosensors with metal-oxide-based nanowires or nanotubes. *Biosensors and Bioelectronics*, 24(2): 167–177.

MacDonald, D.D. 2006. Reflections on the history of electrochemical impedance spectroscopy.

Electrochimica Acta, 51(8–9): 1376–1388.

Macdonald, J.R. 1987. Impedance spectroscopy and its use in analyzing the steady-state AC response of solid and liquid electrolytes. *Journal of Electroanalytical Chemistry*, 223(1–2): 25–50.

Marbán, G., López, I., Valdés-Solís, T. & Fuertes, A.B. 2008. Highly active structured catalyst made up of mesoporous Co3O4 nanowires supported on a metal wire mesh for the preferential oxidation of CO. *International Journal of Hydrogen Energy*, 33(22): 6687–6695.

Monk, P.M.S. & Ayub, S. 1997. Solid-state properties of thin film electrochromic cobalt-nickel oxide. *Solid State Ionics*, 99(1–2): 115–124.

Nam, K.T. 2006. Virus-Enabled Synthesis and Assembly of Nanowires for Lithium Ion Battery Electrodes. *Science*, 312(5775): 885–888.

Neghmouche, N.S. & Lanez, T. 2013. Calculation of Diffusion Coefficients and Layer Thickness for Oxidation the Ferrocene using Voltammetry Technique. *International Journal of Chemical Studies*, 1(1): 2321–4902.

Neiva, E.G.C., Oliveira, M.M., Bergamini, M.F., Marcolino, L.H. & Zarbin, A.J.G. 2016. One material, multiple functions: Graphene/Ni(OH)2 thin films applied in batteries, electrochromism and sensors. *Scientific Reports*, 6(July): 1–14.

Paredes, P.A., Parellada, J., Fernández, V.M., Katakis, L. & Domínguez, E. 1997. Amperometric mediated carbon paste biosensor based on D-fructose dehydrogenase for the determination of fructose in food analysis. *Biosensors and Bioelectronics*, 12(12): 1233–1243.

Patil, P.., Kadam, L.. & Lokhande, C.. 1998. Studies on electrochromism of spray pyrolyzed cobalt oxide thin films. *Solar Energy Materials and Solar Cells*, 53(3–4): 229–234.

Pavinatto, A., Mercante, L.A., Leandro, C.S., Mattoso, L.H.C. & Correa, D.S. 2015. Layer-by-Layer assembled films of chitosan and multi-walled carbon nanotubes for the electrochemical detection of 17α-ethinylestradiol. *Journal of Electroanalytical Chemistry*, 755: 215–220.

Polo da Fonseca, C.N., De Paoli, M.A. & Gorenstein, A. 1994. Electrochromism in cobalt oxide thin films grown by anodic electroprecipitation. *Solar Energy Materials and Solar Cells*, 33(1): 73–81.

Prabhulkar, S., Tian, H., Wang, X., Zhu, J.-J. & Li, C.-Z. 2012. Engineered Proteins: Redox

Properties and Their Applications. *Antioxidants & Redox Signaling*, 17(12): 1796–1822.

Prasad, R. & Bhat, B.R. 2015. Self-assembly synthesis of Co 3 O 4 /multiwalled carbon nanotube composites: an efficient enzyme-free glucose sensor. *New Journal of Chemistry*, 39(12): 9735–9742.

Qi, X., Watanabe, M., Aida, T.M. & Smith, R.L. 2008. Catalytical conversion of fructose and glucose into 5-hydroxymethylfurfural in hot compressed water by microwave heating. *Catalysis Communications*, 9(13): 2244–2249.

Randviir, E.P. & Banks, C.E. 2013. Electrochemical impedance spectroscopy: an overview of bioanalytical applications.Analytical Methods,5(5):1098 - 1115.

Randviir, E.P., Brownson, D.A.C., Gómez-Mingot, M., Kampouris, D.K., Iniesta, J. & Banks, C.E. 2012. Electrochemistry of Q-Graphene. *Nanoscale*, 4(20): 6470 - 6480

Rassaei, L. 2008. *Assembly and Characterization of Nanomaterials into Thin Film Electroanalysis*.PhD.Thesis,University of Kuopio,Finland. http://www.oppi.uef.fi/uku/vaitokset/vaitokset/2008/isbn978-951-2709-72-4.pdf

Reitz, E., Jia, W., Gentile, M., Wang, Y. & Lei, Y. 2008. CuO nanospheres based nonenzymatic glucose sensor. *Electroanalysis*, 20(22): 2482–2486.

Riu, J., Maroto, A. & Rius, F.X. 2006. Nanosensors in environmental analysis. *Talanta*, 69(2) : 288–301.

Seike, T., Nagai, J. & Seike Junichi, T.N. 1991. Electrochromism of 3d transition metal oxides. *Solar Energy Materials*, 22(2–3): 107–117.

Shekarchizadeh, H., Kadivar, M. & Ensafi, A.A. 2013. Rapid nonenzymatic monitoring of glucose and fructose using a CuO/multiwalled carbon nanotube nanocomposite-modified glassy carbon electrode. *Chinese Journal of Catalysis*, 34(6): 1208–1215.

Skale, S., Doleček, V. & Slemnik, M. 2007. Substitution of the constant phase element by Warburg impedance for protective coatings. *Corrosion Science*, 49(3): 1045–1055.

Spataru, N., Terashima, C., Tokuhiro, K., Sutanto, I., Tryk, D.A., Park, S.-M. & Fujishima, A. 2003. Electrochemical Behavior of Cobalt Oxide Films Deposited at Conductive Diamond Electrodes.

Journal of The Electrochemical Society, 150(7): E337 - E341.

Stradiotto, N.R., Yamanaka, H. & Zanoni, M.V.B. 2003. Electrochemical Sensors : A Powerful Tool in Analytical Chemistry. *Journal of the BrazilianChemicalSociety.*, 14(2): 159–173.

Stredansky, M., Pizzariello, A., Stredanska, S. & Miertus, S. 1999. Determination of D-fructose in foodstuffs by an improved amperometric biosensor based on a solid binding matrix. *Analytical Communications*, 36(2): 57–61.

Sung, W.J. & Bae, Y.H. 2000. A glucose oxidase electrode based on electropolymerized conducting polymer with polyanion-enzyme conjugated dopant. *Analytical chemistry*, 72(9): 2177–2181.

Suzuki, E. 2002. High-resolution scanning electron microscopy of immunogold-labelled cells by the use of thin plasma coating of osmium. *Journal of Microscopy-Oxford*, 208(December): 153–157.

Swann, M.J., Bloor, D., Haruyama, T. & Aizawa, M. 1997. The role of polypyrrole as charge transfer mediator and immobilization matrix for D-fructose dehydrogenase in a fructose sensor. *Biosensors and Bioelectronics*, 12(12): 1169–1182.

Thevenot, D., Toth, K., Durst, R., Wilson, G.. 2001. Electrochemical biosensors : recommended definitions and classification. *Biosensors & Bioelectronics*, 16 (1 - 2): 121–131.

Tkáč, J., Voštiar, I., Šturdík, E., Gemeiner, P., Mastihuba, V. & Annus, J. 2001. Fructose biosensor based on D-fructose dehydrogenase immobilised on a ferrocene-embedded cellulose acetate membrane. *Analytica Chimica Acta*, 439(1): 39–46.

Tominaga, M., Hashimoto, S., Misaka, A. & Nakashima, N. 1999. Thermal stability and electrode reaction of chlorella ferredoxin embedded in artificial lipid bilayer membrane films on a graphite electrode. *Analytical Chemistry*, 71(14): 2790–2796.

Trivedi, U.B., Lakshminarayana, D., Kothari, I.L., Patel, P.B. & Panchal, C.J. 2009. Amperometric fructose biosensor based on fructose dehydrogenase enzyme. *Sensors and Actuators, B: Chemical*, 136(1): 45–51.

Urdea, M., Penny, L. A, Olmsted, S.S., Giovanni, M.Y., Kaspar, P., Shepherd, A., Wilson, P., Dahl, C.A , Buchsbaum, S., Moeller, G. & Burgess, D.C.H. 2006. Requirements for high impact diagnostics in the developing world. *Nature*, 73–79.

Veqter Technologies. 2018. X-ray Diffraction Technique. Online.Available at: http://www.veqter.co.uk/assets/files/rsm-techniques/veqter-x-ray-diffraction-technique.pdf. [Accessed April,30 2018].

Walter, G.W. 1986. A review of impedance plot methods used for corrosion performance analysis of painted metals. *Corrosion Science*, 26(9): 681–703.

Wang, H. & Pilon, L. 2012. Intrinsic limitations of impedance measurements in determining electric double layer capacitances. *Electrochimica Acta*, 63: 55–63.

Wang, L., Zhao, J., He, X., Gao, J., Li, J., Wan, C. and Jiang, C. 2012. Electrochemical Impedance Spectroscopy (EIS) Study of LiNi1/3Co1/3Mn1/3O2 for Li-ion Batteries. *International Journal of Electrochemical Science*, 7(1): 345–353.

Wang, H., Zhang, L., Tan, X., Holt, C.M.B., Zahiri, B., Olsen, B.C. & Mitlin, D. 2011. Supercapacitive Properties of Hydrothermally Synthesized Co3O4 Nanostructures. *Journal of Physics Chemical C*, 115: 17599–17605.

Wang, W., Gao, S. & Wang, B. 1999. Building fluorescent sensors by template polymerization: the preparation of a fluorescent sensor for D-fructose. *Organic letters*, 1(8): 1209–12.

Wang, X., Hu, C., Liu, H., Du, G., He, X. & Xi, Y. 2010. Synthesis of CuO nanostructures and their application for nonenzymatic glucose sensing. *Sensors and Actuators, B: Chemical*, 144(1): 220–225.

Wang, X., Zhi, L. & Müllen, K. 2008. Transparent, conductive graphene electrodes for dye-sensitized solar cells. *Nano Letters*, 8(1): 323–327.

Wang, Y., Wang, W. & Song, W. 2011. Binary CuO/Co3O4 nanofibers for ultrafast and amplified electrochemical sensing of fructose. *Electrochimica Acta*, 56(27): 10191–10196.

Williams,D.B.1984.Practical analytical electron microscopy in materials science.Deerfield beach,Electron optics publishing group.Florida.

Wu, J., Yuan, X.Z., Wang, H., Blanco, M., Martin, J.J. & Zhang, J. 2008. Diagnostic tools in PEM fuel cell research: Part I Electrochemical techniques. *International Journal of Hydrogen Energy*, 33(6): 1735–1746.

Xu, D., Luo, L., Ding, Y., Jiang, L., Zhang, Y., Ouyang, X. & Liu, B. 2014a. A novel nonenzymatic fructose sensor based on electrospun LaMnO3 fibers. *Journal of Electroanalytical Chemistry*, 727: 21–26.

Xu, D., Luo, L., Ding, Y., Jiang, L., Zhang, Y., Ouyang, X. & Liu, B. 2014b. A novel nonenzymatic fructose sensor based on electrospun LaMnO3 fibers. *Journal of Electroanalytical Chemistry*, 727: 21–26.

Yabuki, S. & Mizutani, F. 1997. D-fructose sensing electrode based on electron transfer of D-fructose dehydrogenase at colloidal gold enzyme modified electrode. *Electroanalysis*, 9(1): 23–25.

Yamada, Y., Aida, K. & Uemura, T. 1966. A new enzyme, d-fructose dehydrogenase. *Agricultural and Biological Chemistry*, 30(1): 95–96.

Yang, J., Jiang, L.C., Zhang, W.D. & Gunasekaran, S. 2010. A highly sensitive non-enzymatic glucose sensor based on a simple two-step electrodeposition of cupric oxide (CuO) nanoparticles onto multi-walled carbon nanotube arrays. *Talanta*, 82(1): 25–33.

Yang, P., Zheng, Q., Xu, H., Liu, J. & Jin, L. 2012. A highly sensitive electrochemical impedance spectroscopy immunosensor for determination of 1-pyrenebutyric acid based on the bifunctionality of Nafion/gold nanoparticles composite electrode. *Chinese Journal of Chemistry*, 30(5): 1155–1162.

Yuan, P., Zhang, N., Zhang, D., Liu, T., Chen, L., Liu, X., Ma, R. & Qiu, G. 2014. Fabrication of nickel-foam-supported layered zinc–cobalt hydroxide nanoflakes for high electrochemical performance in supercapacitors. *Chemical Communications*, 50(76): 11188.

Zaban, A., Zinigrad, E. & Aurbach, D. 1996. Impedance spectroscopy of Li electrodes. 4. A general simple model of the Li-solution interphase in polar aprotic systems. *Journal of Physical Chemistry*, 100(8): 3089–3101.

Zhai, T., Fang, X., Liao, M., Xu, X., Zeng, H., Yoshio, B. & Golberg, D. 2009. A comprehensive review of one-dimensional metal-oxide nanostructure photodetectors. *Sensors*, 9(8): 6504–6529.

Zhou, S., Wei, D., Shi, H., Feng, X., Xue, K., Zhang, F. & Song, W. 2013. Sodium dodecyl benzene sulfonate functionalized graphene for confined electrochemical growth of metal/oxide nanocomposites for sensing application. *Talanta*, 107: 349–355.

Full Paper

Wiley Online Library

ELECTROANALYSIS

DOI: 10.1002/elan.201700503

Non-enzymatic Fructose Sensor Based on Co_3O_4 Thin Film

Tatenda Gota,[a, b] Mahabubur Chowdhury,*[a, b] and Tunde Ojumu[a, b]

Abstract: In this study, we report on the selective of fructose on Co_3O_4 thin film electrode surface. A facile chemical solution deposition technique was used to fabricate Co_3O_4 thin film on fluorine doped tin oxide, FTO, glass. Electrode characterization was done using XRD, HRTEM, SEM, AFM, and EIS. The constructed sensor exhibited two distinctive linear ranges (0.021–1.74 mM; 1.74–~15 mM) covering a wide linear range of up to ~15 mM at an applied potential of +0.6 V vs Ag/AgCl in 0.1 M NaOH solution. The sensor demonstrated high, reproducible and repeatable (R.S.D of <5%) sensitivity of 495 (lower concentration range) & 53 (higher concentration range) $\mu A\,cm^{-2}\,mM^{-1}$. The sensor produced a low detection limit of ~1.7 μM ($S/N = 3$). The electrode was characterised by a fast response time of < 6 s and long term stability. The repeatability and stability of the electrode resulted from the chemical stability of Co_3O_4 thin film. The sensor was highly selective towards fructose compared to the presence of other key interferences i.e. AA, AC, UA. The ease of the electrode fabrication coupled with good electrochemical activity makes Co_3O_4 thin film, a promising candidate for non-enzymatic fructose detection.

Keywords: Biosensor · Thin film · Cobalt oxide · Voltammetry · D-fructose

1 Introduction

Fast, sensitive, selective and economical fructose detection is highly demanded; because fructose detection is incredibly important to clinical and food and beverage industries. Fructose is a characteristic dietary source of carbohydrates mostly found in fruits [1], honey, soft drinks [2] and processed foods [3] etc. Fructose is also found in various physiological fluids such as blood serum and urine [1]. The average physiological fructose concentration in serum lies in the ranges of 6.1–9.1 μmol/L, whilst concentrations in urine are anything between 14.7– 60 μmol/day [1]. Recent studies have indicated increased serum and urinary fructose concentrations in diabetic patients [4,5] besides glucose. A variety of conventional laboratory techniques are currently available for the detection of fructose, e.g., chromatography [6]; flourometry [5,7,8], colorimetry [5,9], electrophoresis, titration, spectrophotometry [5,10,11] etc. Although these methods can provide an accurate determination of fructose, the methods are tedious, require rigorous sample pre-treatment, sophisticated equipment, highly trained personnel, immense amount of attention in the analysis [12,13]. Therefore, a simple, fast and sensitive method for the determination of fructose is a vital step in food research, as well as in industry of medical devices for personal use [14]. Currently electrochemical detection of fructose can be considered as a cheap and viable mode of fructose detection. Electrochemical fructose sensors are classified into two categories: fructose dehydrogenase (FDH)-based sensor (enzymatic sensors) and non-enzymatic sensor. Several literatures have reported FDH-based biosensors [15,16,17,18]. However, FDH-based biosensors suffer from problems; such as, stability, requirements for different cofactors and the complexity of the immobilisation procedures [5,19,20]; despite of its high sensitivity and selectivity to fructose over a broad range of pH.

Metal oxide based non-enzymatic sensors are interesting due to their ability for the electrocatalytic oxidation of both organic and inorganic materials. However, very limited number of studies have been reported on non-enzymatic detection of fructose [21,22], [23,24,25]. However, previous studies on non-enzymatic fructose detection reported on low sensitivity, high detection limit and short linear range for fructose detection. The use of various cobalt oxides such as, cobaltous oxide (CoO), cobaltic oxide (Co_2O_3) and cobaltosic oxide (Co_3O_4) is increasingly gaining attention [26] in biosensor applications. Compared to other cobalt oxides, Co_3O_4 has attracted great interests owing to its high specific area and good electrochemical activity [25,27]. However, previous attempts to utilise Co_3O_4 for amperometric detection of fructose is very limited. Various methods have been reported for deposition of various metal oxides including Co_3O_4 on substrates; such as, hydrothermal deposition [28], electrodeposition [29,30,31,32], electroprecipitation [30], sol-gel process [33] and powder immobilization [34]. However, most of these techniques may not be commercially scalable and electrodes prepared via these routes exhibit low electronic conductance due to low electron

[a] T. Gota, M. Chowdhury, T. Ojumu
Flow process and Rheology Centre, Cape Peninsula University of Technology, Cape Town-8000, South Africa
E-mail: chowdhurym@cput.ac.za
[b] T. Gota, M. Chowdhury, T. Ojumu
Department of Chemical Engineering, Cape Peninsula University of Technology, Cape Town-8000, South Africa

Supporting information for this article is available on the WWW under https://doi.org/10.1002/elan.201700503

© 2017 Wiley-VCH Verlag GmbH & Co. KGaA, Weinheim

transport as well as high contact resistances [35,36] due to addition of binders (especially for powder immobilization), which hinders their electrocatalytic efficiency. In addition to this, high vacuum processes such as, plasma sputtering [37], electron beam evaporation [38], atomic layer deposition [39] have also been used to deposit Co_3O_4 directly on substrates. However, these methods are very tedious and the involvement of high vacuum equipment in some of the processes requires maintenance and are capital intensive.

In this study, we have deposited Co_3O_4 thin film on FTO support via a two-step spin coating of chemical solution for fructose detection. The prepared sensor exhibited fast, sensitive and wide linear range detection of fructose.

2 Experimental

2.1 Materials and Chemicals

All reagents and chemicals used in this work were of the analytical reagent grade and used as received without any further purification. D (−) fructose ($C_6H_{12}O_6$), Sodium Hydroxide pellets (NaOH) (99.9%), Phosphate Buffer Solution (PBS, pH 7.4), Toluene ($C_6H_5CH_3$), Ethanol (C_2H_5OH), Ascorbic acid (AA), D(−), Glucose ($C_6H_{12}O_6$), Uric Acid (UA), Acetaminophen (AC), Sodium Chloride (NaCl), Potassium Chloride (KCl), Potassium Ferricyanide Trihydrate ($K_4Fe(CN)_6.3H_2O$) were all obtained from Sigma-Aldrich, South Africa. Deionised water (18.2 MΩ) was used for all aqueous solution preparations.

2.2 Co_3O_4/FTO Electrode Fabrication

A two-step spin-coating procedure of a chemical solution as previously described [40,41] was used to deposit the Co_3O_4 film on FTO glass slide. For this procedure, FTO glass sheets (surface resistivity ~7 Ω/sq) purchased from Sigma-Aldrich, South Africa were cut to size using a diamond glass cutter and a pair of pliers. For the removal of any adsorbed material on the FTO glass surface, such precut FTO glasses were cleaned following standard cleaning procedures. The clean FTO glasses were dried at 60 °C under air. Cleaned FTO glass surfaces were demarcated (1 cm × 1 cm) using transparent tape. Precursor solution was prepared by dissolving 0.09 g of cobalt-oleate in 0.5 cm^3 toluene. 50 µL of the cobalt oleate solution was spin-coated on the demarcated glass surfaces using a spin coater set at 2500 rpm for 30 s and at 4000 rpm for 60 s. Different layers were added to the FTO glass (i.e. N = 1, 2…). Each layer was allowed to calcine at 350 °C for 10 minutes and subsequent layers were added in a similar fashion. The final layer was calcined for 5 h. The modified electrodes were stored at ambient temperature (25 °C) before being used in experiments.

2.3 Instrumentation and Measurements

The crystal structure of the electrodes was determined by XRD. The X-ray patterns of the electrodes were recorded using PANalytical X'pert PRO PW 3040/60 diffractometer. An FEI Tecnai F20 TEM operated at 200 kV, equipped with a Gatan GIF-2001 energy filter was utilised to extract high-resolution transmission electron microscopy (HR-TEM) and selected area electron diffraction (SAED) images. Atomic force microscopy (AFM) was used to analyse the surface roughness of the thin film electrode. The AFM measurements were carried out in air under ambient conditions with a commercial Agilent 5500 AFM (Agilent Technologies, USA) in the contact mode at a scanning rate of 1 line per second. All electrochemical measurements were performed using an Autolab PGSTAT302N potentiostat (Metrohm Autolab, Netherlands). A three electrode setup; graphite rod, prepared electrode and Ag/AgCl electrodes were used as counter electrode, working electrode and reference electrodes respectively. Cyclic voltammetry and chronoamperometry studies were conducted in a 0.1 M NaOH electrolyte solution. Chronoamperometric studies were carried out at an applied potential of +0.60 V vs Ag/AgCl. For this procedure, various concentrations of fructose were added in the electrolyte solution at a 30 s interval. Electrochemical impedance spectroscopy (EIS) studies were performed in PBS solution containing 5.0 mM $K_4Fe(CN)_6.3H_2O$ at an applied bias potential of 0.25 V with 5 mV amplitude, in the frequency range 0.1 Hz to 100 kHz [42]. The results were plotted as Bode plots.

3 Results and Discussion

3.1 Surface Morphology of the Co_3O_4 Modified FTO Electrode

High-resolution SEM and TEM were used to evaluate the morphology and structure of the solution deposited film. The SEM and TEM images of the as prepared film is shown in Figure 1. The resulted film thickness was found to be 665 nm as was measured from the cross sectional view of the film (Figure 1a). The film has interconnected aggregated porosity and a rough surface, as can be observed from the SEM (Figure 1b) and AFM topography image (Figure 1c). The roughness of the film can provide increased surface area for enhanced electrocatalytic oxidation of fructose. The aggregated particles are nanoclusters of a single crystalline state as was observed from the HR-TEM image (Figure 1d). The first three diffraction patterns (SAED, Figure 1e) from the film yields d (111) = 0.481 nm, d (220) = 0.294 nm and d (311) = 0.249 nm, with a lattice constant a = 0.831 nm which corresponds largely to the diffraction from the Co_3O_4 lattice. XRD patterns (Figure 1f) matches very well with the diffraction pattern of crystalline cubic Co_3O_4 structure (JCPDS card no: 76–1802) with the exposed {111} facet corresponding to the exposure of high density, low surface

 © 2017 Wiley-VCH Verlag GmbH & Co. KGaA, Weinheim

Cape Peninsula University of Technology

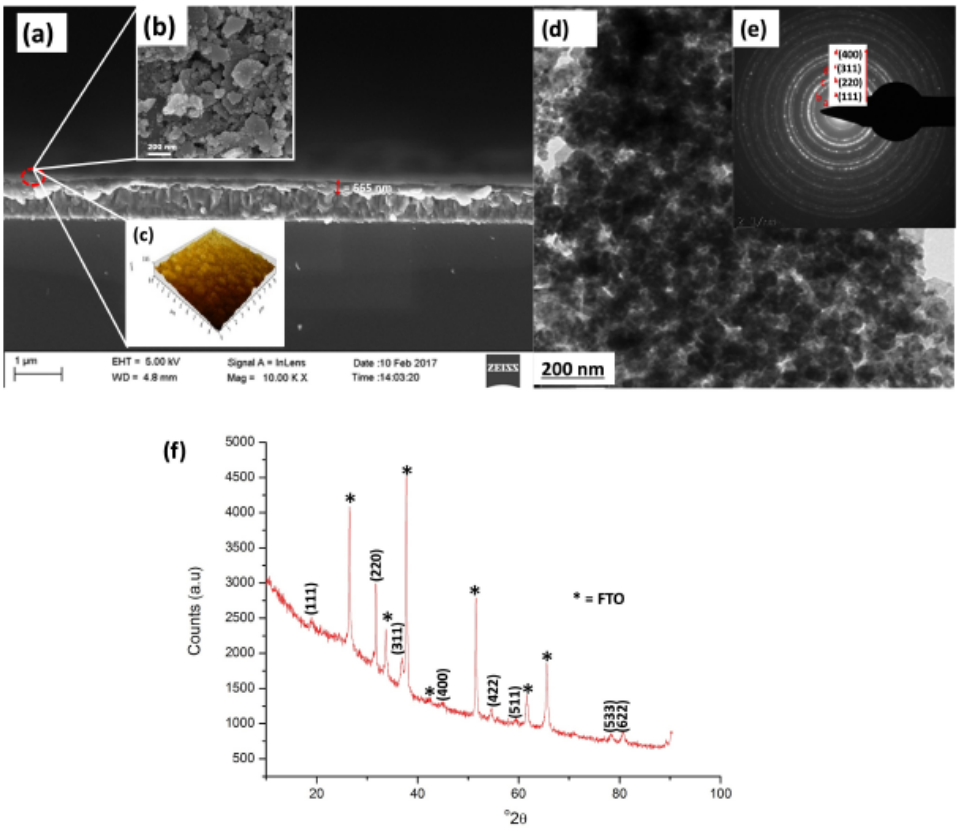

Fig. 1. (a) Cross sectional SEM image of the Co_3O4 film deposited on FTO (inset b & c: SEM and AFM image of the surface of the film respectively), (d) TEM image of the Co_3O_4 film (inset e: SAED of the Co_3O_4 particles) & (f) XRD pattern of the Co_3O_4 modified thin film electrode.

energy planes. The XRD results correspond very well with the recorded SAED patterns of the Co_3O_4 film.

3.2 Electrochemical Behaviour of the Co_3O_4 Modified FTO

Cyclic voltammetry (CV) was used to evaluate the performance of Co_3O_4 modified electrode for the electrocatalytic detection of fructose in 0.1 M NaOH solution (unless otherwise stated). The CV's were recorded in the potential range of −0.2 to +0.8 V vs. Ag/AgCl. Figure 2a demonstrates the CV's of Co_3O_4 electrode both in the absence and presence of 1 mM fructose at 25 $mV\,s^{-1}$. It can be seen from Figure 2a that FTO displayed no oxidation behaviour both in the absence and presence of fructose in the potential window of −0.2 to +0.8 V. The Co_3O_4 thin film electrode resulted in an increase in both the anodic current in the presence and absence of fructose. Two sets of redox peaks were observed from Figure 2a. The first set of peak is (I/II) attributed to the reversible transition between Co and CoOOH. The second redox pair (III/IV) is attributed to the conversion between CoOOH and CoO_2 [43]. The anodic current increased significantly in the presence of fructose due to the Co_3O_4 catalytic oxidation of fructose. The mechanism of electrocatalytic oxidation of fructose by Co_3O_4 in alkaline media is not well understood [44]. The electrocatalytic mechanism of fructose sensing on the Co_3O_4 surface is a multistep process which can be presented in the following manner [44]:

$$Co(III) \leftrightarrow Co(IV) + e \quad (1)$$

$$Co(IV) + fructose \rightarrow Intermediate + Co(III) \quad (2)$$

$$Co(IV) + Intermediate \rightarrow Product + Co(III) \quad (3)$$

It is considered that initially the Co(III) is oxidised to Co(IV) in a reversible aqueous reaction as in Equa-

 © 2017 Wiley-VCH Verlag GmbH & Co. KGaA, Weinheim

Cape Peninsula University of Technology

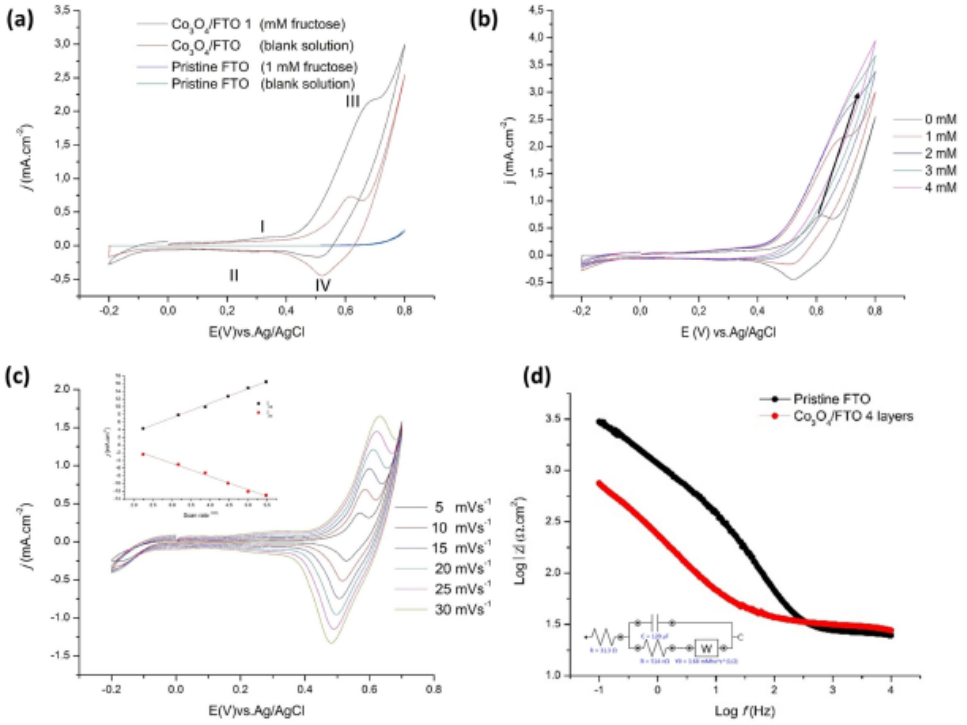

Fig. 2. (a) Electrochemical behaviour of the Co_3O_4 thin film electrode in the presence and absence of 1 mM fructose at 25 mVs^{-1}, (b) CV's of the Co_3O_4 electrode in the presence of 0–5 mM fructose concentration at 25 mVs^{-1}, (c) CV's at various scan rate (inset: relationship between peak current and square root of scan rate) and (d) Bode plot of the Co_3O_4 electrode.

tion (1). The addition of fructose enhances a surface-based reaction which further leads to the oxidation of the hydroxyl (OH) group of the fructose to give a reactive intermediate and Co(III) through and irreversible reaction as indicated by Equation (2). The intermediate reacts with the Co (IV) to generate the product and regenerate the Co (III) as in Equation (3). Thus, it is likely that the Co(IV) generated in reaction (2) is the active species, which is effective in the speeding up the oxidation of fructose.

It is worthy of emphasis that an increment in the concentration of fructose results in proportionally linear enhancement of the anodic peak current and a shift in the peak current toward the positive potential window (see Figure 2b). However, no significant shift in cathodic peak current was observed. The changes in the peak definitions of the cyclic voltammetry can be attributed to the changes of CoO_2 and CoOOH (redox peak III / IV) species concentrations [45]. The results clearly show that the Co_3O_4 nanoparticles are suitable mediators for the shuttling of electrons between the fructose molecules and the working electrode, resulting in high catalytic activity for fructose oxidation. This may be due to the morphology of the Co_3O_4 which not only offers larger space for ion diffusion, but also increase the available catalytic material for fructose oxidation.

Various concentration of electrolytes (0.05, 0.1, 0.5 and 1 M NaOH) were used to evaluate the effect of OH^- ions on the oxidation of fructose (Supplementary document, S1). The anodic currents increased with increasing electrolyte concentration indicating an increase in the specific capacitance. It is, therefore, most likely that the CV of the solution was influenced significantly by the presence of the OH^-. However, in this study 0.1 M NaOH solution was used as a base electrolyte for comparison purpose with previous literature [25,46,47].

A comparison of the CV's at various scan rates (Figure 2c) were conducted and a direct correlation between the peak current and the square root of the scan rate was found. This linearity indicated that the kinetics of the reaction was diffusion based, surface controlled [48] electrochemical reaction.

EIS was used to gain insight of the interfacial properties of the Co_3O_4 thin film electrode. Figure 2d shows the corresponding Bode plot obtained for the FTO and Co_3O_4/FTO coated electrodes (N = 4, where N is the

 © 2017 Wiley-VCH Verlag GmbH & Co. KGaA, Weinheim

Cape Peninsula University of Technology

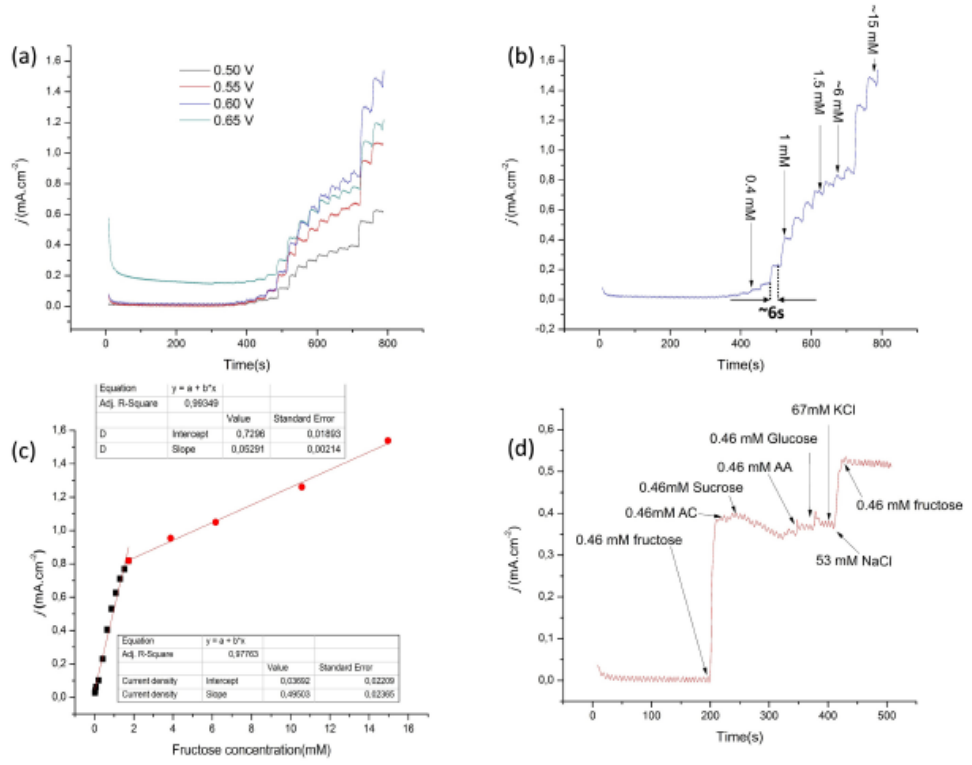

Fig. 3. (a) Chronoamperometry data of the electrode at various applied potential, (b) chronoamperometry data at an applied potential of +0.6 V, (c) dose response curve obtained at various fructose concentration and (d) selectivity performance of the Co3O4 thin film electrode.

number of layers) at 0.25 V (applied bias potential). The comparison of log |Z| vs log *f* for the FTO and the Co_3O_4 distinctively shows that the charge transfer resistance decrease significantly with the presence of Co_3O_4; highlighting the good electrochemical activity of the Co_3O_4. Various layers of Co_3O_4 were also deposited on the FTO glass slide. It could be seen from the Nyquist plot that by the addition of each layer charge transferability increases (Supplementary document, S2 a), resulting in enhanced electrochemical activity (Supplementary document, S2 b). However, it was seen from the CV data that the oxidation potential shifts slightly towards more positive value when 6 layers of Co_3O_4 were deposited. This can be due to the rate of the catalysis of fructose being faster than its diffusion due to increased film thickness. Hence, only 4 layer of Co_3O_4 was considered as optimum in this study.

3.3 Chronoamperometric Studies on Fructose Detection

Chronoamperometry under stirring condition was used to evaluate the performance of the Co_3O_4/FTO thin film electrode toward the direct fructose detection (in 0.1 M NaOH solution). Various potential was applied to find the optimum potential for fructose detection (Figure 3a). Typical step response was obtained for all applied potential. The current density increased with increasing applied potential in the potential rang of +0.5 to +0.6 V. However, at +0.65 V the back ground current increased significantly, but the oxidation current decreased, compared to +0.6 V. This can be due to the initiation of parasitic reaction from the electrolysis of water. Hence, +0.6 V was chosen to be suitable potential for fructose detection. A fast response time of 6 s (to reach 95% steady state after injection) was recorded during the successive addition of fructose (Figure 3b). A fast response time translates to a facile electron transfer process on the Co_3O_4 surface. It could be observed that there was a slight baseline drift at high fructose concentration. This is due to the variation of the localised pH, the rate of the catalysis of fructose being faster than its diffusion and also adsorption of intermediates on catalyst surface [45].

 © 2017 Wiley-VCH Verlag GmbH & Co. KGaA, Weinheim

Cape Peninsula University of Technology

Table 1. Comparison of the fructose sensing characteristics of various nanomaterial modified electrodes prepared by different methods.

Electrode materials	Electrode preparation route	Supporting electrode	Applied potential V vs. Ag/AgCl	Linear range (mM)	Sensitivity ($\mu A.cm^{-2}.mM^{-1}$)	LOD (μM)	Response time (s)	Reference
$LaMnO_3$	Electrospinning	Glassy Carbon	+0.60	0.4–4	1238.5	63	15	[21]
SDBS/Co-Cu	Electrodeposition	Graphene	+0.40	0.003–1	932	–	<1	[22]
CNT-NiCo-oxide	Simple deposition	Screen-printed	0.35	0.02–0.675 0.675–12.12	2.5 ± 0.8 1.08 ± 0.009	9.5	-	[23]
CuO/Co_3O_4	Electrospinning	Glassy carbon	+0.30	0.01–3	18.988	3	1	[24]
Au/Co	Electrochemical & hydrothermal	Au	+0.26	0.001–0.01	12.5	0.005	<1	[46]
Nano-Ni(II)-curcumin	Electrodeposition	Glassy Carbon	+0.70	0.01–0.10	8.8285	≈0.98	~10	[47]
CS-PDDA-nano-PB/nano-Au/MPBA	Solution casting	Glassy Carbon	–	0.1–0.5	0.94	0.022	~10	[52]
Co/Al layered double hydroxide	Electrodepoition	Pt	+0.5	–	70	10		[53]
Co_3O_4	Spin-coating	FTO	+0.6	0.021–1.74 1.74–~15	398 & 53	1.7	~6	This work

Figure 3c demonstrates two distinctive linear ranges (0.021–1.74 mM; 1.74–~15 mM) covering a wide linear range of up to ~15 mM obtained from the dose response curve. The sensor exhibited a high sensitivity of 495 $\mu A\ cm^{-2} mM^{-1}$ for the lower concentration range. For higher concentration range the sensitivity was calculated to be 53 $\mu A\ cm^{-2} mM^{-1}$. The detection limit (LOD) of fructose (at $S/N = 3$) was calculated to be 1.7 μM. The serum fructose concentration is 7.1–9 μM in healthy patients and 8.2–15.8 μM in diabetic patients [1]. This falls well within the range of LOD for the developed sensor.

The selectivity of the fructose sensor in the presence of the key species that are contained in typical biological fluids, such as, glucose, ascorbic acid (AA), uric acid, acetaminophen (AC), potassium chloride (KCl) and sodium chloride (NaCl) was examined. The results in Figure 3d indicated that glucose and other key interference species did not cause any significant response. Prevention of interference species (AA, AC and UA) oxidation at +0.6 V can be due to the repelling effect on the Co_3O_4 surface [20] as the Co_3O_4 surface and the anionic species are negative in 0.1 M NaOH solution. It has been reported previously that chloride poisoning is a challenge for most of the precious metal and alloy based non-enzymatic glucose/fructose sensor [27,49]. It is noticeable from Figure 3d that injection of chloride ions did not result in significant amperometric response. However, consecutive addition of 0.46 mM fructose resulted in lower amperometric current response compared to initial injection of fructose. This can be due to the blocking of reactive sites due to the successive additions of high concentrations of interference. It is also understood that fructose is isomeric with glucose in many biological and food items [50] and that there is a coexistence between the two, and that it is difficult to detect glucose when fructose is present [51]. Ding and co-authors [20] coated Co_3O_4 with nafion to increase selectivity towards glucose. In our previous studies [45,41] we have doped Zn and Sn in Co_3O_4 host lattice to increase selectivity, linear ranges towards glucose oxidation as pristine Co_3O_4 presented very high and low LOD and linear ranges respectively (data not shown). Hence, it can be postulated that the developed Co_3O_4 thin film is more selective towards fructose oxidation compared to glucose (when the glucose concentration is less than 1 mM). It must be noted that the aim of this study was to demonstrate the potential of Co_3O_4 thin film for fructose oxidation. Hence, no real sample was utilised for evaluation purposes. Table 1 presents a performance summary of the various sensors reported for fructose detection.

3.4 Reproducibility, Stability and Shelf Life of the Co_3O_4 Thin Film Electrode

In order to evaluate the reproducibility of the Co_3O_4 sensor, a series of 6 electrodes were prepared and CV's were carried out. Each of the electrodes was stored under ambient temperature. The relative standard deviation (RSD) of 3.97% (n = 6) for 1 mM fructose demonstrated good inter-electrode reproducibility (Figure 4a). Chemical stability and repeatability of the sensor was determined by conducting CV experiments for 50 cycles in 1 mM fructose solution at a scan rate of 25 mV/s (Figure 4b). No new redox pairs were observed and no significant changes occurred in the existing redox peaks. This highlights good chemical stability and repeatability of the sensor. Additionally, the long-term stability was also an important parameter in the evaluation of the performance of the fabricated Co_3O_4 sensor. The shelf-life of the Co_3O_4 electrode was investigated by the consecutive measure-

 © 2017 Wiley-VCH Verlag GmbH & Co. KGaA, Weinheim

Cape Peninsula University of Technology

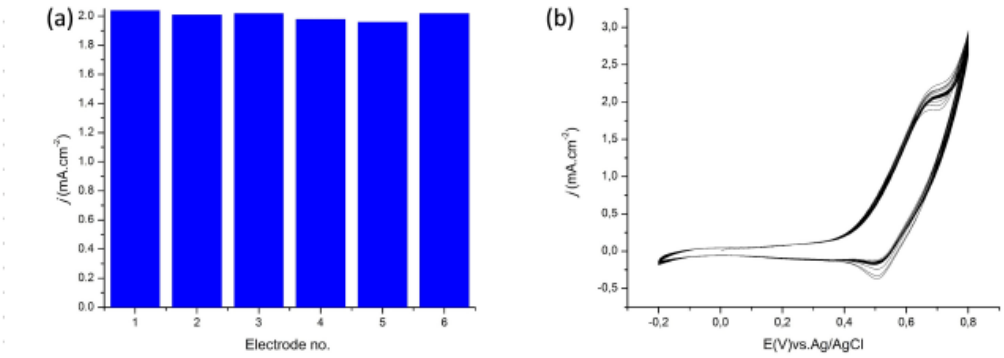

Fig. 4. (a) Inter electrode reproducibility and (b) chemical stability of the Co_3O_4 thin film electrode.

ments of the current response for 1 mM fructose solution over a 4-week period. During this period the sensor was stored at an ambient temperature of 25±2 °C under air, when not in use. The sensor maintained an 83% of its initial peak current response highlighting a good shelf-life (Supplementary document, S3).

4 Conclusions

This work demonstrated that Co_3O_4 thin film electrode, prepared via simple spin-coating of chemical solution can be utilised in rapid, sensitive, selective and wide linear range detection of fructose. The constructed sensor exhibited a wide linear range of up to ~15 mM and a LOD of 1.7 μM at a fast response rate of 6 s. This electrode have the potential to be applied as a sugar sensor in various hazardous environments.

Acknowledgements

Mahabubur Chowdhury would like to thank the National research foundation South Africa (Grant no: 88220) for supporting this study.

References

[1] T. Kawasaki, H. Akanuma, T. Yamanouchi, *Diabetes Care* **2002**, *25*, 353–357.
[2] S. S. Elliott, N. L. Keim, J. S. Stern, K. Teff, P. J. Havel, *Am. J. Clin. Nutr.* **2002**, *76*, 911–922.
[3] I. Šakinyte, J. Barkauskas, J. Gaidukevič, J. Razumiene, *Talanta* **2015**, *144*, 1096–1103.
[4] H. Yoshii, H. Uchino, C. Ohmura, K. Watanabe, Y. Tanaka, R. Kawamori, *Diabetes Res. Clin. Pract.* **2001**, *51*, 115–123.
[5] D. Thevenot, K. Toth, R. Durst, G. Wilson, D. Thevenot, K. Toth, R. Durst, G. Wilson, *Biosens. Bioelectron.* **2001**, *16*, 121–131.
[6] P. N. Wahjudi, M. E. Patterson, S. Lim, J. K. Yee, C. S. Mao, W. N. P. Lee, *Clin. Biochem.* **2010**, *43*, 198–207.
[7] J. L. Pablos, S. Vallejos, S. Ibeas, A. Muñoz, F. Serna, F. C. García, J. M. García, *ACS Macro Lett.* **2015**, *4*, 979–983.
[8] L. Feng, N. Yin, X. Wang, Z. Wang, *Sensors Actuators, B Chem.* **2013**, *181*, 730–734.
[9] O. B. Ayyub, M. B. Ibrahim, R. M. Briber, P. Kofinas, *Biosens. Bioelectron.* **2013**, *46*, 124–129.
[10] J. Biscay, E. Costa Rama, M. B. González García, A. Julio Reviejo, J. M. Pingarrón Carrazón, A. C. García, *Talanta* **2012**, *88*, 432–438.
[11] R. Antiochia, G. Vinci, L. Gorton, *Food Chem.* **2013**, *140*, 742–747.
[12] R. Antiochia, L. Gorton, *Sensors Actuators, B Chem.* **2014**, *195*, 287–293.
[13] H. Li, C. Yang, X. Zhu, H. Zhang, *Spectrochim. Acta Part A Mol. Biomol. Spectrosc.* **2017**, *180*, 199–203.
[14] F. Sun, T. Bai, L. Zhang, S. Liu, A. K. Nowinski, S. Jiang, Q. Yu, *Anal. Chem.* **2014**, *86*, 2387–2394.
[15] U. B. Trivedi, D. Lakshminarayana, I. L. Kothari, P. B. Patel, C. J. Panchal, *Sensors Actuators, B Chem.* **2009**, *136*, 45–51.
[16] J. Tkáč, I. Voštiar, E. Šturdík, P. Gemeiner, V. Mastihuba, J. Annus, *Anal. Chim. Acta* **2001**, 439, 39–46.
[17] C. A. B. Garcia, G. De Oliveira Neto, L. T. Kubota, *Anal. Chim. Acta* **1998**, *374*, 201–208.
[18] M. Tominaga, S. Nomura, I. Taniguchi, *Biosens. Bioelectron.* **2009**, *24*, 1184–1188.
[19] P. A. Paredes, J. Parellada, V. M. Fernandez, I. Katakis, E. Dominguez, *Biosens. Bioelectron. Elsevier Applied Science*, **1989**.
[20] Y. Ding, Y. Wang, L. Su, M. Bellagamba, H. Zhang, Y. Lei, *Biosens. Bioelectron.* **2010**, *26*, 542–548.
[21] D. Xu, L. Luo, Y. Ding, L. Jiang, Y. Zhang, X. Ouyang, B. Liu, J. *Electroanal. Chem.* **2014**, 727, 21–26.
[22] S. Zhou, D. Wei, H. Shi, X. Feng, K. Xue, F. Zhang, W. Song, *Talanta* **2013**, *107*, 349–355.
[23] A. Arvinte, A. M. Sesay, V. Virtanen, *Talanta* **2011**, *84*, 180–186.
[24] Y. Wang, W. Wang, W. Song, *Electrochim. Acta* **2011**, *56*, 10191–10196.
[25] X. Wang, C. Hu, H. Liu, G. Du, X. He, Y. Xi, *Sensors Actuators, B Chem.* **2010**, *144*, 220–225.
[26] P. M. S. Monk, S. Ayub, *Solid State Ionics* **1997**, *99*, 115–124.
[27] E. Reitz, W. Jia, M. Gentile, Y. Wang, Y. Lei, *Electroanalysis* **2008**, *20*, 2482–2486.
[28] H. Wang, L. Zhang, X. Tan, C. M. B. Holt, B. Zahiri, B. C. Olsen, D. Mitlin, *J. Phys. Chem. C* **2011**, *115*, 17599–17605.
[29] J. A. Koza, Z. He, A. S. Miller, J. A. Switzer, *Chem. Mater.* **2012**, *24*, 3567–3573.

 © 2017 Wiley-VCH Verlag GmbH & Co. KGaA, Weinheim

Cape Peninsula University of Technology

[30] C. N. Polo da Fonseca, M. A. De Paoli, A. Gorenstein, *Sol. Energy Mater. Sol. Cells* **1994**, *33*, 73–81.
[31] I. G. Casella, *J. Electroanal. Chem.* **2002**, *520*, 119–125.
[32] P. Patil, L. Kadam, C. Lokhande, *Sol. Energy Mater. Sol. Cells* **1998**, *53*, 229–234.
[33] S. Buratti, B. Brunetti, S. Mannino, *Talanta* **2008**, *76*, 454–457.
[34] S. P. Jiang, A. C. C. Tseung, *J. Electrochem. Soc.* **1990**, *137*, 3442–3446.
[35] S. R. Gowda, A. Leela Mohana Reddy, X. Zhan, H. R. Jafry, P. M. Ajayan, *Nano Lett.* **2012**, *12*, 1198–1202.
[36] Y. Ding, Y. Liu, J. Parisi, L. Zhang, Y. Lei, *Biosens. Bioelectron.* **2011**, *28*, 393–398.
[37] E. R. Arriola, A. C. Cordón, *AIP Conf. Proc.* **2010**, *1322*, 483–487.
[38] T. Seike, J. Nagai, T. N. Seike Junichi, *Sol. Energy Mater.* **1991**, *22*, 107–117.
[39] M. E. Donders, H. C. M. Knoops, M. C. M. van, W. M. M. Kessels, P. H. L. Notten , *J. Electrochem. Soc.* **2011**, *158*, G92.
[40] M. Chowdhury, F. Cummings, M. Kebede, V. Fester, *Electroanalysis* **2017**, *29*, 578–586.
[41] M. Chowdhury, C. Ossinga, F. Cummings, J. Chamier, M. Kebede, *Electroanalysis* **2017**, *29*, 1876–1886.
[42] C. Guo, X. Zhang, H. Huo, C. Xu, X. Han, *Analyst* **2013**, *138*, 6727.
[43] P. Yuan, N. Zhang, D. Zhang, T. Liu, L. Chen, X. Liu, R. Ma, G. Qiu, *Chem. Commun.* **2014**, *50*, 11188.
[44] G. Karim-Nezhad, M. Hasanzadeh, L. Saghatforoush, N. Shadjou, S. Earshad, B. Khalilzadeh, *J. Braz. Chem. Soc.* **2009**, *20*, 141–151.
[45] M. Chowdhury, F. Cummings, M. Kebede, V. Fester, **2017**, 578–586.
[46] X.-Y. Lang, H.-Y. Fu, C. Hou, G.-F. Han, P. Yang, Y.-B. Liu, Q. Jiang, *Nat. Commun.* **2013**, *4*, 1–8.
[47] M. Y. Elahi, M. F. Mousavi, S. Ghasemi, *Electrochim. Acta* **2008**, *54*, 490–498.
[48] J. Chen, W. De Zhang, J. S. Ye, *Electrochem. Commun.* **2008**, *10*, 1268–1271.
[49] S. Park, T. D. Chung, H. C. Kim, *Anal. Chem.* **2003**, *75*, 3046–3049.
[50] X. Qi, M. Watanabe, T. M. Aida, R. L. Smith, *Catal. Commun.* **2008**, *9*, 2244–2249.
[51] B. Fang, A. Gu, G. Wang, W. Wang, Y. Feng, C. Zhang, X. Zhang, *ACS Appl. Mater. Interfaces* **2009**, *1*, 2829–2834.
[52] X. Z. Bian, H. Q. Luo, N. B. Li, *Bioprocess Biosyst. Eng.* **2010**, *33*, 971–978.
[53] I. Gualandi, E. Scavetta, Y. Vlamidis, A. Casagrande, D. Tonelli, *Electrochim. Acta* **2015**, *173*, 67–75.

Received: August 23, 2017
Accepted: September 30, 2017
Published online on October 13, 2017

 © 2017 Wiley-VCH Verlag GmbH & Co. KGaA, Weinheim

Cape Peninsula University of Technology